A deadly hug:
contact-dependent killing by *Caulobacter crescentus*, via cell surface-associated glycine-zipper proteins

by

Leonor García-Bayona

B. Sc. Microbiology and B. Eng. Chemical Engineering
Universidad de los Andes, Bogota, Colombia (2009)

M.Sc. Biological Sciences, sp. Microbiology
Universidad de los Andes, Bogota, Colombia (2010)

SUBMITTED TO THE GRADUATE PROGRAM IN MICROBIOLOGY
IN PARTIAL FULFILLMENT OF THE REQUIREMENTS FOR THE DEGREE OF

DOCTOR OF PHILOSOPHY AT THE
MASSACHUSETTS INSTITUTE OF TECHNOLOGY

SEPTEMBER 2017
©2017 Leonor García-Bayona. All rights reserved.

The author hereby grants MIT permission to reproduce and distribute publicly
paper and electronic copies of this thesis document in whole or in part in any medium now
known or hereafter created

Signature of Author: _____
Leonor García-Bayona
Graduate Program in Microbiology
August 31st, 2017

Certified by: _____
Michael T. Laub
Professor of Biology
Thesis Supervisor

Accepted by: _____
Martin F. Polz
Professor of Civil and Environmental Engineering
Co-director, Microbiology Graduate Program

POLE POLE NDIO MWENDO

A deadly hug: contact-dependent killing by *Caulobacter crescentus*, via cell surface-associated glycine-zipper proteins

by
Leonor García-Bayona
Submitted to the Graduate Program in Microbiology on August 31st, 2017
in partial fulfillment of the requirements for the degree of Doctor of Philosophy in Microbiology

ABSTRACT

In the battle for resources within microbial communities, antagonistic interactions between bacterial species are often mediated by diffusible inhibitory compounds, which can be diffusible or delivered in a contact-dependent manner. Bacteriocins are one ubiquitous type of such antimicrobials, and collectively constitute a very diverse group of ribosomally-synthesized diffusible proteinaceous toxins. The majority of well-characterized bacteriocin systems belong to a limited group of bacterial clades and environments. In contrast, interbacterial interactions are poorly characterized in the nutrient-poor aquatic environments where the α-proteobacterium *Caulobacter crescentus* thrives.

Here, I describe the discovery and characterization of a new type of bacteriocin in *C. crescentus*. The Cdz toxin is composed of two small hydrophobic proteins, each harboring an extended glycine-zipper motif often found in amyloids. These proteins are retained on the surface of producer cells where they form large, insoluble aggregates. I show that Cdz mediates cell contact-dependent killing of closely related species. The Cdz bacteriocin uses a type I secretion system and is unrelated to previously described contact-dependent inhibition systems. Delivering the bacteriocin directly to the recipient, rather than secreting it into the extracellular milieu, likely enables *C. crescentus* to avoid the dilemma of producing an expensive common good that would rapidly diffuse away in its aqueous environment. Furthermore, Cdz-like systems are found in many clades of bacteria, including pathogens such as *Klebsiella pneumoniae* and *Pseudomonas aeruginosa*, suggesting that this form of contact-dependent inhibition is widespread.

Using a cationic membrane stain, I showed that the Cdz bacteriocin causes inner membrane depolarization in the target cells. To further characterize the mechanism of delivery and toxicity, I conducted a suppressor screen to identify mutations that confer Cdz resistance to a target strain. I identified the putative surface receptor for the Cdz toxins, PerA, a protein harboring several pentapeptide-repeat motifs thought to adopt a quadrilateral β-helical fold. PerA plays an important role in envelope homeostasis. Additionally, I identified two envelope-remodeling genes whose upregulation confers resistance to Cdz-mediated killing. Taken together, my work has expanded the repertoire of bacteriocins, demonstrating that these antimicrobials can be contact-dependent and, consequently, advantageous in a wider range of environments than previously anticipated.

Thesis Supervisor: Michael T. Laub
Title: Professor of Biology

ACKNOWLEDGEMENTS

I am indebted to the many people who had the patience to teach me how to do science, kept me sane(ish) and who made the last six years a really fun and extraordinary experience.

To my advisor, Michael Laub, for showing me that doing science can be exciting and extremely rigorous at the same time. Thank you for giving me the right amount of freedom to develop my ideas and for keeping me somewhat focused. I will try my best to stay true to the amazing science communication skills that I (hopefully) learned in the lab. But most of all, thank you for showing the cat gifs at my defense, that moment is my proudest grad career accomplishment!

To my committee members Alan Grossman and Martin Polz, for all your scientific advice and useful input over the years. Alan, there are several very specific nuggets of wisdom that I keep going back to (i.e. "you get what you screen for, not what you want to screen for"). Thank you also for all the wise career advice at times where I felt most confused. Carine Gibbs, thank you for serving on my defense committee.

To members of the Laub lab. I feel honored to have been part of such an scarily talented and hard-working group of people. Thank you for all the scientific guidance and input, but mostly thank you for your support and for making the lab such a fun place. In particular to my three baymates for letting me vent and for making me smile when I lost perspective. Emma, thank you for being the original crazy cat lady, I hope I've been a worthy successor. Jayme and Michele, it was an honor seeing you go through such a special time in your lives, I learned more than I wanted about pregnancy, and I truly admire you. Monica and James, thanks for all the experimental and career advice and for debriefing me in all the TV shows so that I remember why I never watch them. But most of all, Monica thank you for the Tiny Cat book! Mary, thank you for my super cutesy defense cartoon, it gave me the extra motivation I needed to be able to stand in front of people and speak. Tung, thank you for sharing all your technical knowledge and your plasmids.

Nicki Watson, thank you for all your help with troubleshooting EM experiments. The Grossman, Sauer, Baker and Bell labs for being great neighbors and sharing your knowledge, equipment and reagents. Dr. Constanza Moreno, thank you for giving me a working right hand that I used for all the pipetting described in this work. Thank you also for convincing my parents to let me travel two days after surgery. Silvia Restrepo and Barbara Zimmermann, thank you for giving me my first opportunity to do research in a lab.

To the micro 2011 class, I hope we can keep biofilming for a long time... please no one move away from Boston so that the quorum sensing signal doesn't dilute! Kat and Aleja (+Andres), thanks for being my Cambridge family. To my friends in Boston and beyond, mi gente linda de las fiestas hasta las 5, mis bridesmaids locas, my science brothers Manu and Gabo, Georgios, Lu, Dani, my former housemates.

To my dad, for raising me into an infinitely curious girl, telling me how colors are a brain construct before I knew how to read. How could I not grow up into a scientist when my early childhood memories involve explanations of diverse aspects of human physiology and the philosophy of a paradox? My Mom, the master tinkerer and the most persevering person I know, for all your love and for being such a great role model of kindness and empathy. To my sister, Cocos, for being so centered and sensible and making sure I don't go off the rails, and for being such a goofball. To the memory of my grandparents, Mario and Leonor, for showing me that sometimes there is no other recourse but to be the Quixote ("Colombia es un país de Quijotes"). To my brother and Renee for coming to my defense, it meant a lot to have you around!

To Juanjo, the best and most loyal teammate/travelmate/adventuremate in life; your love and support is definitely worth all the bad puns and the dad jokes. Without you, this last 6 years would have been gray. Finally, to Eureka, Tommy, Daly and especially Momo for showing me that cats are the best cronopios and effectively turning me into a crazy cat lady.

TABLE OF CONTENTS

Abstract 3

Acknowledgements 4

Table of Contents 6

List of Figures 11

List of Tables 13

Chapter 1 Introduction: Interbacterial antagonism mediated by proteinaceous toxins 14

I. Introduction 15

II. Bacteriocins 16

General description 16

Classification 17

Two-peptide bacteriocins in gram positive bacteria 22

Class II microcins from gram-negatives 23

Bacteriocin detection and purification techniques 25

Potential applications 27

Bacteriocin ecology and evolution 28

III. Contact-dependent polymorphic toxin systems 29

The Contact-Dependent Inhibition (CDI) “toxin on a stick” 30

The Type VI Secretion System "speargun" 33

Other types of contact-dependent killing systems 34

IV. Ecology of the model organism Caulobacter crescentus 35

V. Research summary 36

References 37

Chapter 2: Identification of Cdz, a novel type of contact-dependent killing system in *Caulobacter crescentus* mediated by cell surface-associated glycine zipper proteins 48

Abstract 49

Introduction 50

Results 52

A *C. crescentus* bacteriocin gene cluster is induced in stationary phase 52

Cells harboring the cdz gene cluster can kill cells lacking it 54

CdzC, CdzD, and a type I secretion system are required for killing 55

Immunity to *cdz* is conferred by the small transmembrane protein CdzI 58

CdzC and CdzD promote lysis of target cells 60

Cdz-based killing requires physical contact between producer and indicator cells 61

CdzC and CdzD localize to the outer membrane of producer cells 65

CdzC forms large aggregates on the surface of producer cells 69

Cdz can drive interspecies killing and Cdz-like systems are widespread in bacteria..... 73

Discussion 77

A novel contact-dependent killing system 77

Mechanism of secretion and toxin delivery 78

Mechanism of killing by CdzC and CdzD 79

Cdz-like bacteriocins may be widespread in proteobacteria 81

Final Perspective 82

Matherials and methods 83

Bacterial strains and growth conditions 83

Competition experiments 83

Testing for inhibitory activity in culture supernatants 84

Split-well competition experiments 85

RNA-seq and transcriptional reporters 85

Immunoblotting 86

Fluorescence microscopy of competitions 87

Immunogold labeling and transmission electron microscopy 87

Immunofluorescence 88

Flow cytometry 88

Subcellular fractionation 89

Computational prediction of aggregation and searches for Cdz-like systems 89

Acknowledgements 102

References 102

Chapter 3: Mechanisms of resistance to Cdz-mediated killing 109

Abstract 110

Introduction 111

Results 114

A suppressor screen to identify mutations that render the indicator cells resistant to Cdz 114

Increased expression of the envelope-associated *zerRAB* operon confers resistance to Cdz 116

The pentapeptide-repeat protein PerA probably acts as CdzC/D surface receptor 121

PerA is required for normal cell envelope homeostasis 125

Discussion 129

Use of spontaneous suppressor mutations and deep sequencing to identify genes involved in bacteriocin sensitivity 129

A new type of receptor for a new type of toxin 130

A newly identified member of the pentapeptide-repeat family has a role in envelope homeostasis 131

Newly identified envelope remodeling genes in *C. crescentus* 132

Materials and Methods 134

Bacterial strains and growth conditions 134

Competition experiments 134

Suppressor screening and mapping 135

Membrane depolarization staining 135

Fluorescence and transmission electron microscopy 135

Triton X-100 fractionation and western blotting 136

Immunofluorescence 136

Alignment visualization and 3D model prediction 136

Acknowledgements 143

References 143

Chapter 4: Conclusions and future directions 149

Conclusions 150

Future directions 152

Validation of CDZ-like systems in other bacteria 152

Understanding the mechanism of CdzC/D delivery and its link to aggregation 153

Understanding the physiological role of PerA and ZerA/B 154

Regulation of the CDZ system 155

Discovery of other genes involved in community behaviors in *C. crescentus* 158

References 159

LIST OF FIGURES

Figure 1.1. Representation of bacteriocins from different classes in gram-positive and gram-negative bacteria 18

Figure 1.2. Type I secretion system (T1SS) for microcin secretion 24

Figure 1.3. Testing for bacteriocin activity by the spot-on-lawn method or by agar overlay 26

Figure 1.4. Architecture of the polymorphic toxin systems (PTS) in bacteria. 30

Figure 1.5. Types of contact-dependent killing systems in bacteria 32

Figure 2.1. The *cdz* gene cluster is very highly expressed in stationary phase 53

Figure 2.2. Growth curve for cells expressing a P_{cdzC}-YFP reporter..... 54

Figure 2.3. The *cdz* gene cluster encodes a two-peptide bacteriocin, secreted via a type I secretion system, and a small transmembrane immunity protein 56

Figure 2.4. Control experiments for the genetic dissection of the Cdz system 57

Figure 2.5. CdzC and CdzD kill an indicator strain in co-culture 59

Figure 2.6. Control experiments for the microscopy-based analysis of Cdz-dependent killing 60

Figure 2.7. Cdz-mediated killing requires cell-cell contact between a producer and an indicator..... 62

Figure 2.8. CdzC can be detected in a concentrated culture supernatant 63

Figure 2.9. Controls for flow cytometry analysis of cell-cell attachment 64

Figure 2.10. CdzC and CdzD localize to the outer membranes of cells, while CdzI is an inner membrane protein 66

Figure 2.11. Controls for cell-fractionation experiments 68

Figure 2.12. CdzC aggregates on the surface of producer cells 70

Figure 2.13. Controls for the visualization of Cdz in the surface of producer cells via immunogold labeling and transmission electron microscopy 71

Figure 2.14. CdzC can be detected in the surface of producer cells by immunofluorescence..... 72

Figure 2.15. Phylogenetic distribution of putative Cdz-like systems in bacteria 74

Figure 2.16. Cdz can mediate killing of closely related species 75

Figure 3.1. Identification of mutations that confer resistance to Cdz-mediated killing 115

Figure 3.2. Increased expression of the *zerRAB* operon leads to Cdz resistance 117

Figure 3.3. Expression of the *zerRAB* causes cell-envelope and morphology alterations 119

Figure 3.4. *zerA/B* overexpression inhibits growth 121

Figure 3.5. PerA acts as a receptor for Cdz 122

Figure 3.6. PerA is a surface-exposed outer membrane protein 124

Figure 3.7. PerA is a pentapeptide-repeat protein required for normal cell growth 126

Figure 3.8. Altered cell morphology caused by a perA deletion 127

Figure 4.1. Cdz-like gene cluster in *Pseudomonas aeruginosa* PAO1 152

Figure 4.2. CdzC and CdzD can be produced in two separate cells for killing 154

Figure 4.3. Regulation of the Cdz system 157

LIST OF TABLES

Table 1.1. Summary of characterized bacteriocin diversity in gram-positive bacteria 20

Table 1.2. Summary of characterized bacteriocin diversity in gram-negative bacteria 21

Table 2.1. Oligonucleotides 91

Table 2.2. Strains 93

Table 2.3. Plasmids 98

Table 3.1. Oligonucleotides 137

Table 3.2. Strains 138

Table 3.3. Plasmids 141

Chapter 1
Introduction: Interbacterial antagonism mediated by proteinaceous toxins

I. Introduction

Bacteria are, by biomass, the most abundant organism on the planet and they have the ability to colonize almost any type of environment (Nee, 2004; Whitman et al., 1998), including the human gut (Donaldson et al., 2015), the plant rhizosphere (Andreote and Pereira e Silva, 2017) and even the tropospheric clouds (DeLeon-Rodriguez et al., 2013). Moreover, bacterial metabolic activity often plays a major role in shaping ecosystems (Konopka, 2009; Nee, 2004; Nicholson et al., 2012). In their environments, bacteria frequently form complex microbial communities, where each individual species needs to compete with community members for a set of limited resources, particularly specific nutrients and physical space (Cornforth and Foster, 2013; Hibbing et al., 2010). Bacteria also display an array of cooperative community behaviors, including quorum sensing, biofilm formation, and syntrophic interactions (cross-feeding) (Parsek and Greenberg, 2005; Stubbendieck et al., 2016). These antagonistic and cooperative interactions can determine the ability of a given species to establish and thrive within a community (Hibbing et al., 2010; Stubbendieck et al., 2016) and, consequently, these interactions can influence the overall structure and composition of a community. Antimicrobial-producing populations can act as cohesive units such that the inhibitory molecules mostly mediate competition between populations rather between individuals within a community (Cordero et al., 2012). One compelling example of such community dynamics is the role that the normal human gut microbiota plays in protecting the colon from colonization by the pathogen *Clostridium difficile.* Following antibiotic treatment that causes a drop in the normal resident gut microbiota, the pathogen can proliferate, causing antibiotic-associated diarrhea (Abt et al., 2016).

Broadly, ecological competition can be classified into two main types: indirect competition where one species preferentially consumes the resources required by the other (exploitative competition), and direct competition where one species inhibits the growth of the other by causing harm (interference competition). The latter is often implemented via secretion of diffusible antimicrobials such as antibiotics, or through contact-dependent killing mechanisms. The presence of antagonistic molecules often drives the co-evolution of protective mechanisms in some target cells, for example the acquisition of antibiotic resistance genes. Even so, the

ecological and evolutionary dynamics of a killer-prey system are in large part also determined by the characteristics of the environment (Cornforth and Foster, 2013; Hibbing et al., 2010).

Also frequently involved in interference competition are bacteriocins, which are ribosomally-synthesized proteinaceous antimicrobial molecules produced by bacteria, that usually target relatively closely related species (Riley and Wertz, 2002). Although these toxins are ubiquitous and extraordinarily diverse, the bulk of well-characterized bacteriocin systems belong to a restricted group of bacterial clades and environments (Rebuffat, 2011a; Riley, 2009). Considering that bacteriocins constitute a potential alternative to address the pressing issue of antibiotic resistance in pathogens (Cotter et al., 2012; Hassan et al., 2012), there is a need to discover and characterize new bacteriocin families from a wider taxonomic set of bacteria in a range of environments. The α-proteobacterium *Caulobacter crescentus,* a well-established and genetically tractable model organism, represents a suitable platform to expand this field, as it thrives in freshwater oligotrophic environments (Poindexter, 1981; Tsokos and Laub, 2012), where the limited resources and dilute conditions may call for different bacteriocin types and dynamics than previously characterized. Prior to the work described in this thesis, no bacteriocins had been characterized in *C. crescentus* or related species.

In this chapter, I review the general characteristics of this type of toxic proteins, with an emphasis on small bacteriocins produced by Gram-negative bacteria. I also recapitulate the current knowledge of toxin systems that act in a contact-dependent manner, and compare and contrast these two different types of inhibitory systems.

II. Bacteriocins

General description

The first observation of bacteriocin activity dates back to 1877 when Louis Pasteur and Jules François Joubert reported that bacteria isolated from urine samples inhibited the growth of *Bacillus anthracis* (Pasteur and Joubert, 1877; Rea et al., 2011). The main distinguishing feature

of bacteriocins relative to other antimicrobials is that these proteinaceous toxins or their precursor peptides are genetically-encoded and produced using the cellular translation machinery, after which they may undergo post-translational modifications (PTMs) (Riley, 2009). Conversely, non-ribosomal peptide antibiotics such as penicillin are synthesized through a series of catalytic steps requiring enzymes (Montesinos, 2007). In contrast to antibiotics, bacteriocins often (but not always) have a narrow killing spectrum, being toxic only to close relatives of the producing strain (Cotter et al., 2012; Riley, 2011). This range of action can be determined by the nature of its cellular target, but is most often defined by the requirement for a specific cell-surface receptor molecule in the prey cell, that mediates attachment and sometimes import into the cell (Nes, 2011; Rebuffat, 2011a). Another feature that differentiates bacteriocins from antibiotics is their potency, since they are usually active at pico- or nanomolar concentrations, orders of magnitude less that the minimal inhibitory concentration for most antibiotics (Cotter et al., 2012; Nes, 2011; Rebuffat, 2012). Interestingly, some of the most potent bacteriocins can have dual modes of action combining involvement of more than one cellular target (Rebuffat, 2012).

Bacteriocins are ubiquitous, as there is evidence of their production across all major groups of archaea and bacteria. Within a given species, there can be great variation in the number and type of bacteriocins produced by each isolate (Riley, 2009, 2011). In general, they are encoded within gene clusters that can be on plasmids or in the chromosome and are often subject to horizontal gene transfer (Rankin et al., 2011; Riley, 2009). These gene clusters comprise all the genes required for synthesis, PTM and export, along with an immunity gene that protects the producer cell from its cognate bacteriocin (Rea et al., 2011; Rebuffat, 2011a). Other types of genes are sometimes associated with these gene clusters, such as those involved in regulation (histidine kinase-response regulator pairs), synthesis of signaling molecules, and genes of unknown function (de Jong et al., 2011; Rea et al., 2011).

Classification

Bacteriocins are very heterogeneous, ranging in size from large toxins (˜95 kDa) to small peptides of less than 5 kDa, and have a variety of cellular targets. Broadly, these toxins can be divided into

those produced by Gram-positive and Gram-negative bacteria. Further class divisions are based on size, type and extent of PTMs and cellular targets. Historically, most studies have focused on bacteriocins produced by lactic acid bacteria (LAB) and enterobacteria, which is why their bacteriocins are used as the base for classification. I summarize the most prevalent classification and describe the main features of characterized bacteriocins in Tables 1.1 and 1.2 (Ghequire and De Mot, 2014; Gordon et al., 2007; Heng et al., 2007; Kaškonienė et al., 2017; Rea et al., 2011; Rebuffat, 2011a, 2012). Schematic representations of some examples are presented in Fig 1.1. The subsequent sections focus on two-peptide bacteriocins form LAB and class II microcins, the two types of bacteriocins that bear most resemblance to the bacteriocin system that I identified in *C. crescentus*.

Figure 1.1. Representation of bacteriocins from different classes in gram-positive and gram-negative bacteria. A. Nisin A, a lantibiotic produced by *Lactococcus lactis*. Residues involved in lanthionine (Ala-S-Ala) or β-methyllanthionine (Abu-S-Ala) structures are shaded in grey, other modified residues are in black (*Dha* dehydroalanine, *Dhb* dehydrobutyrine). Adapted from (Rea et al., 2011). **B.** Lactococcin C, a two-peptide pore-forming unmodified bacteriocin produced by *Lactococcus lactis*. Adapted from (Nissen-Meyer et al., 2010). **C.** Lysostaphin, a bacteriolysin produced by *Staphyloccocus aureus* (PDB 1QWY). **D.** Colicin B (*E. coli*). Pore-forming domains are shown in blue and brown (hydrophobic hairpin); connecting helix is red; translocation domain is green. Adapted from (Zakharov et al., 2004). **E.** Pyocin R2, a phage tail-like bacteriocin from *P. aeruginosa.* Adapted from (Ghequire and De Mot, 2015). **F.** Microcin E492, a pore-forming siderophore-microcin from *K. pneumoniae* (only C-terminus of peptide is shown). Adapted from (Fischbach et al., 2006). **G.** Microcin J25, a lasso-peptide RNA-polymerase inhibitor from *E. coli*. Adapted from (Pattabiraman and Bode, 2011).

A. Nisin A (lantibiotic)

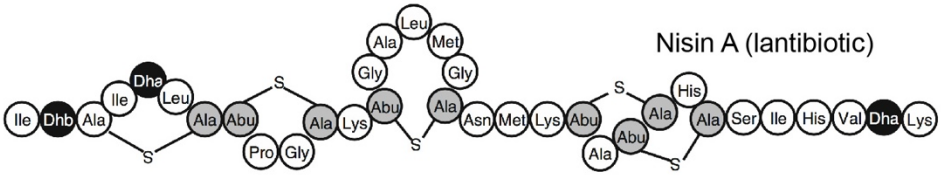

B. Lactococcin C (class IIb)

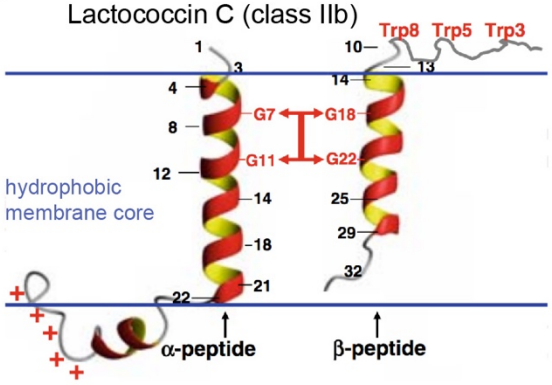

C.

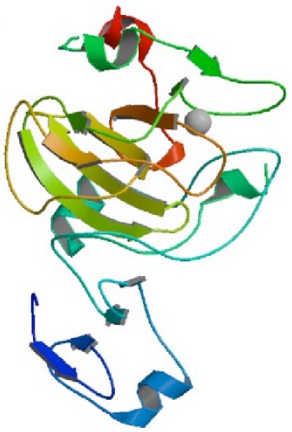

Lysostaphin (bacteriolysin)

D. Colicin B

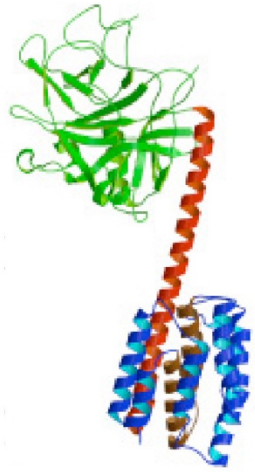

E. Pyocin R2 (tailocin)

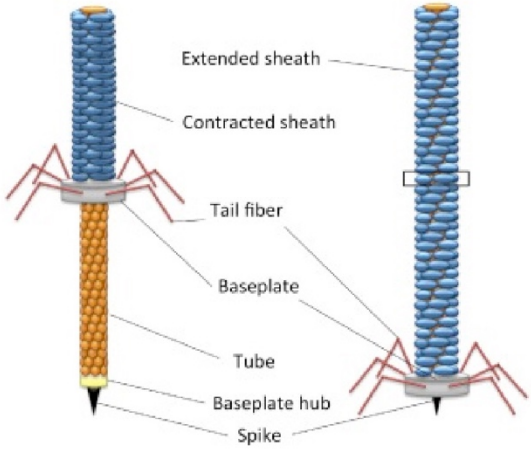

F. Microcin E492 (class II)

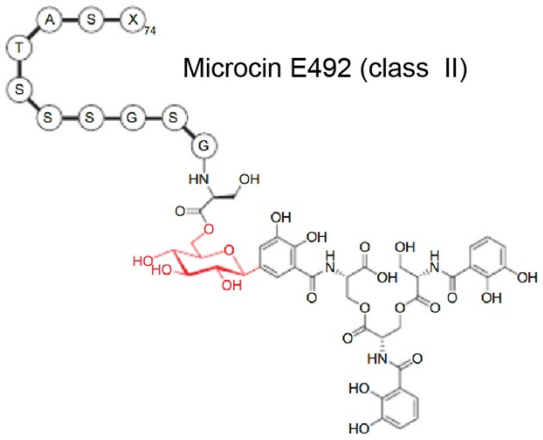

G.

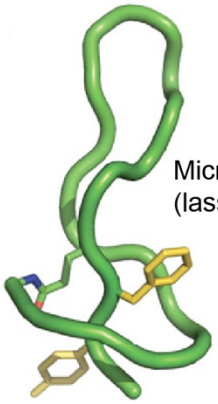

Microcin J25
(lasso-peptide)

Table 1.1. Summary of characterized bacteriocin diversity in Gram-positive bacteria.

Gram-positive bacteriocins						
	Description	**Size**	**Distinctive features**	**Synthesis and export**	**Target(s)**	**Examples**
Class I	Small, post-translationally modified (Lantibiotics)	<5 kDa, 19-28 residues	- Extensive PTM, most contain the modified amino acids lanthionine or ß-methyllanthionine and dehydrated residues. - Can be single or two-component. - Can be linear, globular, a few are cyclic.	- Modification enzymes anchor on the leader peptide, some can catalyze cyclisation - ABC transporter secretion, serine proteinases cleave the leader peptide	Membrane pore-forming and/or peptidoglycan synthesis inhibition (lipid II)	Nisin A (*Lactococcus lactis*) shown in Fig 1.1A, subtilin (*B. subtilis*), cynnamicin (*Streptomyces cinnamoneus*)
Class II	Small, unmodified	<10 kDa	**class IIa:** pediocin-like (N-terminal pediocin box YGNGV), inhibit *Listeria monocitogenes* **class IIb:** two-peptide bacteriocins, GxxxG dimerization motif, form amphiphilic α-helices **class IIc:** circular, heat stable, protease-resistant, inhibit *L. monocytogenes* **class IId:** linear, non pediocin-like	Secretion by ABC transporter and accessory protein or sec-dependent secretion, cleavage during secretion of leader peptide at double-glycine (GG)	Form membrane pores (leakage and loss of membrane potential)	Pediocin PA-1 (*Pediococcus acidilactici*), Thermophilin 13 (*Streptococcus thermophilus*), uberolysin (S*treptococcus uberis*), lactococcin C (*L. lactis*) shown in Fig 1.1B
Bacteriolysins (class III)	Bacteriolytic enzymes	15-80 kDa	- Large, heat-labile - Have specific domains for translocation, receptor binding and killing.	Self-export	Peptidoglycan cleavage	Helveticin J (*Lactobacillus helveticus*), enterolysin A (*Enterococcus faecalis*), lysostaphin (*Staphylococcus aureus*) shown in Fig 1.1C
Class IV	Bacteriocins with non-protein moieties	12 kDa	- Glycoproteins or lipoproteins - Heat stable, sensitive to protease treatment - bacteriostatic		Inhibit protein synthesis through an unknown mechanism	Lactocin 27 (*L. helveticus*), lacstrepcin (*Streptococcus lactis*)

Table 1.2. Summary of characterized bacteriocin diversity in Gram-negative bacteria.

Gram-negative bacteriocins						
	Description	**Size**	**Distinctive features**	**Synthesis and export**	**Target(s)**	**Examples**
Colicins and colicin-like bacteriocins	Modular with separate domains for receptor binding, translocation and killing (C-terminus).	30-95 kDa	-High molecular weight. - Induced by SOS-response - Usually encoded in plasmids - Protease-sensitive and heat-labile - Target cell attachment requires a specific surface receptor normally involved in the uptake of essential nutrients - Translocation inside the target may require a second outer membrane protein.	- Release requires a lysis protein and is lethal for the producer cell - Immunity gene protects cells not expressing the colicin	- Form voltage-dependent channels in the inner membrane - Nucleases (DNA, RNA, tRNA) - Peptidoglycan degradation	Colicin B shown in Fig 1.1D, colicin E2 (*E. coli*), pyocins-S1 (*P. aeruginosa*), klebicin C (*K. pneumoniae*)
Tailocins	Resemble bacteriophage tails	>80 kDa	- Induced by DNA damage (SOS-independent mechanism) - Upon target contact the sheath contracts and the tailocin core is inserted into the cell envelope (R-type) - Receptor is usually lipopolysaccharide - Some are protease-resistant - Gene cluster with 40+ genes, up to ˜40 kb	- Release requires a lysis protein and is lethal for the producer cell - Immunity gene protects cells not expressing the tailocin	- Form a channel through the inner membrane that causes depolarization	Pyocin R2 shown in Fig 1.1E, pyocin F2 (*P. aeruginosa*)
Microcins	Small, unmodified or post-translationally modified	1-10 kDa	- Stable, hydrophobic - Generally produced under stress conditions - Can have an attached moiety produced by non-ribosomal synthesis, added to serine-rich C-terminus - "Trojan horse" recognition by target cell receptor: PTM is a siderophore (siderophore-microcins) or nucleotide - Can be linear or lasso-peptides (knotted) -Two classes: **Class I** are plasmid-encoded, <5 KDa, extensive PTM **Class II** are 5-10 kDa, can be unmodified or modified at the C-terminus, can be chromosomal	- Export through Type-I secretion system - Cleavage of leader peptide during secretion, at GG/GA/GS	- Inner membrane pore formation - RNA polymerase inhibition - Asp-tRNA-synthase inhibition - Gyrase inhibition	Microcin J25 shown in shown in Fig 1.1G, microcin M (E. coli), microcin E492 (*K. pneumoniae*) shown in Fig 1.1F

Two-peptide bacteriocins in Gram-positive bacteria

To date, more than a dozen two-peptide bacteriocins (class IIb) from lactic acid bacteria have been characterized. These systems are composed of two unmodified small proteins of less than 10 kDa (30 to 50 residues). Usually, the genes encoding the peptides are co-operonic and are part of a gene cluster that also includes the genes required for secretion and an immunity gene that protects the producer cell from self-intoxication. Some class IIb bacteriocins are constitutively expressed, whereas others are regulated by a two-component system (a histidine kinase and a response regulator) that respond to a peptide quorum signal also encoded within the bacteriocin gene cluster. Although sometimes one of the individual peptides can display low antimicrobial activity, both peptides are required in approximately equal amounts to achieve full potency. The peptides are usually amphipathic or hydrophobic and have a 15-30 residue leader peptide that is cleaved at a double-glycine residue pair during secretion through an ABC transporter (Nissen-Meyer et al., 2011).

The two peptides are unstructured after secretion into the aqueous environment and only adopt an α-helical conformation upon contact with target cell membranes. Their dimerization/oligomerization requires the presence of a GxxxG motif (x=any residue). The two glycines in this motif are on the same side of the helix and form a flat surface that allows close contact between the helices (Fig 1.1B) (Nissen-Meyer et al., 2010). Interestingly, the two purified peptides of lactococcin G can be added to the target cell in a sequential manner to cause cytotoxicity, indicating that they do not need to interact with each other before reaching the target cell. In contrast, each peptide cannot diffuse to another cell once bound to the surface of a target cell, as determined by experiments in which prey cells that had been treated with one of the peptides were mixed with target cells pre-treated with the other peptide. In this setup, no antimicrobial activity was detected (Moll et al., 1998).

Most type IIb bacteriocins are narrow spectrum and are extremely potent. Their cytotoxic effects typically stem from the formation of membrane pores that cause leakage of cytosolic contents. Remarkably, these bacteriocins do not disrupt the membrane in a detergent-like manner, as they display some specificity with regard to the type of molecules the pores can transport. Indeed,

different bacteriocins cause leakage of different and specific subsets of molecules (Nissen-Meyer et al., 2011). For instance plantaricin EF causes leakage of monovalent (but not divalent) ions, with a preference for cations; and lactococcin G leads to increased permeability to Na^+, K^+, Li^+, Cs^+ and Rb^+ but not H+, divalent cations nor anions (Moll et al., 1999). Therefore, a proposed mode of action is that the two bacteriocin peptides could interact with their integral membrane receptor in the target cell (usually a transport protein), causing structural alterations preventing it from properly closing. However, the cell receptor for only two similar class IIb bacteriocins (lactococcin G and enterocin 1071) has been identified, which is UppP, a membrane protein involved in peptidoglycan synthesis (Kjos et al., 2014). Some studies suggest hydrophobic two-peptide bacteriocins may not need specific cellular receptors (Gao et al., 1999; Marciset et al., 1997). The mechanism of action of the immunity proteins remains poorly understood, but is thought to function through a cellular component, most likely the receptor, as its effect is dependent on the type of cells where the immunity gene is expressed. This toxin-neutralizing effect is thought to happen at the membrane, since many immunity genes for two-peptide bacteriocins have several predicted transmembrane helices (Nissen-Meyer et al., 2011).

Class II microcins from Gram-negatives

Nine class II microcin clusters have been characterized so far, which can be in plasmids or in the chromosome. In the latter case, the gene clusters can be flanked by a transposase and insertion sequences, suggesting they are subject to horizontal gene transfer. The clusters can also be part of a larger pathogenicity island, for instance the MccM microcin cluster in some uropathogenic *E. coli* strains (Vassiliadis et al., 2011). Similar in many regards to two-peptide bacteriocins from LAB, class II microcins from Gram-negatives are small (5 to 10 kDa) bacteriocins with an unmodified peptide backbone, that are often stable to heat, pH extremes and protease treatment (Rebuffat, 2011b). They are proposed to target inner membrane proteins or are membrane-active and have a dedicated immunity gene that is associated with the inner membrane. Like their Gram-positive counterparts, they are secreted via an ATP-binding cassette (ABC) transporter in the inner membrane, in this case part of a type I secretion system (T1SS) that also includes a membrane fusion protein (MFP) in the periplasm and an outer membrane channel

(OMP) (Fig 1.2). The latter is usually not part of the bacteriocin gene cluster and is located elsewhere in the chromosome. The ABC transporter recognizes a peptide secretion leader that is cleaved at a double-glycine (also GA or GS for this system) during secretion (Vassiliadis et al., 2011).

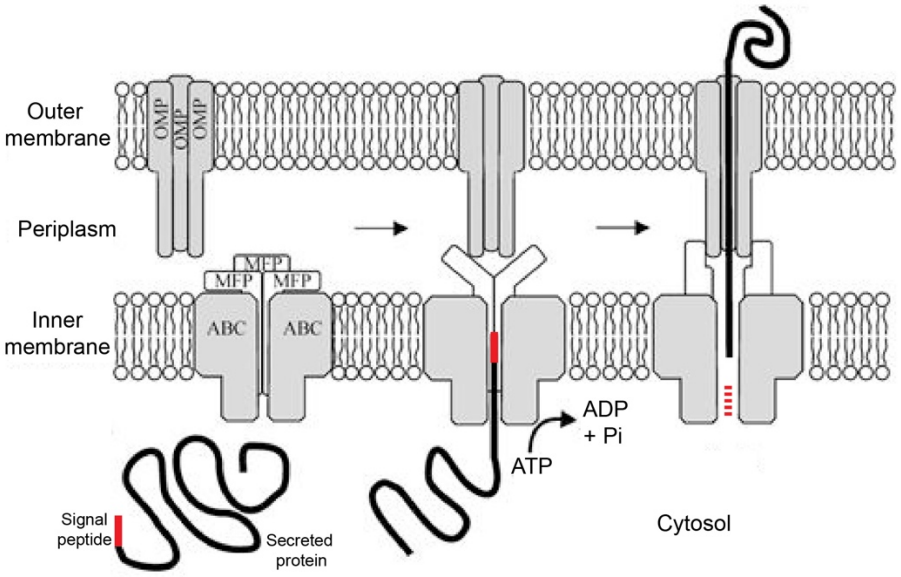

Figure 1.2. Type I secretion system (T1SS) for microcin secretion. Adapted from (Wells and Henderson, 2013).

However, in contrast to two-peptide bacteriocins, all class IIb microcins described to date are single-peptide, and some can have PTMs. Microcin IIb gene clusters often also encode the enzymes for synthesizing a catecholate-siderophore molecule that is post-translationally attached to the C-terminus of the microcin after recognition of a conserved 10-residue serine-rich sequence (Fig 1.1F) (Vassiliadis et al., 2011). Siderophores are small secreted diffusible high-affinity iron chelators that allow the producer cell to take up iron (Fe^{3+}) when it is present in very low concentrations in the environment. These molecules are imported by specific siderophore receptors in the outer membrane, which rely on TonB to couple import with energy from the proton-motive force (PMF) of the inner membrane (Braun and Braun, 2002). Therefore, siderophore-peptide microcins, produced under iron limiting conditions, use a Trojan horse strategy where prey cells that would be competing for iron import the siderophore, taking the toxic cargo along with it (Vassiliadis et al., 2011). Due to the requirement for these receptors, siderophore-microcins usually are only active against a few genera of enterobacteria. Interestingly, unmodified class II microcins MccV and MccL are also thought to target

catecholate-siderophore receptors in a TonB and PMF-dependent manner, through an unknown mechanism, but have a broader killing spectrum that includes some *Pseudomonas* species (Chehade and Braun, 1988; Pons et al., 2004).

Although class II microcins are thought to kill by membrane permeabilization, only four of them have been extensively characterized, so the killing mechanism for most remains unknown. MccE492 can form ion channels when added to planar lipid bi-layers (Lagos et al., 1993), and *in vivo* it causes membrane depolarization in the target cells (de Lorenzo and Pugsley, 1985). This effect is dependent on the presence of the inner membrane component of the mannose permease ManYZ (Bieler et al., 2006). Both MccH47 (a siderophore-peptide) and MccPDI (an unmodified peptide) target the F_0F_1 ATP synthase (Rodriguez and Lavina, 2003; Zhao et al., 2015). The mechanism by which immunity genes counteract their cognate toxin in the producer cell remains to be characterized, but like Gram-positive two-peptide bacteriocin immunity genes, their microcin equivalents are thought to be membrane associated. In the case of MccE492, the immunity gene does not preclude binding of the toxin to the ManYZ target, yet it somehow protects the cells from membrane leakage and depolarization (Biéler et al., 2010).

Bacteriocin detection and purification techniques

Bacteriocin-producing strains can be identified using several techniques; the most widely used are the spot-on-lawn method and the soft-agar overlay. All methods rely on the use of an indicator strain (target) that is allowed to form a lawn on agar plates. Candidate producer strains are tested for inhibitory activity, which is visible as a zone of clearing (inhibition halo) in the opaque indicator lawn (Kaškonienė et al., 2017; O'Bryan et al., 2015). In the spot-on-lawn method, the indicator strain is grown in liquid and a small volume is added to soft agar which is homogenized and spread on top of a firmer agar base plate, allowing it to grow and form a lawn in the soft agar. The strains to be tested are grown in liquid culture under conditions thought to induce bacteriocin production (stationary phase, iron limitation, etc.), and a small drop of the culture is spotted on top of the indicator soft agar (Gratia, 1946). Alternatively, a cell-free supernatant obtained by centrifugation of the culture is spotted. Bacteriocin activity will be detectable as an inhibitory halo in the indicator lawn, around the producer drop (Fig. 1.3). The

soft-agar overlay is a variation of the former technique, in which the candidate producer strains are allowed to form colonies on the plate, prior to addition of the soft agar layer that will form a lawn of the indicator strain. Other alternatives for testing the inhibitory activity of a culture supernatant or a sample from intermediate purification steps is to pipet it into wells punched into the soft agar indicator lawn or to immerse paper discs in the sample to be tested (Kaškonienė et al., 2017; O'Bryan et al., 2015). Additionally, several computational tools are also available for the identification of candidate bacteriocin clusters in sequenced genomes, including BAGEL (van Heel et al., 2013), BACTIBASE (Hammami et al., 2007), antiSMASH (Weber et al., 2015) and BOA (Morton et al., 2015).

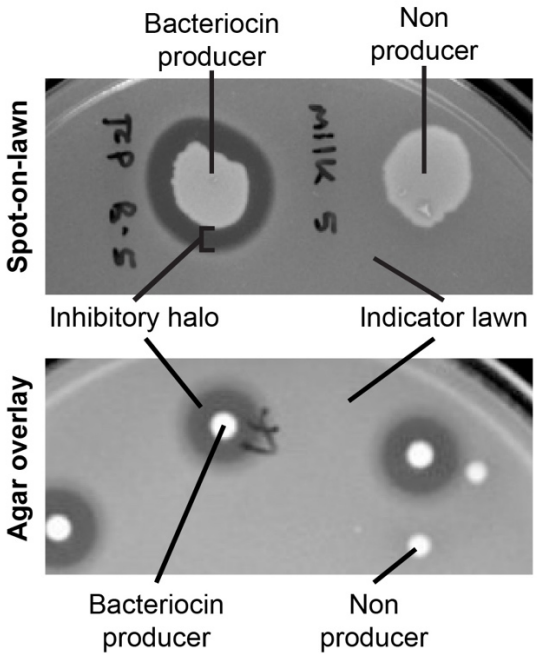

Figure 1.3. Testing for bacteriocin activity by the spot-on-lawn method or by agar overlay. Adapted from (Henning et al., 2015).

Bacteriocin purification protocols vary depending on the biochemical properties of each toxin, but in general start by concentrating the culture supernatant using ammonium sulfate precipitation or trichloroacetic acid, followed by a succession of ion-exchange chromatography, hydrophobic interaction chromatography, gel filtration and/or RP-HPLC (Kaškonienė et al., 2017; Saavedra and Sesma, 2011). For many bacteriocins from LAB, the number of purification steps can be significantly reduced by taking advantage of the fact that soluble bacteriocins become

adsorbed to the surface of producer cells when the pH of the culture medium is adjusted to close to neutral. The cells can then be pelleted down, washed and re-suspended in buffer where the pH is acidified, causing release of the adsorbed bacteriocin molecules into the buffer (Yang et al., 1992).

Potential applications

Traditionally, bacteriocins from LAB have been studied for their ability to kill foodborne pathogens and spoilage microorganisms, in particular *L. monocytogenes*. Since antibiotics are not suitable food additives, the addition of purified bacteriocins or their producer organisms has been deemed a valuable strategy for food preservation. To date, the most widely used bacteriocin in this context is nisin, which is licensed for food use. One of the main limitations for more widespread use of bacteriocins in food is the high cost of large-scale production and purification (Cotter et al., 2012; López-Cuellar et al., 2016).

More recently, bacteriocins have also been postulated as a suitable alternative to antibiotics, to overcome the emerging problem of antibiotic resistance. Their main advantages are their high potency, low human toxicity, and their narrow inhibitory spectrum, with characterized bacteriocins that can specifically target some pathogens (Cotter et al., 2012). For instance, lanthibiotics have been studied as effective inhibitors of staphylococci and enterococci in catheters (Fontana et al., 2006). Similarly, nisin F has been shown to be active intravenously, intranasally, or when incorporated into bone cement, to inhibit *S. pneumoniae* and *S. aureus* (De Kwaadsteniet et al., 2009; van Staden et al., 2012). Other promising preliminary results include mersacidin as an effective treatment for MRSA in the nasal cavity (Kruszewska, 2004), and planosporicin to treat *S. pyogenes* septicemia in a mouse model (Castiglione et al., 2007). Finally, the class IIa bacteriocin E50-52 was shown to successfully inhibit the intracellular growth of *M. tuberculosis* in an acute-tuberculosis mouse model (Sosunov et al., 2007).

Additionally, bacteriocins could be amenable to production *in situ* by probiotic strains. For instance, the bacteriocin-producing probiotic strain *Lactobacillus salivarius* DPC 6005 has been shown to successfully control *Salmonella typhimurium*-induced diarrhea in pigs (Casey et al.,

2007). Likewise, oral administration of *L. salivarius* UCC118 allowed control of a *Listeria monocytogenes* infection, via the production of the class IIb bacteriocin ABP118 (Corr et al., 2007). Furthermore, a bacteriocin-producing strain of *S. mutans* has been developed by Oragenics to control plaque formation in the oral cavity, showing great success in human clinical trials by excluding plaque-forming *S. mutans* strains for up to 14 years after a single inoculation (Hillman, 2002).

It should be noted that, similar to antibiotics, bacteriocins are also susceptible to the emergence of resistance in the target cells. Indeed, resistant isolates have been identified for many well characterized bacteriocins, usually due to loss of the surface receptor or modification of the cellular target (Cotter et al., 2012). Therefore, bacteriocins may need to be deployed in a clinical setting in a judicious manner, so as to delay the proliferation of resistant isolates.

Ecology and evolution

Despite the ubiquitous nature of bacteriocins across environments and taxonomic lineages, little is known about the ecological relevance and population dynamics of most bacteriocin systems. Most studies on the ecological and evolutionary dynamics of bacteriocins have almost exclusively focused on colicins, which are SOS-induced and require lysis of the producer cell for release. In that particular context, only a small percentage of the potential producer cells turn on the bacteriocin synthesis (Chavan and Riley, 2007). Therefore, studies of such systems may not be informative about the dynamics of other types of bacteriocins, where stress conditions induce most producer-competent cells to synthesize and secrete bacteriocin, without cell lysis (Dykes and Hastings, 1997).

Indeed, in an unstructured environment (*e.g.* a shaken culture flask), a LAB bacteriocin producer will invade and persist in an established sensitive strain population (Ruiz-Barba et al., 1994). In contrast, if inoculated at a low frequency, a colicin producer strain cannot invade the sensitive strain population due to the fitness cost of producing the bacteriocin (*i.e.* lethality to the producer cells that turn on the system), while the benefits are distributed at random. For colicin producers in liquid culture, a cheater strain that has the immunity gene or a resistant mutation

and benefits from the colicin public good but does not pay the fitness cost of bacteriocin production can sweep an established producer population. In contrast, in a structured environment (*e.g.* an agar plate), a rock-paper-scissors dynamic emerges where all three strains (sensitive, cheater, producer) can co-exist in different parts of the plate, as the producer strain can directly benefit from the resources made available by killing (Riley, 2011).

Several hypotheses have been put forward about the main forces affecting bacteriocin dynamics in natural populations. Some evidence suggests that bacteriocins play a role in maintaining microbial diversity at the population and community levels in soil communities (Czaran et al., 2002; Kerr et al., 2002). Bacteriocins may also serve to limit the advance of neighboring cells, preclude the invasion of a sensitive strain into an established population, or conversely, they may allow a producer strain to invade an already colonized niche (Kerr, 2007; Rao et al., 2005; Riley, 2011; Tait and Sutherland, 2002). Sequence analysis of some of the more widely distributed, modular colicins has shown that there is co-variation between the immunity gene and the immunity-binding region of the toxin. Furthermore, these regions, generally towards the C-terminal part of the colicin, are subject to frequent recombination to acquire different variants of the toxin-immunity region (Fig 1.3) (Chavan and Riley, 2007; Jamet and Nassif, 2015). These sequences are under strong diversifying positive selection, hinting that under some contexts the newly arisen variants can confer a fitness advantage to the producer cell (Chavan and Riley, 2007). Experimental testing of this hypothesis showed that in liquid culture, new variants with a promiscuous immunity gene (and a corresponding mutation in the cognate bacteriocin) can invade and sweep a population expressing the ancestral variant of the colicin (Tan and Riley, 1996).

III. Contact-dependent polymorphic toxin systems

As an alternative to the secretion of diffusible toxic molecules, bacteria can target direct neighbors in a contact-dependent manner. Like bacteriocins, these systems are also based on proteinaceous toxin-immunity pairs, but in this case the toxic effectors are directly delivered to the prey cells via a variety of secretion systems. It should be noted that some of these secretion

systems are related to systems involved in the secretion of effector molecules geared towards eukaryotic hosts, although the two types can usually be distinguished by sequence analysis. In an analogous way to colicins, the sequence of the majority of a contact-dependent system is conserved, with a variable region corresponding to the toxin-immunity pair, which is likely often subjected to diversification by recombination (Fig. 1.4). The immunity gene is usually immediately downstream of the toxin. Gene clusters encoding these polymorphic toxin systems (PTS) can also include additional orphan toxin-immunity pairs that only include the variable but not the conserved part of the toxin.

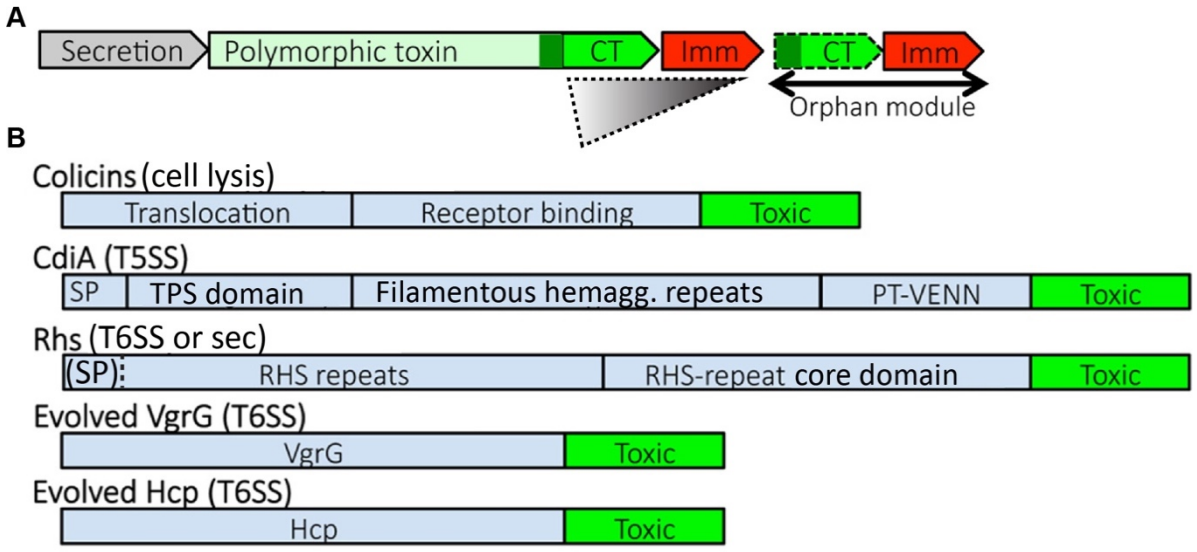

Figure 1.4. Architecture of the polymorphic toxin systems (PTS) in bacteria. A. Gene cluster organization for a canonical PTS. Dark green region indicates consensus sequence where toxin moiety is cleaved off for release. Shaded triangle indicates the variable region subject to recombination. CT = C-terminal toxic domain, Imm = immunity gene. **B.** Domain architecture for some characterized PTSs. Parentheses after the name indicate the secretion mechanism. SP = secretion signal peptide. Hcp and VgrG are core components of the T6SS needle. Adapted from (Jamet and Nassif, 2015).

The Contact Dependent Inhibition (CDI) "toxin on a stick"

The first contact-dependent system to be characterized, *cdiBAI,* was originally discovered in *E. coli* EC93 but similar systems are now known to be widespread in Gram-negative organisms (Aoki, 2005; Aoki et al., 2010; Jamet and Nassif, 2015). CdiA and CdiB are the components of a type V secretion system subclass called two-partner secretion. Both proteins use the Sec complex for

translocation across the inner membrane. CdiB is an outer membrane β-barrel transporter that mediates translocation of CdiA to the cell surface. CdiA is a modular, very large (>3000 amino acid) filamentous protein with both adhesion and toxic domains. The filamentous part contains hemagglutinin repeats and adopts a β-helix fold that extends from the cell-surface, with the C-terminus containing a much smaller (100-200 residues) toxin moiety separated from the rest of the protein by a conserved VENN motif. Therefore, CDI can be compared to a stick with a variable toxin tip (Fig. 1.5A). CdiI is the small immunity protein encoded directly downstream (Aoki et al., 2011).

CDI systems can be deployed in liquid culture or in biofilms (Aoki, 2005; Ruhe et al., 2015). Toxin delivery into the target cell requires stable cell-to-cell contact between CdiA on the producer cell and specific receptors on the surface of the target (BamA, OmpC, or Tsx, depending on the CdiA variant), required for cell attachment and toxin import (Ruhe et al., 2017). Once contact is established, the toxin moiety is cleaved off at the VENN region and imported into the periplasm (Webb et al., 2013). For toxins that require cytosolic import to exert their inhibitory effect, translocation requires the proton motive force and interaction with specific inner membrane receptors (Ruhe et al., 2014; Willett et al., 2015). The characterized toxin moieties are pore forming toxins, DNases, or tRNases, with several other putative toxin types having unknown functions function (Ruhe et al., 2017).

Interestingly, the role of the CDI system in *Burkholderia thailandensis* is not limited to mediating interbacterial competition, as it is also required for biofilm formation. This role is independent of the toxic activity, although the C-terminal toxin moiety is still required. It has been hypothesized that the mechanism by which this nuclease toxin influences biofilm formation is by causing modifications in the extracellular DNA within the biofilm matrix (Garcia et al., 2013). CDI systems are also required for biofilm formation in other bacteria, suggesting that in some species this polymorphic toxin system may serve a kin discrimination role, enabling the coordination of cooperative behaviors only with close relatives (Ruhe et al., 2013).

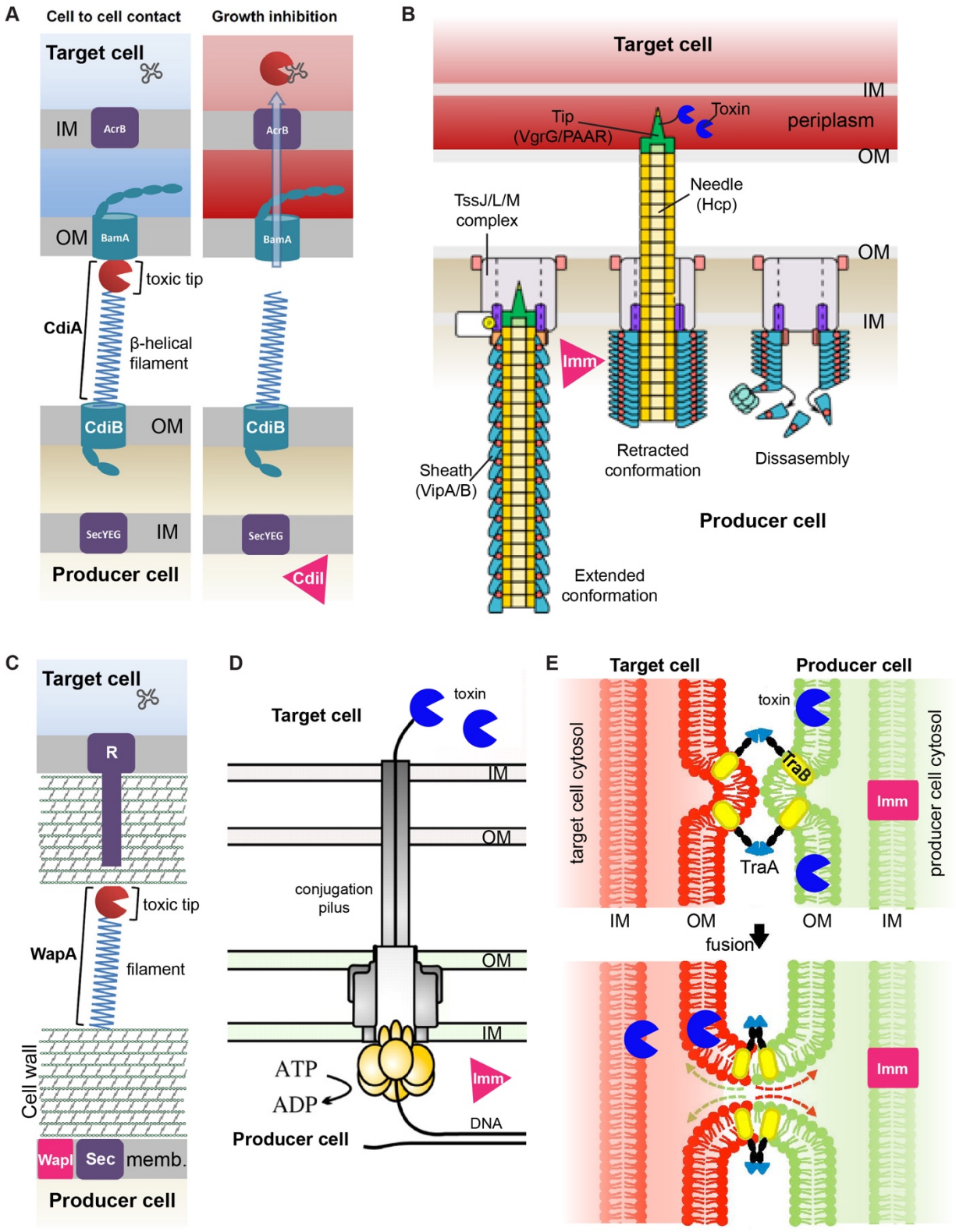
A
Cell to cell contact
Growth inhibition
Target cell
IM
AcrB
OM
BamA
toxic tip
CdiA
β-helical filament
CdiB
OM
SecYEG
IM
Producer cell
CdiI
B
Target cell
IM
Tip (VgrG/PAAR)
Toxin
periplasm
OM
Needle (Hcp)
TssJ/L/M complex
OM
IM
Imm
Sheath (VipA/B)
Retracted conformation
Dissasembly
Producer cell
Extended conformation
C
Target cell
R
toxic tip
WapA
filament
Cell wall
WapI
Sec
memb.
Producer cell
D
toxin
Target cell
IM
OM
conjugation pilus
OM
IM
ATP
ADP
Imm
DNA
Producer cell
E
Target cell
Producer cell
toxin
target cell cytosol
TraB
Imm
producer cell cytosol
TraA
IM
OM
OM
IM
fusion
Imm

Figure 1.5. Types of contact-dependent killing systems in bacteria. IM = inner membrane, OM = outer membrane, Imm = immunity gene **A.** Contact-dependent inhibition (*CdiABI*) uses a type V secretion system. Adapted from (Jacob-Dubuisson et al., 2013), depicting the Cdi system of *E. coli* strain EC93. CdiI is the immunity gene. **B.** Type VI secretion system (T6SS). Adapted from (Kube et al., 2015). **C.** Recombination hotspot protein (Rhs) WapAI in *B. subtilis*, memb = cell membrane. **D.** Type IV secretion system (T4SS) interbacterial inhibition in *X. citri*, WapI is the immunity gene, the surface receptor (R) is unknown. Adapted from (Zechner et al., 2012). **E.** Outer-membrane protein exchange in *M. xanthus*. Adapted from (Cao et al., 2015).

The Type VI Secretion System "speargun"

Type VI secretion systems (T6SS) are widespread in proteobacteria, including several pathogens (Boyer et al., 2009), and in the Gram-negative Bacteroidales that are a major component of the human gut microbiota (Coyne et al., 2016). The T6SS apparatus allows producer bacteria to inject toxins directly into the periplasm of target cells, when co-cultured on agar or in mixed-species biofilms (Hood et al., 2010; Russell et al., 2011). This multiprotein complex spans the cell envelope and shares structural homology to the T4 contractile bacteriophage tail (Fig. 1.5B). The core components are assembled in the cytosol of the producer cell and loaded with the toxic effectors prior to firing. A spike-tipped needle is surrounded by a contractile sheath, which, through a rapid conformational change, propels outward the needle, piercing the outer membrane of the prey cell and delivering the toxic cargo. Individual systems can deliver multiple distinct toxins. The contracted T6SS is then disassembled in an ATP-dependent manner (Ho et al., 2014; Russell et al., 2014).

T6SS gene clusters are typically large and contain all the structural and regulatory components, along with a variable number of accessory genes. The toxin-immunity pairs can be standalone bicistronic units, or the toxin can be fused to the C-terminal end of the spike protein (Li et al., 2015). The toxic effectors characterized to date can target the cell wall (peptidoglycan hydrolases), the inner membrane (phospholipases and pore forming toxins), or can have a cytosolic effect (nucleases and NAD(P) degradation enzymes) (Jamet and Nassif, 2015; Whitney et al., 2015). All characterized T6SS target Gram-negative bacteria, but the prey can be distantly related to the producer cell (Russell et al., 2014). Additionally, in *Proteus mirabilis* the T6SS can also be involved in kin discrimination independent of toxic effectors, allowing a producer strain

to coordinate community behaviors (Cardarelli et al., 2015; Gibbs et al., 2008). Other non-canonical T6SS roles have also been identified recently that are not directly related to interbacterial antagonism (Lin et al., 2017).

Other types of contact-dependent killing systems

Recombination hotspot proteins (Rhs) are large (>1500 residues) multidomain proteins with similar architecture to CdiA (Fig 1.5C): a conserved N-terminal region that determines their mode of secretion and/or attachment to the producer cell, a central region with Rhs repeats that adopt a filamentous fold, and a variable C-terminal toxic domain. The cognate immunity gene is immediately downstream (Koskiniemi et al., 2013; Poole et al., 2011). Gram-negative Rhs toxins have been shown to be secreted in a contact-dependent manner via a T6SS (Ma et al., 2017). In contrast, Rhs proteins from Gram-positive bacteria are most likely secreted via the general secretory pathway, yet still exhibit a contact-dependent killing phenotype, as was shown for the tRNase WapAI system in *B. subtilis* (Koskiniemi et al., 2013). WapA has been shown to remain associated to the cell wall (Foster, 1993) and is thought to mediate attachment and toxin delivery by a mechanism similar to CDI (Koskiniemi et al., 2013).

Type IV secretion systems (T4SS) can transfer protein-DNA complexes into neighboring cells in a contact-dependent manner (Fig 1.5D). This ATP-dependent multi-protein complex has a translocation channel that spans the whole cell envelope and an extracellular pilus. It is an extremely versatile system that is an important host colonization tool for many pathogens of eukaryotes (notably *Agrobacterium tumefaciens* tumor formation in plant cells). The conjugation machinery in bacteria is also a T4SS, while a different type of T4SS mediates DNA uptake from the extracellular environment (Peña and Arechaga, 2013; Wallden et al., 2010). Recently, this system was also associated with contact-dependent interbacterial competition in *Xanthomonas citri* via secretion of lipases or amidases, while the producer cells are protected from self-harming by a cognate immunity gene. This role in interbacterial antagonism for T4SS is thought to be more widespread in bacteria (Souza et al., 2015).

Finally, outer membrane exchange (OME) in the social bacterium *Myxococcus xanthus* is a kind discrimination system regulated by the polymorphic TraA cell surface receptor (Fig 1.5E). Homotypic TraA interactions between cells lead to transient outer membrane fusion and exchange of their protein contents. However, depending on the strain combination, OME may lead to killing of one of the participating isolates. The genetic mechanism underlying this phenomenon has not been fully characterized yet, but is likely due to toxin-immunity pairs associated with the outer membrane. This type of system would allow *M. xanthus* to fine tune a kin recognition system, so that it can identify more closely related species (actual kin) rather than just the "greenbeard" kind discrimination that TraA provides (Dey et al., 2016).

IV. Ecology of the model organism *Caulobacter crescentus*

Caulobacter crescentus is a well-established and genetically tractable model system, mostly used to study cell cycle regulation and determinants of cell morphology in bacteria. One of its main advantages for this purpose is that it divides asymmetrically, producing daughter cells with different structure and function. One of the daughter cells can immediately undergo a new round of DNA replication. This 'stalked cell' is sessile and has a polar stalk that allows it to attach to various substrates via an adhesive holdfast composed of proteins and polysaccharides. The other cell, the swarmer cell, is motile, chemotactic and replication-incompetent, such that it must first differentiate into a stalked cell before starting a new round of DNA replication. DNA replication is a highly regulated process in *C. crescentus*, and is only initiated once per cell cycle under all conditions. Together, these features make *Caulobacter* easily synchronizable and allow the easy tracking of cells as they proceed through the cell cycle. As a result, the genetic regulatory network and signal transduction pathways involved in cell cycle progression, differentiation, and morphogenesis are well characterized (Tsokos and Laub, 2012; Woldemeskel and Goley, 2017).

In contrast, our understanding of the environmental biology of *C. crescentus* and related species is very limited. One salient feature of this α-proteobacterium is its ability to thrive in dilute, nutrient poor aquatic environments (Poindexter, 1981). The arsenal of genetic adaptations that allow it to proliferate in the face of such limitation has not been studied extensively, although

some steps have been taken to understand how it copes with carbon, iron, and phosphate limitation (Boutte and Crosson, 2013; Leslie et al., 2015; Lubin et al., 2016; da Silva Neto et al., 2013). Additionally, the *Caulobacter* genomes are notably enriched in membrane receptors, particularly TonB-dependent transporters, which probably mediate the import of a diverse array of nutrients available at low concentrations, but their specific substrates remain obscure (Ash et al., 2014).

Similarly, community dynamics have not been well studied in this model organism. To date, no quorum sensing system has been identified. A panel of 11 *Caulobacter* isolates was screened for production of diffusible antibacterials, based on spot-on-lawn assays against the rest of the panel. Four strains, including *C. crescentus* CB15, were shown to be likely "bacteriocin" producers, causing very small (<1 mm) inhibitory halos in a few of the indicator strains. However, the genetic determinants of the phenotype and the biochemical nature of the inhibitory molecules have not been identified. In contrast to the modest inhibitory activity of the *Caulobacter* strains, the related species *Sphingomonas leidiyi* was shown to produce large (3-4 mm) inhibitory halos against most of the strains in the panel (Schoenlein and Ely, 1983).

C. crescentus has the ability to form stable biofilms that adhere to submerged surfaces, consisting of stalked cells arranged in a monolayer or in multicellular "mushroom" structures. Interestingly, in contrast to the structural role that extracellular DNA plays in the biofilms of other species, *Caulobacter* eDNA released due to cell death has the ability to promote biofilm dispersal by preventing the attachment of new cells, in a species specific manner (*i.e.* DNA from other species does not promote disassembly). It has been proposed that this could be part of a biofilm homeostasis mechanism in response to unfavorable conditions (Berne et al., 2010).

V. Research summary

During the course of my doctoral research, I identified and characterized a new type of bacteriocin system in *C. crescentus*, that allows it to inhibit the growth of closely related species. The system bears some similarity to microcins and two-peptide bacteriocins from LAB, but differs in some fundamental aspects. In chapter 2, I describe the initial characterization of this

unmodified two-protein bacteriocin, and show that it remains surface associated, acting in a contact-dependent manner, in sharp contrast to the canonical diffusible bacteriocins. In Chapter 3, I present a study of the mechanisms that allow prey cells to escape killing by this atypical bacteriocin, which in turn provide insights into previously unknown aspects of cell envelope physiology. To conclude, in chapter 4 I summarize some of the open questions and outline future research directions that will provide a better understanding of the biology of this system and of bacteriocins in general.

REFERENCES

Abt, M.C., McKenney, P.T., and Pamer, E.G. (2016). Clostridium difficile colitis: pathogenesis and host defence. Nat. Rev. Microbiol. *14*, 609–620.

Andreote, F.D., and Pereira e Silva, M. de C. (2017). Microbial communities associated with plants: learning from nature to apply it in agriculture. Curr. Opin. Microbiol. *37*, 29–34.

Aoki, S.K. (2005). Contact-Dependent Inhibition of Growth in Escherichia coli. Science *309*, 1245–1248.

Aoki, S.K., Diner, E.J., de Roodenbeke, C. t'Kint, Burgess, B.R., Poole, S.J., Braaten, B.A., Jones, A.M., Webb, J.S., Hayes, C.S., Cotter, P.A., et al. (2010). A widespread family of polymorphic contact-dependent toxin delivery systems in bacteria. Nature *468*, 439–442.

Aoki, S.K., Poole, S.J., Hayes, C.S., and Low, D.A. (2011). Toxin on a stick: Modular CDI toxin delivery systems play roles in bacterial competition. Virulence *2*, 356–359.

Ash, K., Brown, T., Watford, T., Scott, L.E., Stephens, C., and Ely, B. (2014). A comparison of the Caulobacter NA1000 and K31 genomes reveals extensive genome rearrangements and differences in metabolic potential. Open Biol. *4*, 140128–140128.

Berne, C., Kysela, D.T., and Brun, Y.V. (2010). A bacterial extracellular DNA inhibits settling of motile progeny cells within a biofilm: Biofilm inhibition by extracellular DNA. Mol. Microbiol. *77*, 815–829.

Bieler, S., Silva, F., Soto, C., and Belin, D. (2006). Bactericidal Activity of both Secreted and Nonsecreted Microcin E492 Requires the Mannose Permease. J. Bacteriol. *188*, 7049–7061.

Biéler, S., Silva, F., and Belin, D. (2010). The polypeptide core of Microcin E492 stably associates with the mannose permease and interferes with mannose metabolism. Res. Microbiol. *161*, 706–710.

Boutte, C.C., and Crosson, S. (2013). Bacterial lifestyle shapes stringent response activation. Trends Microbiol. *21*, 174–180.

Boyer, F., Fichant, G., Berthod, J., Vandenbrouck, Y., and Attree, I. (2009). Dissecting the bacterial type VI secretion system by a genome wide in silico analysis: what can be learned from available microbial genomic resources? BMC Genomics *10*, 104.

Braun, V., and Braun, M. (2002). Active transport of iron and siderophore antibiotics. Curr. Opin. Microbiol. *5*, 194–201.

Cao, P., Dey, A., Vassallo, C.N., and Wall, D. (2015). How Myxobacteria Cooperate. J. Mol. Biol. *427*, 3709–3721.

Cardarelli, L., Saak, C., and Gibbs, K.A. (2015). Two Proteins Form a Heteromeric Bacterial Self-Recognition Complex in Which Variable Subdomains Determine Allele-Restricted Binding. mBio *6*, e00251-15.

Casey, P.G., Gardiner, G.E., Casey, G., Bradshaw, B., Lawlor, P.G., Lynch, P.B., Leonard, F.C., Stanton, C., Ross, R.P., Fitzgerald, G.F., et al. (2007). A Five-Strain Probiotic Combination Reduces Pathogen Shedding and Alleviates Disease Signs in Pigs Challenged with Salmonella enterica Serovar Typhimurium. Appl. Environ. Microbiol. *73*, 1858–1863.

Castiglione, F., Cavaletti, L., Losi, D., Lazzarini, A., Carrano, L., Feroggio, M., Ciciliato, I., Corti, E., Candiani, G., Marinelli, F., et al. (2007). A Novel Lantibiotic Acting on Bacterial Cell Wall Synthesis Produced by the Uncommon Actinomycete *Planomonospora* sp. Biochemistry (Mosc.) *46*, 5884–5895.

Chavan, M.A., and Riley, M.A. (2007). Molecular Evolution of Bacteriocins in Gram-Negative Bacteria. In Bacteriocins, M.A. Riley, and M.A. Chavan, eds. (Berlin, Heidelberg: Springer Berlin Heidelberg), pp. 19–43.

Chehade, H., and Braun, V. (1988). Iron-regulated synthesis and uptake of colicin V. FEMS Microbiol. Lett. *52*, 177–181.

Cordero, O.X., Wildschutte, H., Kirkup, B., Proehl, S., Ngo, L., Hussain, F., Le Roux, F., Mincer, T., and Polz, M.F. (2012). Ecological Populations of Bacteria Act as Socially Cohesive Units of Antibiotic Production and Resistance. Science *337*, 1228–1231.

Cornforth, D.M., and Foster, K.R. (2013). Competition sensing: the social side of bacterial stress responses. Nat. Rev. Microbiol. *11*, 285–293.

Corr, S.C., Li, Y., Riedel, C.U., O'Toole, P.W., Hill, C., and Gahan, C.G.M. (2007). Bacteriocin production as a mechanism for the antiinfective activity of Lactobacillus salivarius UCC118. Proc. Natl. Acad. Sci. U. S. A. *104*, 7617–7621.

Cotter, P.D., Ross, R.P., and Hill, C. (2012). Bacteriocins — a viable alternative to antibiotics? Nat. Rev. Microbiol. *11*, 95–105.

Coyne, M.J., Roelofs, K.G., and Comstock, L.E. (2016). Type VI secretion systems of human gut Bacteroidales segregate into three genetic architectures, two of which are contained on mobile genetic elements. BMC Genomics *17*.

Czaran, T.L., Hoekstra, R.F., and Pagie, L. (2002). Chemical warfare between microbes promotes biodiversity. Proc. Natl. Acad. Sci. *99*, 786–790.

De Kwaadsteniet, M., Doeschate, K.T., and Dicks, L.M.T. (2009). Nisin F in the treatment of respiratory tract infections caused by *Staphylococcus aureus*. Lett. Appl. Microbiol. *48*, 65–70.

DeLeon-Rodriguez, N., Lathem, T.L., Rodriguez-R, L.M., Barazesh, J.M., Anderson, B.E., Beyersdorf, A.J., Ziemba, L.D., Bergin, M., Nenes, A., and Konstantinidis, K.T. (2013). Microbiome of the upper troposphere: Species composition and prevalence, effects of tropical storms, and atmospheric implications. Proc. Natl. Acad. Sci. *110*, 2575–2580.

Dey, A., Vassallo, C.N., Conklin, A.C., Pathak, D.T., Troselj, V., and Wall, D. (2016). Sibling Rivalry in Myxococcus xanthus Is Mediated by Kin Recognition and a Polyploid Prophage. J. Bacteriol. *198*, 994–1004.

Donaldson, G.P., Lee, S.M., and Mazmanian, S.K. (2015). Gut biogeography of the bacterial microbiota. Nat. Rev. Microbiol. *14*, 20–32.

Dykes, G.A., and Hastings, J.W. (1997). Selection and fitness in bacteriocin-producing bacteria. Proc. R. Soc. B Biol. Sci. *264*, 683–687.

Fischbach, M.A., Lin, H., Liu, D.R., and Walsh, C.T. (2006). How pathogenic bacteria evade mammalian sabotage in the battle for iron. Nat. Chem. Biol. *2*, 132–138.

Fontana, M.B.C., de Bastos, M. do C.F., and Brandelli, A. (2006). Bacteriocins Pep5 and Epidermin Inhibit Staphylococcus epidermidis Adhesion to Catheters. Curr. Microbiol. *52*, 350–353.

Foster, S.J. (1993). Molecular analysis of three major wall-associated proteins of Bacillus subtilis 168: evidence for processing of the product of a gene encoding a 258 kDa precursor two-domain ligand-binding protein. Mol. Microbiol. *8*, 299–310.

Gao, Y., van Belkum, M.J., and Stiles, M.E. (1999). The outer membrane of gram-negative bacteria inhibits antibacterial activity of brochocin-C. Appl. Environ. Microbiol. *65*, 4329–4333.

Garcia, E.C., Anderson, M.S., Hagar, J.A., and Cotter, P.A. (2013). Burkholderia BcpA mediates biofilm formation independently of interbacterial contact-dependent growth inhibition. Mol. Microbiol. *89*, 1213–1225.

Ghequire, M.G.K., and De Mot, R. (2014). Ribosomally encoded antibacterial proteins and peptides from *Pseudomonas*. FEMS Microbiol. Rev. *38*, 523–568.

Ghequire, M.G.K., and De Mot, R. (2015). The Tailocin Tale: Peeling off Phage Tails. Trends Microbiol. *23*, 587–590.

Gibbs, K.A., Urbanowski, M.L., and Greenberg, E.P. (2008). Genetic Determinants of Self Identity and Social Recognition in Bacteria. Science *321*, 256–259.

Gordon, D.M., Oliver, E., and Littlefield-Wyer, J. (2007). The Diversity of Bacteriocins in Gram-Negative Bacteria. In Bacteriocins, M.A. Riley, and M.A. Chavan, eds. (Berlin, Heidelberg: Springer Berlin Heidelberg), pp. 5–18.

Gratia, A. (1946). Techniques sélectives pour la recherche systématique des germes antibiotiques. C. R. Seances Soc. Biol. Fil. *140*, 1053–1055.

Hammami, R., Zouhir, A., Ben Hamida, J., and Fliss, I. (2007). BACTIBASE: a new web-accessible database for bacteriocin characterization. BMC Microbiol. *7*, 89.

Hassan, M., Kjos, M., Nes, I.F., Diep, D.B., and Lotfipour, F. (2012). Natural antimicrobial peptides from bacteria: characteristics and potential applications to fight against antibiotic resistance. J. Appl. Microbiol. *113*, 723–736.

van Heel, A.J., de Jong, A., Montalban-Lopez, M., Kok, J., and Kuipers, O.P. (2013). BAGEL3: automated identification of genes encoding bacteriocins and (non-)bactericidal posttranslationally modified peptides. Nucleic Acids Res. *41*, W448–W453.

Heng, N.C.K., Wescombe, P.A., Burton, J.P., Jack, R.W., and Tagg, J.R. (2007). The Diversity of Bacteriocins in Gram-Positive Bacteria. In Bacteriocins, M.A. Riley, and M.A. Chavan, eds. (Berlin, Heidelberg: Springer Berlin Heidelberg), pp. 45–92.

Henning, C., Gautam, D., and Muriana, P. (2015). Identification of Multiple Bacteriocins in Enterococcus spp. Using an Enterococcus-Specific Bacteriocin PCR Array. Microorganisms *3*, 1–16.

Hibbing, M.E., Fuqua, C., Parsek, M.R., and Peterson, S.B. (2010). Bacterial competition: surviving and thriving in the microbial jungle. Nat. Rev. Microbiol. *8*, 15–25.

Hillman, J.D. (2002). Genetically modified Streptococcus mutans for the prevention of dental caries. Antonie Van Leeuwenhoek *82*, 361–366.

Ho, B.T., Dong, T.G., and Mekalanos, J.J. (2014). A View to a Kill: The Bacterial Type VI Secretion System. Cell Host Microbe *15*, 9–21.

Hood, R.D., Singh, P., Hsu, F., Güvener, T., Carl, M.A., Trinidad, R.R.S., Silverman, J.M., Ohlson, B.B., Hicks, K.G., Plemel, R.L., et al. (2010). A Type VI Secretion System of Pseudomonas aeruginosa Targets a Toxin to Bacteria. Cell Host Microbe *7*, 25–37.

Jacob-Dubuisson, F., Guérin, J., Baelen, S., and Clantin, B. (2013). Two-partner secretion: as simple as it sounds? Res. Microbiol. *164*, 583–595.

Jamet, A., and Nassif, X. (2015). New Players in the Toxin Field: Polymorphic Toxin Systems in Bacteria. mBio *6*, e00285-15.

de Jong, A., van Heel, A.J., and Kuipers, O.P. (2011). Genome Exploitation and Bioinformatics Tools. In Prokaryotic Antimicrobial Peptides, D. Drider, and S. Rebuffat, eds. (New York, NY: Springer New York), pp. 75–80.

Kaškonienė, V., Stankevičius, M., Bimbiraitė-Survilienė, K., Naujokaitytė, G., Šernienė, L., Mulkytė, K., Malakauskas, M., and Maruška, A. (2017). Current state of purification, isolation and analysis of bacteriocins produced by lactic acid bacteria. Appl. Microbiol. Biotechnol. *101*, 1323–1335.

Kerr, B. (2007). The Ecological and Evolutionary Dynamics of Model Bacteriocin Communities. In Bacteriocins, M.A. Riley, and M.A. Chavan, eds. (Berlin, Heidelberg: Springer Berlin Heidelberg), pp. 111–134.

Kerr, B., Riley, M.A., Feldman, M.W., and Bohannan, B.J.M. (2002). Local dispersal promotes biodiversity in a real-life game of rock–paper–scissors. Nature *418*, 171–174.

Kjos, M., Oppegård, C., Diep, D.B., Nes, I.F., Veening, J.-W., Nissen-Meyer, J., and Kristensen, T. (2014). Sensitivity to the two-peptide bacteriocin lactococcin G is dependent on UppP, an enzyme involved in cell-wall synthesis: Lactococcin G receptor. Mol. Microbiol. *92*, 1177–1187.

Konopka, A. (2009). What is microbial community ecology? ISME J. *3*, 1223–1230.

Koskiniemi, S., Lamoureux, J.G., Nikolakakis, K.C., t'Kint de Roodenbeke, C., Kaplan, M.D., Low, D.A., and Hayes, C.S. (2013). Rhs proteins from diverse bacteria mediate intercellular competition. Proc. Natl. Acad. Sci. *110*, 7032–7037.

Kruszewska, D. (2004). Mersacidin eradicates methicillin-resistant Staphylococcus aureus (MRSA) in a mouse rhinitis model. J. Antimicrob. Chemother. *54*, 648–653.

Kube, S., Wendler, P., and Gene Center Munich, Ludwig-Maximilians-Universität München, Feodor-Lynen-Strasse 25, D-81377 Munich, Germany (2015). Structural comparison of contractile nanomachines. AIMS Biophys. *2*, 88–115.

Lagos, R., Wilkens, M., Vergara, C., Cecchi, X., and Monasterio, O. (1993). Microcin E492 forms ion channels in phospholipid bilayer membranes. FEBS Lett. *321*, 145–148.

Leslie, D.J., Heinen, C., Schramm, F.D., Thüring, M., Aakre, C.D., Murray, S.M., Laub, M.T., and Jonas, K. (2015). Nutritional Control of DNA Replication Initiation through the Proteolysis and Regulated Translation of DnaA. PLOS Genet. *11*, e1005342.

Li, J., Yao, Y., Xu, H.H., Hao, L., Deng, Z., Rajakumar, K., and Ou, H.-Y. (2015). SecReT6: a web-based resource for type VI secretion systems found in bacteria: Genomics update. Environ. Microbiol. *17*, 2196–2202.

Lin, J., Zhang, W., Cheng, J., Yang, X., Zhu, K., Wang, Y., Wei, G., Qian, P.-Y., Luo, Z.-Q., and Shen, X. (2017). A Pseudomonas T6SS effector recruits PQS-containing outer membrane vesicles for iron acquisition. Nat. Commun. *8*, 14888.

López-Cuellar, M. del R., Rodríguez-Hernández, A.-I., and Chavarría-Hernández, N. (2016). LAB bacteriocin applications in the last decade. Biotechnol. Biotechnol. Equip. 1–12.

de Lorenzo, V., and Pugsley, A.P. (1985). Microcin E492, a low-molecular-weight peptide antibiotic which causes depolarization of the Escherichia coli cytoplasmic membrane. Antimicrob. Agents Chemother. *27*, 666–669.

Lubin, E.A., Henry, J.T., Fiebig, A., Crosson, S., and Laub, M.T. (2016). Identification of the PhoB Regulon and Role of PhoU in the Phosphate Starvation Response of Caulobacter crescentus. J. Bacteriol. *198*, 187–200.

Ma, J., Sun, M., Dong, W., Pan, Z., Lu, C., and Yao, H. (2017). PAAR-Rhs proteins harbor various C-terminal toxins to diversify the antibacterial pathways of type VI secretion systems: The antibacterial pathways of type VI secretion systems. Environ. Microbiol. *19*, 345–360.

Marciset, O., Jeronimus-Stratingh, M.C., Mollet, B., and Poolman, B. (1997). Thermophilin 13, a nontypical antilisterial poration complex bacteriocin, that functions without a receptor. J. Biol. Chem. *272*, 14277–14284.

Moll, G., Hildeng-Hauge, H., Nissen-Meyer, J., Nes, I.F., Konings, W.N., and Driessen, A.J. (1998). Mechanistic properties of the two-component bacteriocin lactococcin G. J. Bacteriol. *180*, 96–99.

Moll, G.N., van den Akker, E., Hauge, H.H., Nissen-Meyer, J., Nes, I.F., Konings, W.N., and Driessen, A.J. (1999). Complementary and overlapping selectivity of the two-peptide bacteriocins plantaricin EF and JK. J. Bacteriol. *181*, 4848–4852.

Montesinos, E. (2007). Antimicrobial peptides and plant disease control. FEMS Microbiol. Lett. *270*, 1–11.

Morton, J.T., Freed, S.D., Lee, S.W., and Friedberg, I. (2015). A large scale prediction of bacteriocin gene blocks suggests a wide functional spectrum for bacteriocins. BMC Bioinformatics *16*.

Nee, S. (2004). More than meets the eye. Nature *429*, 804–805.

Nes, I.F. (2011). History, Current Knowledge, and Future Directions on Bacteriocin Research in Lactic Acid Bacteria. In Prokaryotic Antimicrobial Peptides, D. Drider, and S. Rebuffat, eds. (New York, NY: Springer New York), pp. 3–12.

Nicholson, J.K., Holmes, E., Kinross, J., Burcelin, R., Gibson, G., Jia, W., and Pettersson, S. (2012). Host-Gut Microbiota Metabolic Interactions. Science *336*, 1262–1267.

Nissen-Meyer, J., Oppegård, C., Rogne, P., Haugen, H.S., and Kristiansen, P.E. (2010). Structure and Mode-of-Action of the Two-Peptide (Class-IIb) Bacteriocins. Probiotics Antimicrob. Proteins *2*, 52–60.

Nissen-Meyer, J., Oppegård, C., Rogne, P., Haugen, H.S., and Kristiansen, P.E. (2011). The Two-Peptide (Class-IIb) Bacteriocins: Genetics, Biosynthesis, Structure, and Mode of Action. In Prokaryotic Antimicrobial Peptides, D. Drider, and S. Rebuffat, eds. (New York, NY: Springer New York), pp. 197–212.

O'Bryan, C.A., Crandall, P.G., Ricke, S.C., and Ndahetuye, J.B. (2015). Lactic acid bacteria (LAB) as antimicrobials in food products. In Handbook of Natural Antimicrobials for Food Safety and Quality, (Elsevier), pp. 137–151.

Parsek, M.R., and Greenberg, E.P. (2005). Sociomicrobiology: the connections between quorum sensing and biofilms. Trends Microbiol. *13*, 27–33.

Pasteur, L., and Joubert, J. (1877). In Charbon et Septicemie., (C R Soc Biol Paris), pp. 101–115.

Pattabiraman, V.R., and Bode, J.W. (2011). Rethinking amide bond synthesis. Nature *480*, 471–479.

Peña, A., and Arechaga, I. (2013). Molecular Motors in Bacterial Secretion. J. Mol. Microbiol. Biotechnol. *23*, 357–369.

Poindexter, J. (1981). The caulobacters: ubiquitous unusual bacteria. Microbiol. Rev. *45*, 123–179.

Pons, A.-M., Delalande, F., Duarte, M., Benoit, S., Lanneluc, I., Sable, S., Van Dorsselaer, A., and Cottenceau, G. (2004). Genetic Analysis and Complete Primary Structure of Microcin L. Antimicrob. Agents Chemother. *48*, 505–513.

Poole, S.J., Diner, E.J., Aoki, S.K., Braaten, B.A., t'Kint de Roodenbeke, C., Low, D.A., and Hayes, C.S. (2011). Identification of Functional Toxin/Immunity Genes Linked to Contact-Dependent Growth Inhibition (CDI) and Rearrangement Hotspot (Rhs) Systems. PLoS Genet. *7*, e1002217.

Rankin, D.J., Rocha, E.P.C., and Brown, S.P. (2011). What traits are carried on mobile genetic elements, and why? Heredity *106*, 1–10.

Rao, D., Webb, J.S., and Kjelleberg, S. (2005). Competitive Interactions in Mixed-Species Biofilms Containing the Marine Bacterium Pseudoalteromonas tunicata. Appl. Environ. Microbiol. *71*, 1729–1736.

Rea, M.C., Ross, R.P., Cotter, P.D., and Hill, C. (2011). Classification of Bacteriocins from Gram-Positive Bacteria. In Prokaryotic Antimicrobial Peptides, D. Drider, and S. Rebuffat, eds. (New York, NY: Springer New York), pp. 29–53.

Rebuffat, S. (2011a). Bacteriocins from Gram-Negative Bacteria: A Classification? In Prokaryotic Antimicrobial Peptides, D. Drider, and S. Rebuffat, eds. (New York, NY: Springer New York), pp. 55–72.

Rebuffat, S. (2011b). Microcins from Enterobacteria: On the Edge Between Gram-Positive Bacteriocins and Colicins. In Prokaryotic Antimicrobial Peptides, D. Drider, and S. Rebuffat, eds. (New York, NY: Springer New York), pp. 333–349.

Rebuffat, S. (2012). Microcins in action: amazing defence strategies of Enterobacteria. Biochem. Soc. Trans. *40*, 1456–1462.

Riley, M.A. (2009). Bacteriocins, Biology, Ecology, and Evolution. In Encyclopedia of Microbiology, (Elsevier), pp. 32–44.

Riley, M.A. (2011). Bacteriocin-Mediated Competitive Interactions of Bacterial Populations and Communities. In Prokaryotic Antimicrobial Peptides, D. Drider, and S. Rebuffat, eds. (New York, NY: Springer New York), pp. 13–26.

Riley, M.A., and Wertz, J.E. (2002). Bacteriocins: Evolution, Ecology, and Application. Annu. Rev. Microbiol. *56*, 117–137.

Rodriguez, E., and Lavina, M. (2003). The Proton Channel Is the Minimal Structure of ATP Synthase Necessary and Sufficient for Microcin H47 Antibiotic Action. Antimicrob. Agents Chemother. *47*, 181–187.

Ruhe, Z.C., Wallace, A.B., Low, D.A., and Hayes, C.S. (2013). Receptor Polymorphism Restricts Contact-Dependent Growth Inhibition to Members of the Same Species. mBio *4*, e00480-13-e00480-13.

Ruhe, Z.C., Nguyen, J.Y., Beck, C.M., Low, D.A., and Hayes, C.S. (2014). The proton-motive force is required for translocation of CDI toxins across the inner membrane of target bacteria: Translocation of CDI toxins. Mol. Microbiol. *94*, 466–481.

Ruhe, Z.C., Townsley, L., Wallace, A.B., King, A., Van der Woude, M.W., Low, D.A., Yildiz, F.H., and Hayes, C.S. (2015). CdiA promotes receptor-independent intercellular adhesion: BamA-independent CdiA-mediated adhesion. Mol. Microbiol. *98*, 175–192.

Ruhe, Z.C., Nguyen, J.Y., Xiong, J., Koskiniemi, S., Beck, C.M., Perkins, B.R., Low, D.A., and Hayes, C.S. (2017). CdiA Effectors Use Modular Receptor-Binding Domains To Recognize Target Bacteria. mBio *8*, e00290-17.

Ruiz-Barba, J.L., Cathcart, D.P., Warner, P.J., and Jiménez-Díaz, R. (1994). Use of Lactobacillus plantarum LPCO10, a Bacteriocin Producer, as a Starter Culture in Spanish-Style Green Olive Fermentations. Appl. Environ. Microbiol. *60*, 2059–2064.

Russell, A.B., Hood, R.D., Bui, N.K., LeRoux, M., Vollmer, W., and Mougous, J.D. (2011). Type VI secretion delivers bacteriolytic effectors to target cells. Nature *475*, 343–347.

Russell, A.B., Peterson, S.B., and Mougous, J.D. (2014). Type VI secretion system effectors: poisons with a purpose. Nat. Rev. Microbiol. *12*, 137–148.

Saavedra, L., and Sesma, F. (2011). Purification Techniques of Bacteriocins from Lactic Acid Bacteria and Other Gram-Positive Bacteria. In Prokaryotic Antimicrobial Peptides, D. Drider, and S. Rebuffat, eds. (New York, NY: Springer New York), pp. 99–113.

Schoenlein, P., and Ely, B. (1983). Plasmids and bacteriocins in Caulobacter species. *153*, 1092–1094.

da Silva Neto, J.F., Lourenço, R.F., and Marques, M.V. (2013). Global transcriptional response of Caulobacter crescentus to iron availability. BMC Genomics *14*, 549.

Sosunov, V., Mischenko, V., Eruslanov, B., Svetoch, E., Shakina, Y., Stern, N., Majorov, K., Sorokoumova, G., Selishcheva, A., and Apt, A. (2007). Antimycobacterial activity of bacteriocins and their complexes with liposomes. J. Antimicrob. Chemother. *59*, 919–925.

Souza, D.P., Oka, G.U., Alvarez-Martinez, C.E., Bisson-Filho, A.W., Dunger, G., Hobeika, L., Cavalcante, N.S., Alegria, M.C., Barbosa, L.R.S., Salinas, R.K., et al. (2015). Bacterial killing via a type IV secretion system. Nat. Commun. *6*, 6453.

van Staden, A.D., Brand, A.M., and Dicks, L.M.T. (2012). Nisin F-loaded brushite bone cement prevented the growth of Staphylococcus aureus in vivo: Inhibition of S. aureus by nisin F in bone cement. J. Appl. Microbiol. *112*, 831–840.

Stubbendieck, R.M., Vargas-Bautista, C., and Straight, P.D. (2016). Bacterial Communities: Interactions to Scale. Front. Microbiol. *7*.

Tait, K., and Sutherland, I.W. (2002). Antagonistic interactions amongst bacteriocin-producing enteric bacteria in dual species biofilms. J. Appl. Microbiol. *93*, 345–352.

Tan, Y., and Riley, M.A. (1996). Rapid invasion by colicinogenic Escherichia coli with novel immunity functions. Microbiology *142*, 2175–2180.

Tsokos, C.G., and Laub, M.T. (2012). Polarity and cell fate asymmetry in Caulobacter crescentus. Curr. Opin. Microbiol. *15*, 744–750.

Vassiliadis, G., Destoumieux-Garzón, D., and Peduzzi, J. (2011). Class II Microcins. In Prokaryotic Antimicrobial Peptides, D. Drider, and S. Rebuffat, eds. (New York, NY: Springer New York), pp. 309–332.

Wallden, K., Rivera-Calzada, A., and Waksman, G. (2010). Microreview: Type IV secretion systems: versatility and diversity in function: Diversity and versatility of the type IV secretion system. Cell. Microbiol. *12*, 1203–1212.

Webb, J.S., Nikolakakis, K.C., Willett, J.L.E., Aoki, S.K., Hayes, C.S., and Low, D.A. (2013). Delivery of CdiA Nuclease Toxins into Target Cells during Contact-Dependent Growth Inhibition. PLoS ONE *8*, e57609.

Weber, T., Blin, K., Duddela, S., Krug, D., Kim, H.U., Bruccoleri, R., Lee, S.Y., Fischbach, M.A., Müller, R., Wohlleben, W., et al. (2015). antiSMASH 3.0—a comprehensive resource for the genome mining of biosynthetic gene clusters. Nucleic Acids Res. *43*, W237–W243.

Wells, T.J., and Henderson, I.R. (2013). Type 1 and 5 secretion systems and associated toxins. In Escherichia Coli, (Elsevier), pp. 499–532.

Whitman, W.B., Coleman, D.C., and Wiebe, W.J. (1998). Prokaryotes: the unseen majority. Proc. Natl. Acad. Sci. U. S. A. *95*, 6578–6583.

Whitney, J.C., Quentin, D., Sawai, S., LeRoux, M., Harding, B.N., Ledvina, H.E., Tran, B.Q., Robinson, H., Goo, Y.A., Goodlett, D.R., et al. (2015). An Interbacterial NAD(P)+ Glycohydrolase Toxin Requires Elongation Factor Tu for Delivery to Target Cells. Cell *163*, 607–619.

Willett, J.L.E., Gucinski, G.C., Fatherree, J.P., Low, D.A., and Hayes, C.S. (2015). Contact-dependent growth inhibition toxins exploit multiple independent cell-entry pathways. Proc. Natl. Acad. Sci. *112*, 11341–11346.

Woldemeskel, S.A., and Goley, E.D. (2017). Shapeshifting to Survive: Shape Determination and Regulation in Caulobacter crescentus. Trends Microbiol.

Yang, R., Johnson, M.C., and Ray, B. (1992). Novel method to extract large amounts of bacteriocins from lactic acid bacteria. Appl. Environ. Microbiol. *58*, 3355–3359.

Zakharov, S.D., Kotova, E.A., Antonenko, Y.N., and Cramer, W.A. (2004). On the role of lipid in colicin pore formation. Biochim. Biophys. Acta BBA - Biomembr. *1666*, 239–249.

Zechner, E.L., Lang, S., and Schildbach, J.F. (2012). Assembly and mechanisms of bacterial type IV secretion machines. Philos. Trans. R. Soc. B Biol. Sci. *367*, 1073–1087.

Zhao, Z., Eberhart, L.J., Orfe, L.H., Lu, S.-Y., Besser, T.E., and Call, D.R. (2015). Genome-Wide Screening Identifies Six Genes That Are Associated with Susceptibility to Escherichia coli Microcin PDI. Appl. Environ. Microbiol. *81*, 6953–6963.

Chapter 2
Identification of Cdz, a novel type of contact-dependent killing system in *Caulobacter crescentus* mediated by cell surface-associated glycine zipper proteins

This work was published as García-Bayona L, Guo MS, Laub MT. Contact-dependent killing by *Caulobacter crescentus* via cell surface-associated, glycine zipper proteins. *eLife.* 2017 Mar 21;6. pii: e24869. doi: 10.7554/eLife.24869.

ABSTRACT

Most bacteria are in fierce competition with other species for limited nutrients. Some bacteria can kill nearby cells by secreting bacteriocins, a diverse group of proteinaceous antimicrobials. However, bacteriocins are typically freely diffusible, and so of little value to planktonic cells in aqueous environments. Here, we identify an atypical two-protein bacteriocin in the α-proteobacterium *Caulobacter crescentus* that is retained on the surface of producer cells where it mediates cell contact-dependent killing. The bacteriocin-like proteins CdzC and CdzD harbor glycine-zipper motifs, often found in amyloids, and CdzC forms large, insoluble aggregates on the surface of producer cells. These aggregates can drive contact-dependent killing of other organisms, or *Caulobacter* cells not producing the CdzI immunity protein. The Cdz system uses a type I secretion system and is unrelated to previously described contact-dependent inhibition systems. However, Cdz-like systems are found in many bacteria, suggesting that this form of contact-dependent inhibition is common.

INTRODUCTION

To survive within complex microbial communities such as those found in the guts of animals or in soil, bacteria have evolved, and now rely on, a sophisticated array of strategies that allow them to compete for a limited set of resources. This constant battle for space and nutrients often involves the secretion of diffusible antimicrobials, including small-molecule antibiotics and bacteriocins. The secretion of these toxic compounds typically provides a fitness advantage to the producing cell by inhibiting the growth of competing cells and, in some cases, by lysing these competitors to liberate nutrients (Cornforth and Foster, 2013; Hibbing et al., 2010). The production of many antimicrobials is induced by stress signals triggered by crowding or the low availability of specific nutrients (Rebuffat, 2011).

Bacteriocins are ribosomally-synthesized proteinaceous toxins that are also sometimes post-translationally modified (Cotter et al., 2012; James et al., 1992; Nissen-Meyer et al., 2011; Riley and Wertz, 2002). Most small bacteriocins are secreted into the environment through a type I secretion system (De Kwaadsteniet et al., 2006; Rebuffat, 2011). Bacteriocins can be encoded on plasmids or in chromosomal gene clusters that generally contain all of the genes necessary for their synthesis, modification, and secretion, along with an immunity gene that protects the producer cell from self-intoxication. The inhibitory activity of bacteriocins can be broad- or narrow-spectrum, often determined by the nature of their cellular targets or the receptor proteins on target cells that mediate uptake. Diverse cellular targets have been described for bacteriocins. However, many insert into the membranes of target cells, either alone or by associating with integral membrane proteins, producing pores that alter cytosolic membrane permeability, causing the leakage of cellular contents, loss of membrane potential, and eventual cell death (Cotter et al., 2012; Rebuffat, 2011; Vassiliadis et al., 2011).

Producing diffusible, secreted bacteriocins may not be an efficient competitive strategy for many bacteria, particularly in certain growth conditions. For instance, *Caulobacter crescentus* is an α-proteobacterium that thrives in nutrient-poor aquatic conditions (Poindexter, 1981) where a secreted bacteriocin would be quickly washed away or diluted, making it ineffective in killing neighboring cells (Aguirre-von-Wobeser et al., 2015). Additionally, the production of a secreted

toxin, or any "public good", also renders a population of cells sensitive to the proliferation of so-called cheaters that do not pay the energetic cost of producing the toxin, but benefit from its production by others (Riley and Gordon, 1999; Travisano and Velicer, 2004). To circumvent these limitations of secreted toxins, some bacteria have evolved killing systems that require direct contact between a producer and a target cell. This includes the contact-dependent growth inhibition systems found in many Gram-negative pathogens in which a CdiA toxin is anchored to the outer membrane via a type V secretion mechanism, and then delivered directly to a target cell (Aoki et al., 2005, 2010). Similarly, type VI and VII secretion systems are often used to deliver toxins to direct neighbors (Cao et al., 2016; Hood et al., 2010; Russell et al., 2014a). Homologs of these proximity- or contact-dependent inhibition systems are absent from the *C. crescentus* genome (Marks et al., 2010). In fact, aside from an ability to adhere together and form biofilms, no social behavior or cell-cell interaction system such as quorum-sensing has been previously described for *Caulobacter*.

Here, we describe a novel, atypical bacteriocin system in *C. crescentus,* now called the contact-dependent inhibition by glycine zipper proteins (Cdz) system, that enables producing cells to kill other cells in a contact-dependent manner. The Cdz system bears some genetic similarity to the small unmodified two-peptide bacteriocins (class IIb) from Gram-positive bacteria. However, in surprising contrast, the *C. crescentus* Cdz system yields no inhibitory activity in culture supernatant and the two small proteins CdzC and CdzD are only found at very low concentrations in the supernatant. Instead, the CdzC/D proteins remain almost exclusively cell-associated, with the CdzC protein forming large heat- and SDS-stable aggregates via a glycine-zipper repeat structure often seen in amyloid proteins. Together, the surface-associated proteins CdzC and CdzD enable producer cells to kill neighboring cells through direct contact. The Cdz system is massively induced upon entry to stationary phase and drives a nearly complete killing of any neighboring cells lacking the CdzI immunity protein. A computational search identified homologous, but as yet uncharacterized, systems in a range of species, including several clinically relevant pathogens. Our results suggest that contact-dependent inhibition may be more widespread than previously appreciated and has arisen through the modification of systems traditionally thought to produce diffusible toxins.

RESULTS

A *C. crescentus* bacteriocin gene cluster is induced in stationary phase

We hypothesized that, if they exist, *Caulobacter* genes involved in intercellular competition would be upregulated as cells enter stationary phase when cell density increases and nutrients become scarce. Thus, we used RNA-Seq to compare global patterns of gene expression in a culture of wild-type *Caulobacter crescentus* (CB15N) grown to mid-exponential and early stationary phase (Fig. 2.1A). One cluster of genes (CC0681-CC0684 in CB15; CCNA_03931-CCNA_00720 in CB15N) was very highly upregulated, with two of the genes, CCNA_03932 and CCNA_03933, increasing nearly 50-fold in stationary phase relative to exponential phase, reaching levels higher than all other genes in stationary phase.

Careful inspection of this region of the genome revealed five open reading frames in two divergently transcribed operons (Fig. 2.1B). We named these genes *cdzABCD* and *cdzI* for contact-dependent inhibition by glycine zipper proteins based on results below. The genes *cdzA* and *cdzB* are homologous to canonical type I secretion systems. The genes *cdzC* and *cdzD* are predicted to encode small (86 and 84 amino acids, respectively) proteins with weak similarity to bacteriocins (using the Gene Function Identification Tool in KEGG) and N-terminal regions resembling the signal peptides of secreted RTX proteins (Kanonenberg et al., 2013). These analyses suggested that *cdzC* and *cdzD* may represent a previously uncharacterized two-protein bacteriocin. The *cdzI* gene had no obvious sequence homologs, but was predicted by TM-HMM to harbor three transmembrane domains, and could represent an immunity gene that prevents self-intoxication by the bacteriocins (see below).

To confirm induction of the *cdz* genes upon entry to stationary phase, we generated a reporter construct in which the predicted promoter region of cdzC was fused to YFP. Cells were grown in a rich medium from early exponential phase (OD_{600} ~ 0.05) into stationary phase (OD_{600} ~ 1.2) (Fig. 2.2). YFP levels increased dramatically as cells exited exponential phase, exhibiting ~10-fold induction once the culture reached an OD_{600} of 1.0 and ~30-fold after reaching an OD_{600} of 1.2

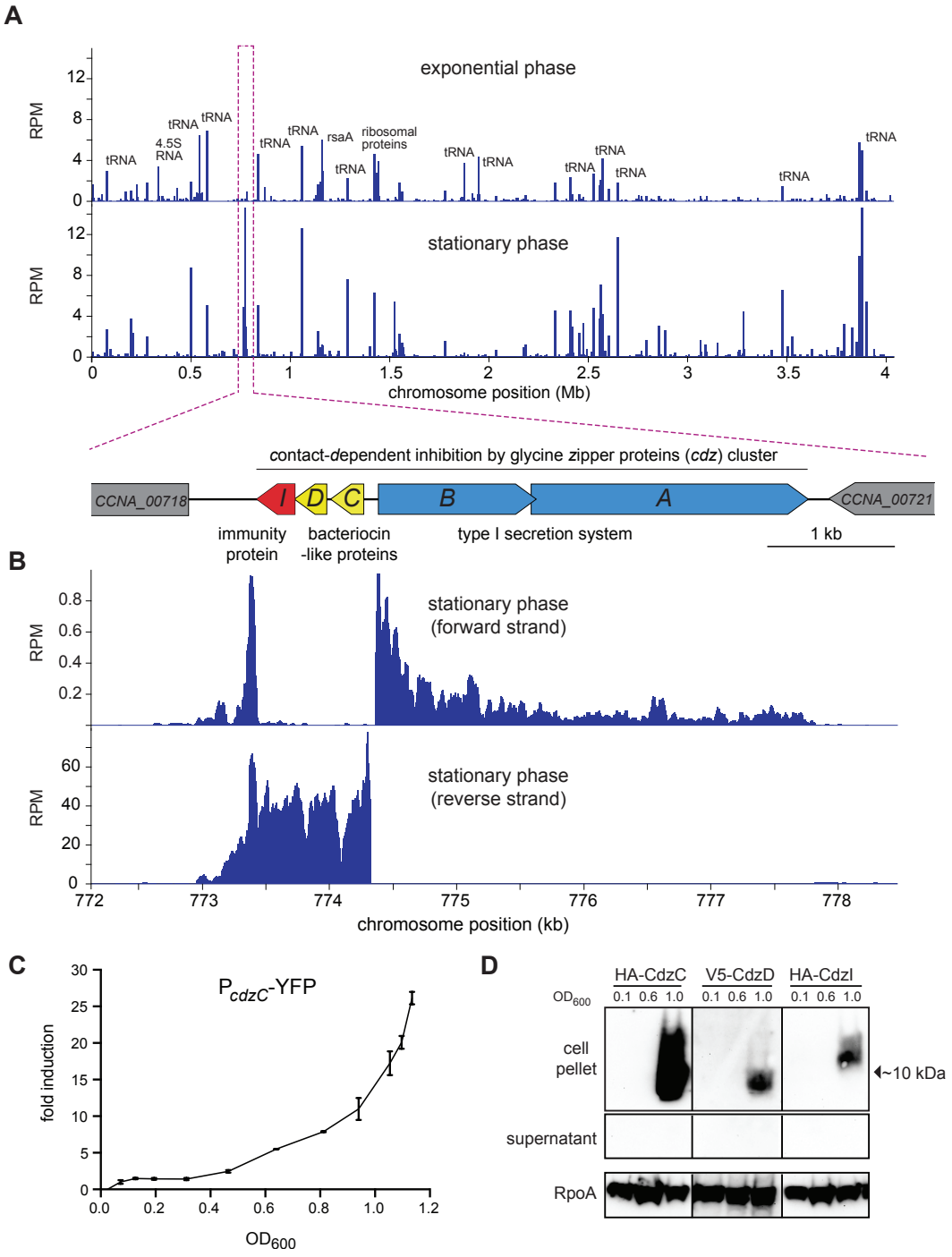

Figure 2.1. The *cdz* gene cluster is very highly expressed in stationary phase. (A) Genome-wide RNA-seq profiles of *C. crescentus* CB15N grown in rich medium to exponential (top) or stationary (bottom) phase. Expression levels (RPM) for both strands combined are plotted as a function of genomic position. A schematic of the *cdz* cluster is shown beneath the RNA-seq profiles. (B) RNA-seq profile of the *cdz* gene cluster in stationary phase. Each strand is shown separately. (C) Activity of a *cdzC* transcriptional reporter (YFP) as a function of culture density (for the corresponding growth curve, see Fig. 2.2). Induction is reported relative to the level when $OD_{600} = 0.025$. Data points are mean of three independent cultures; error bars indicate standard deviation (S.D.). (D) Western blot analysis of epitope-tagged CdzC, CdzD, and CdzI in the cell pellets of supernatant taken from cultures at the OD_{600} values indicated. RpoA is a loading control.

(Fig. 2.1C). Expression of the *cdz* genes may also be regulated by post-transcriptional mechanisms as we noted in our RNA-Seq data that an antisense RNA overlapping the 3' end of the *cdzCDI* operon was expressed during exponential phase, but significantly less so during stationary phase.

To further examine *cdz* induction, we generated strains in which CdzC or CdzD harbored an epitope tag, HA or V5, respectively, immediately following the putative secretion signal; CdzI was tagged with HA at the N-terminus. Western blots of cell extracts indicated that none of these proteins (CdzC, CdzD, or CdzI) were detectable in cultures grown to an OD_{600} of 0.1 or 0.6, but each was easily detected once cells reached an OD_{600} of ~1.0 (Fig. 2.1D), confirming their stationary phase-dependent induction. Surprisingly, the epitope-tagged CdzC and CdzD were detected only in cell pellets, not the cell-free supernatants, suggesting that they are not conventional, secreted bacteriocins and instead remain cell-associated, a possibility explored further below.

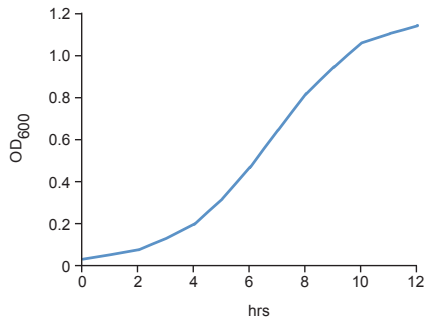

Figure 2.2. Growth curve for cells expressing a P_{cdzC}-YFP reporter.

Cells harboring the *cdz* gene cluster can kill cells lacking it

We hypothesized that CdzC and CdzD form a two-peptide toxin that is secreted via the type I secretion system CdzAB, with CdzI providing immunity against CdzC/D. To test this model and to genetically dissect the *cdz* system, we built an 'indicator' strain in which *cdzABCDI* was deleted. We then mixed this Δ*cdzABCDI* indicator with a 'producer', the wild-type *C. crescentus*, at a ratio of 1:1 and co-cultured the strains from early exponential phase into stationary phase. To quantify

the presence of each strain, we inserted a gentamicin-resistance cassette into the wild-type producer and a tetracycline resistance cassette into the Δ*cdzABCDI* indicator; the colony-forming units of each strain were then assessed at various time points during co-culturing (Fig. 2.3A). The indicator and producer strains maintained a ratio of ~1:1 throughout exponential phase, up to a cell density of ~3 x 10^9 cells/mL (OD_{600} ~ 0.9), at which point the Δ*cdzABCDI* strain began to lose viability, dropping nearly 4 orders of magnitude within ~7 hours. A similar result was obtained for strains in which the antibiotic resistance cassettes were swapped (Fig. 2.4A). As a control, we verified that the Δ*cdzABCDI* indicator strain maintained viability and a 1:1 ratio when co-cultured with another Δ*cdzABCDI* strain harboring a different antibiotic resistance marker (Fig. 2.4B). Similarly, two wild-type producer strains with different antibiotic resistance markers were maintained at a ratio of ~1:1, even in stationary phase (Fig. 2.4C). Finally, we found that a Δ*cdzCDI* indicator strain, grown separately and only to exponential phase, was still killed when mixed 1:1 with a producer strain that had been grown separately to stationary phase (Fig. 2.4D), indicating that the producer gains the ability to kill in stationary phase and susceptible cells need not be in stationary phase.

CdzC, CdzD, and a type I secretion system are required for killing

To further dissect the requirements for Cdz-based killing we generated a series of producer strains and competed each against a Δ*cdzABCDI* indicator, mixing cultures at a 1:1 ratio upon entry in stationary phase (Fig. 2.3B). The competitive index was then calculated as the ratio of indicator to producer at the final time point relative to the same ratio at the initial time point. Producer strains lacking *cdzC*, *cdzD*, *cdzCD*, or *cdzCDI* each failed to kill the indicator (Fig. 2.3C), with competitive indices of ~1 for the indicator in each case, as also seen for a producer lacking the entire *cdz* cluster. For the Δ*cdzC* and Δ*cdzD* producers, full killing activity was restored when a copy of *cdzC* or *cdzD*, respectively, was provided on a plasmid (Fig. 2.4E). Similarly, only a construct harboring both *cdzC* and *cdzD* complemented a Δ*cdzCD* strain (Fig. 2.3D). Together, these results indicate that both bacteriocin-like proteins, CdzC and CdzD, are required for killing.

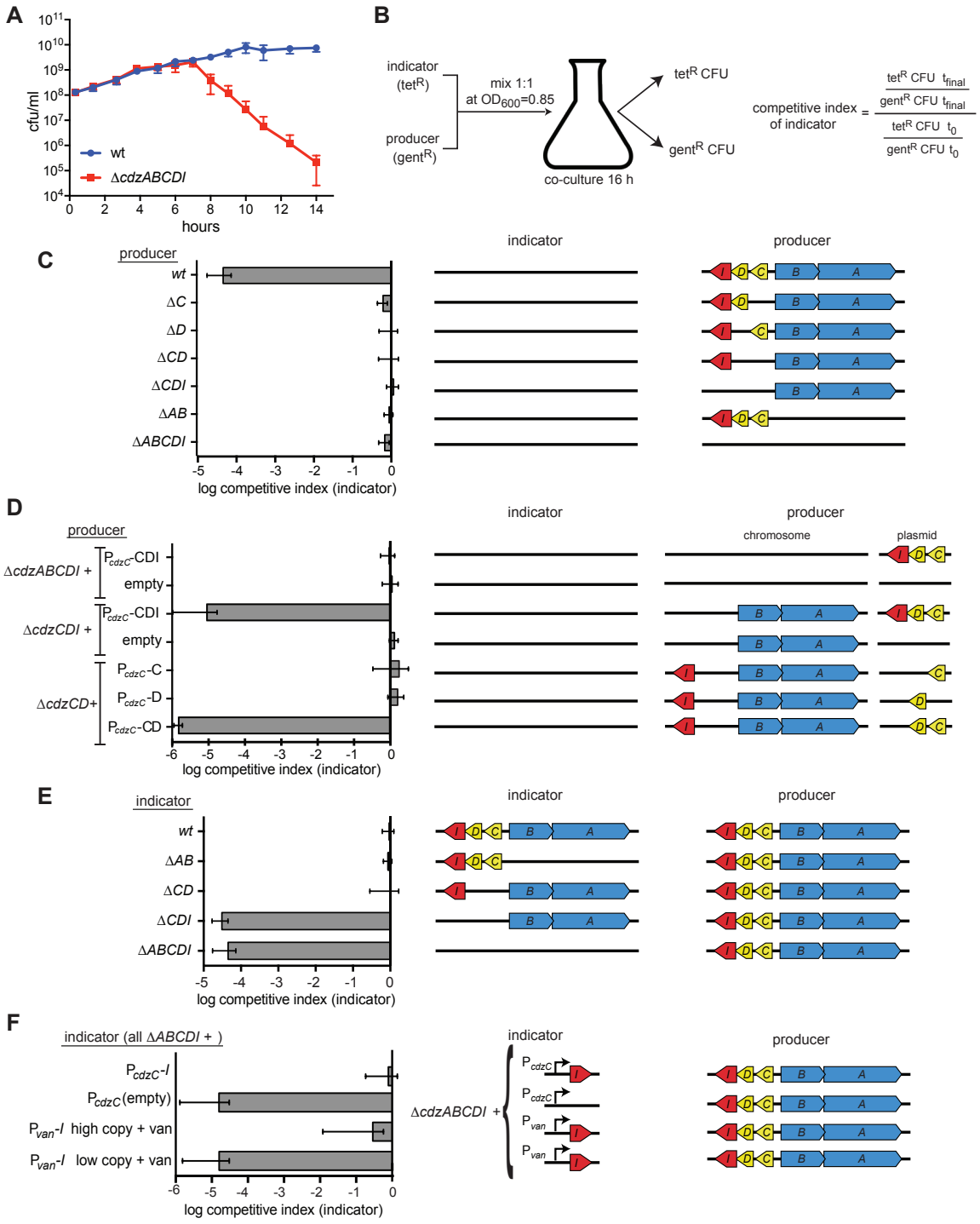

Figure 2.3. The *cdz* gene cluster encodes a two-peptide bacteriocin, secreted via a type I secretion system, and a small transmembrane immunity protein. (A) Co-culture competition of wild-type *C. crescentus* and *ΔcdzABCDI* in rich medium. Strains were mixed 1:1 in exponential phase and co-cultured, with CFUs of each strain measured up to 14 hours. (B) Experimental set-up for co-culture competitions in stationary phase and overview of competitive index calculation. (C-F) Competitions between the indicator and producer strains with the genotypes indicated schematically. Graphs show the competitive index of the indicator strain in each experiment. In each panel, data points represent the mean of at least three independent experiments; error bars indicate S.D. Induction of the P_{van} promoter by vanillate is indicated by '+ van'.

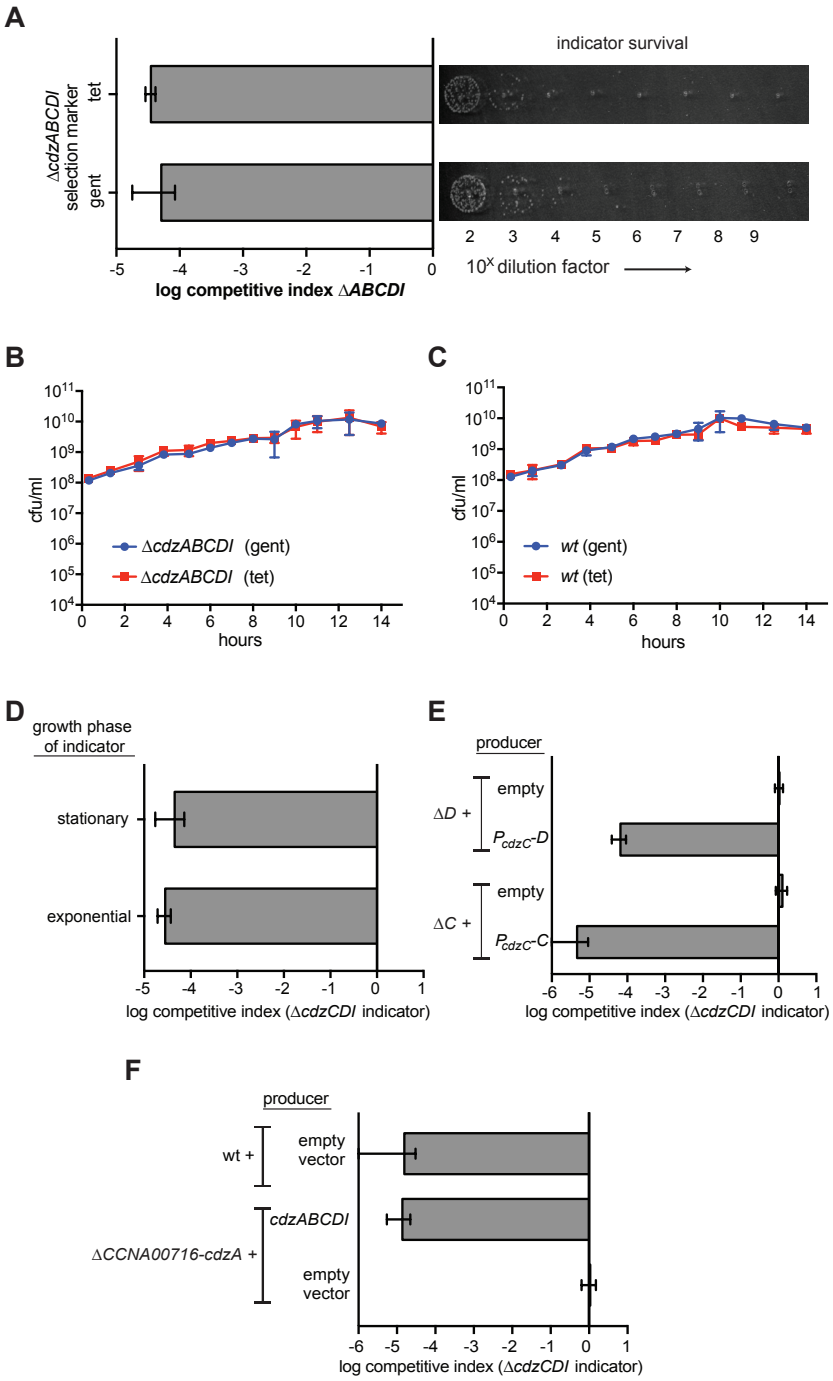

Figure 2.4. Control experiments for the genetic dissection of the Cdz system. (A) Co-culture competition of a wild-type producer and Δ*cdzABCDI* indicator showing that the antibiotic selection marker does not affect the outcome of the competition. (B) Co-culture competition of two *ΔcdzABCDI* strains with different antibiotic markers during growth in rich medium. (C) Co-culture competition of two wild-type strains with different antibiotic markers during growth in rich medium. (D) Competition of wild-type producer cells grown to stationary phase, mixed 1:1 with a *ΔcdzCDI* indicator strain grown to either exponential or stationary phase prior to mixing. (E) Complementation of *ΔcdzC* and *ΔcdzD* strains with the corresponding gene in a low copy number plasmid. The producer strains indicated were co-cultured with a *ΔcdzCDI* indicator. (F) Killing activity of a strain harboring a deletion spanning CCNA_0716 to *cdzA* was complemented with a low copy number plasmid containing only *cdzABCDI*. In each panel, data points represent the mean of at least three independent experiments; error bars indicate S.D.

The putative secretion system formed by CdzA and CdzB was also required for a producer strain to kill a Δ*cdzABCDI* indicator (Fig. 2.3C-D). Canonical type I secretion systems comprise an ATP-binding cassette that resides in the inner membrane (CdzA), an adaptor protein in the periplasm (CdzB), and a TolC-like outer membrane protein (Kanonenberg et al., 2013). As a homolog of the latter is absent from the *cdz* cluster, we suspect killing also requires one of the two TolC homologs in the *C. crescentus* genome that likely associate with many different type I secretion systems.

Bacteriocin gene clusters often contain genes involved in post-translational modification of the toxic protein precursors (James et al., 1992; Nissen-Meyer et al., 2011). To more precisely define the bounds of the *cdz* genomic cluster, we made larger deletions, spanning upstream genes of unknown function, including a predicted membrane-associated CaaX motif protease, often present in bacteriocin clusters. However, the killing activity of strains carrying these larger deletions could be fully complemented by introducing only *cdzABCDI* on a plasmid (Fig. 2.4F) indicating that (i) the neighboring genes are not part of the *cdz* system and (ii) CdzC and CdzD are likely not post-translationally modified, although we cannot fully rule out the possibility of modification by genes encoded elsewhere in the *Caulobacter* genome.

Immunity to *cdz* is conferred by the small transmembrane protein CdzI

To identify the putative immunity gene, which would protect a producer strain from self-intoxication, we made several indicator strains with deletions spanning different regions of *cdz* and tested each for inhibition by a wild-type producer (Fig. 2.3E). Our results indicated that *cdzI* was necessary for immunity, because any deletion including this gene led to killing by the producer, whereas the other *cdz* genes were dispensable for immunity. We could not generate a strain lacking only *cdzI* as this gene is essential for viability, consistent with it providing immunity to CdzC-CdzD. We also tested a Δ*cdzABCDI* strain producing only *cdzI* in *trans* (Fig. 2.3F). Full resistance to a wild-type producer was seen if *cdzI* was driven by its native promoter (the region upstream of *cdzC*), or if *cdzI* was driven by a vanillate-inducible promoter on a high-copy vector with cells grown in the presence of vanillate. Taken together, these results indicate that CdzI is critical for immunity to CdzC-CdzD.

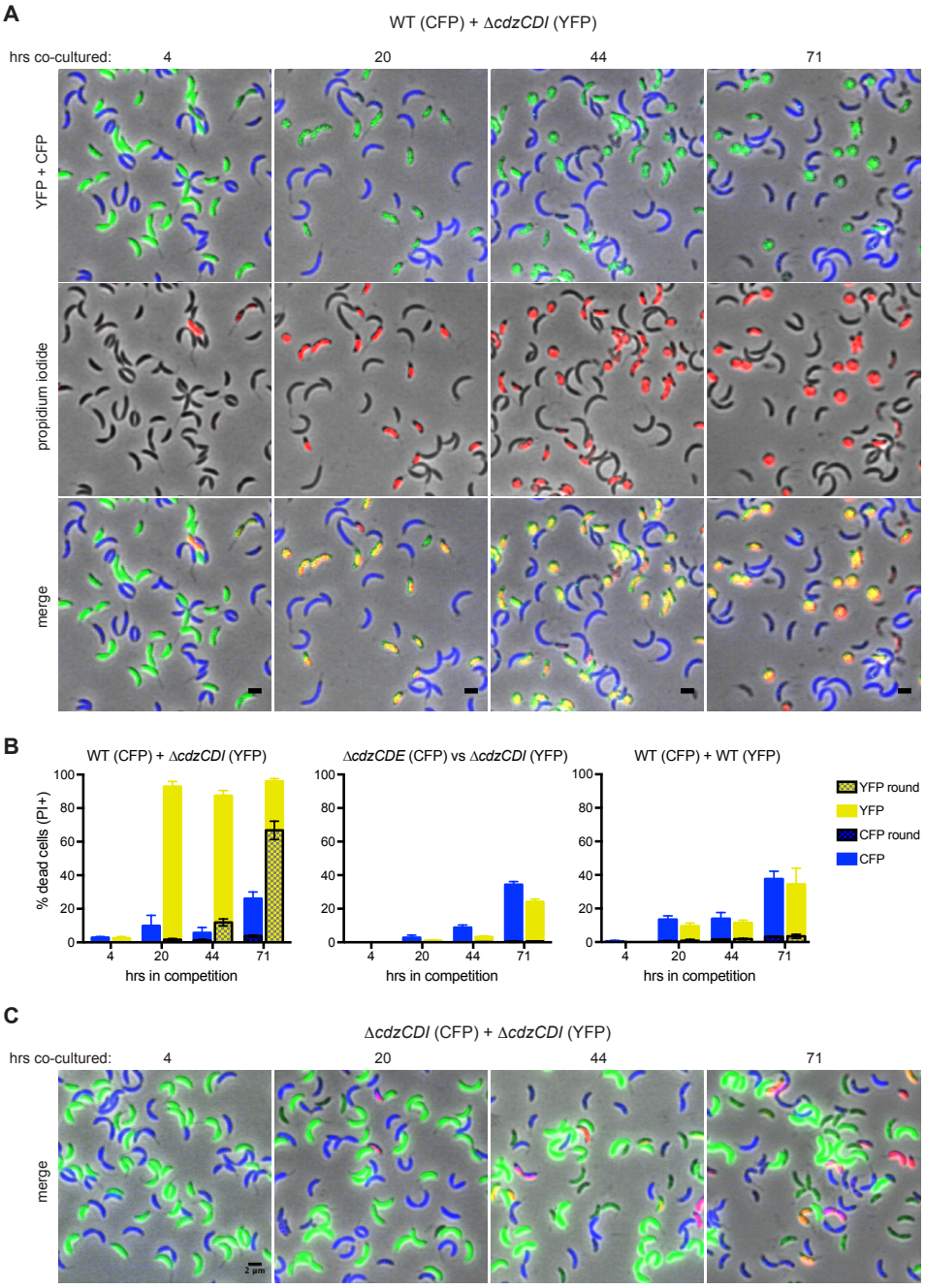

Figure 2.5. CdzC and CdzD kill an indicator strain in co-culture. (A) Microscopy analysis of aliquots taken from co-culture competitions of a wild-type producer synthesizing CFP (false colored blue) and a *ΔcdzCDI* indicator synthesizing YFP (false colored green), and stained with propidium iodide (red) to assess cell permeability. Fields of cells at the time points indicated were imaged by phase and epi-fluorescence microscopy. Phase images were overlaid with the corresponding YFP+CFP images (top), the propidium iodide image (middle), or both (bottom). Cells staining red and green are shown in yellow in the merged image (bottom). (B) Quantification of dead, propidium iodide-stained cells. At least 250 cells in three separate fields of view were counted for each time point of each competition; results were averaged, with error bars indicating S.D. (C) Same as panel A but for a co-culture competition of two indicator strains, synthesizing CFP or YFP.

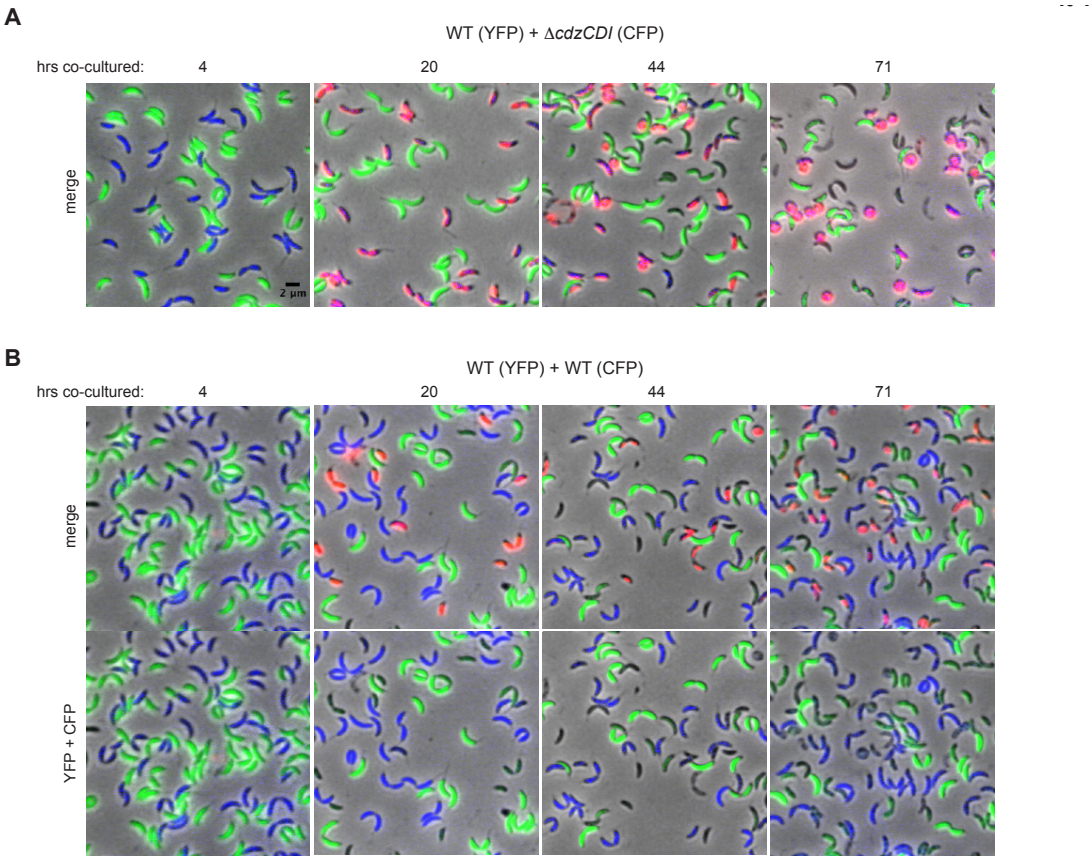

Figure 2.6. Control experiments for the microscopy-based analysis of Cdz-dependent killing. (A) Phase and epifluorescence microscopy of aliquots taken from a co-culture competition of a wild-type producer synthesizing YFP (green) and a *ΔcdzCDI* indicator synthesizing CFP (blue), with the viability stain propidium iodide (red). A merge of phase and all three fluorescence channels is shown at each time point. Cells staining blue and red are shown in magenta. (B) Same as panel A, but for a competition between two wild-type producers synthesizing CFP or YFP.

CdzC and CdzD promote lysis of target cells

The co-culture competition experiments shown in Fig. 2.3 are consistent with the Cdz gene cluster encoding a system that can kill cells lacking the CdzI immunity protein. To more directly assess killing by CdzC/D-producing strains and to gain insight into the mechanism(s) of killing, we used fluorescence microscopy to examine co-cultured cells. We engineered a wild-type producer strain to synthesize CFP and a Δ*cdzCDI* indicator to synthesize YFP. These strains were then mixed at a 1:1 ratio in early stationary phase and co-cultured. At various time points after mixing, we imaged the co-cultured cells in both the YFP and CFP channels. We also stained cells at each time

point with propidium iodide (PI) to label in red cells with compromised membrane integrity that are likely dead.

After 20 hours of co-culturing, >95% of the Δ*cdzCDI* indicator cells were stained by PI and thus were likely dead. In contrast, only ~10% of wild-type producer cells were stained by PI, a frequency comparable to that seen when CFP-labeled WT cells were competed against YFP-labeled WT cells (Fig. 2.5A-B). After 20 hours, nearly all PI-positive indicator cells still had a typical, crescent-shaped morphology and were relatively dark in phase contrast. However, by 44 hours, 30% of PI-positive cells were no longer homogeneously dark in phase contrast, and 13% had become round, a signature of cell lysis. By 71 hours, 70% of the indicator population was comprised of round, PI-positive cells. These results demonstrated that Cdz producers do, in fact, kill cells lacking CdzI, leading to a loss of membrane integrity and, ultimately, cell death. We verified that expression of the fluorophores did not affect the outcome of the competition by swapping CFP and YFP between producer and indicator (Fig. 2.6A). As a control, we also verified that a co-culture of two indicator strains expressing different fluorophores did not lead to the same pervasive cell death (Fig. 2.5B-C).

As noted, we also competed two wild-type producer strains that synthesize different fluorophores. We found that ~10-20% of cells from each population were PI-positive by ~20 hours, with some round cells appearing by day three (Fig. 2.6B). The percentage of PI-positive cells was consistently higher at each time point relative to the experiment competing two Δ*cdzCDI* indicator strains. These results suggest that producer cells harboring CdzI may still be subject to occasional CdzC/D-mediated death, possibly due to variability in the timing or extent of CdzI production in individual cells.

Cdz-based killing requires physical contact between producer and indicator cells

Although similar in some ways to previously described two-peptide bacteriocins (Nissen-Meyer et al., 2011), we suspected that CdzC/D were not secreted, diffusible proteins as both were detected by Western blot analysis in cell pellets, rather than in the culture supernatant (Fig. 2.1D). Additionally, we found that the supernatant from a stationary phase culture of a producer

strain did not kill a Δ*cdzABCDI* indicator strain (Fig. 2. 7A). We also tried concentrating the supernatant from a culture of producer cells using trichloroacetic acid (TCA) or ammonium sulfate precipitation, or by using a centrifugal filter, but did not see any killing (Fig. 2.7A), even though CdzC could now be detected in the concentrated supernatant (Fig. 2.8). These results, along with our initial immunoblots (Fig. 2.1D), strongly suggested that CdzC and CdzD typically remain cell associated and may mediate contact- or proximity-dependent killing.

To directly assess whether CdzC/D-based killing requires cell-to-cell contact, we co-cultured strains using a split-well arrangement in which producer and indicator strains are separated by a porous membrane (Fig. 2.7B). In this setup, any molecules secreted into the growth medium by the producer should be able to target the indicator, unless they form structures larger than the

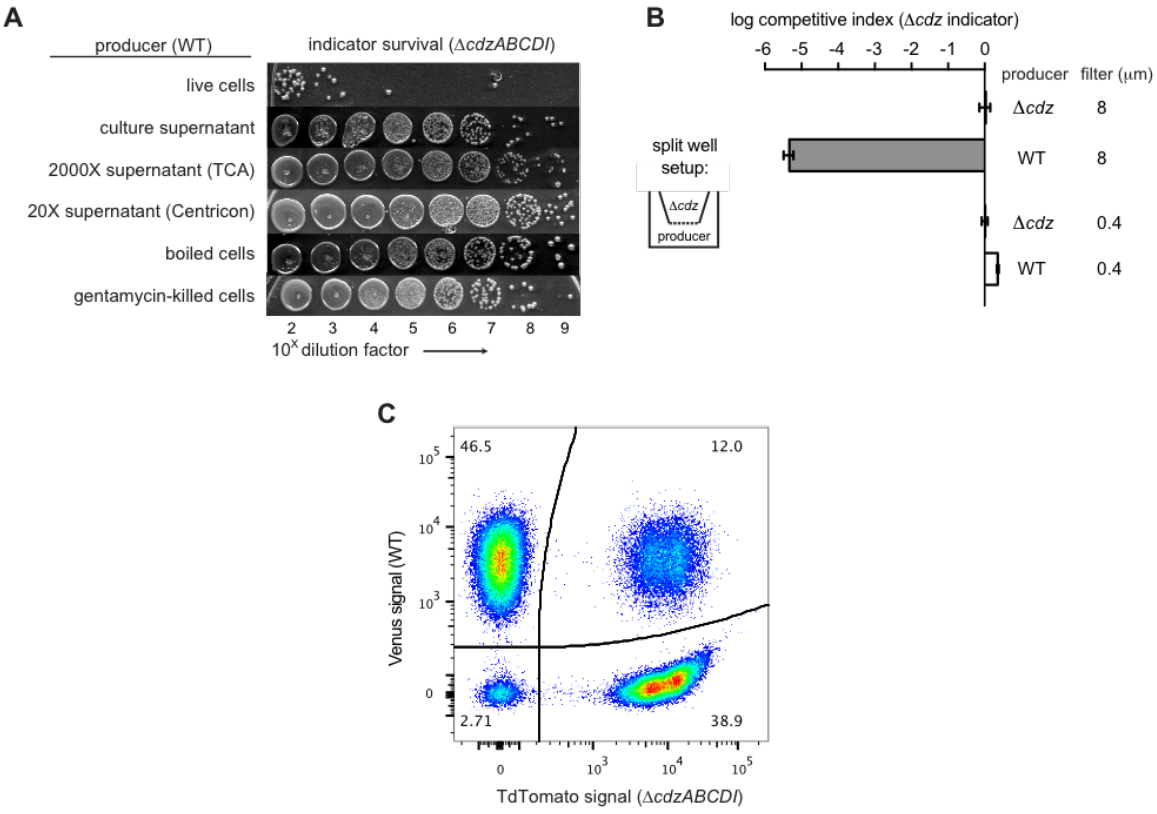

Figure 2.7. Cdz-mediated killing requires cell-cell contact between a producer and an indicator. (A) Survival of a *ΔcdzABCDI* indicator when treated for 16 hours with live producer cells, producer culture supernatant, producer culture supernatant concentrated 2000X by trichloroacetic acid precipitation, producer culture supernatant concentrated 20X by centrifugation, producer cells that were boiled for 5 min, or producer cells treated with gentamicin. (B) Competitive index of *ΔcdzABCDI* indicator grown in co-culture with a wild-type producer or *ΔcdzABCDI* mock-producer using the split-well set-up shown (left). The membrane separating the two compartments had a pore size of 8 or 0.4 μm, as indicated. (C) Flow cytometry analysis of a 1:1 mixture in stationary phase of wt producer cells expressing Venus and *ΔcdzABCDI* indicator cells expressing TdTomato.

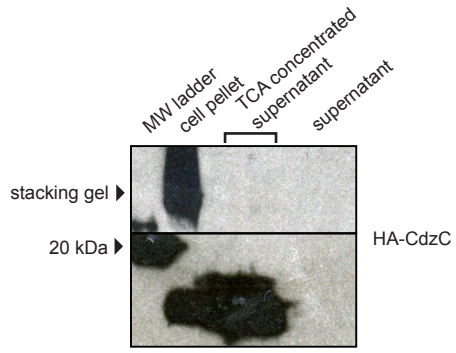

Figure 2.8. CdzC can be detected in a concentrated culture supernatant. Western blot of HA-cdzC in concentrated (TCA-precipitated) culture supernatant

pore size or adhere to the membrane. Strikingly, killing of the indicator occurred when the membrane pores were 8 µm in diameter and able to allow the passage of whole cells, but not when the pores were 0.4 µm, which restricts the exchange of cells.

Our split-well experiments strongly suggested that CdzC/D-based killing requires direct cell contact. On their own, these experiments do not rule out the possibility that the toxins form large aggregates that are released from cells, but that cannot pass through the 0.4 µm filters used. However, neither CdzC nor CdzD was detected in culture supernatant (Fig. 2.1D) and culture supernatant exhibited no killing activity, even if concentrated 2000X (Fig. 2.7A). The preparation of such cell-free supernatants required the centrifugation and pelleting of cells, which could, in principle, also have pelleted large aggregates of toxins that had been released from cells to mediate non-contact-dependent killing. To rule out this possibility, we first killed stationary phase producer cells by boiling for 5 min before adding them, without a centrifugation step, to indicator cells. If large toxin aggregates were present in the supernatant, the indicator should still be killed, but it was not (Fig. 2.7A). Similarly, we pre-treated stationary phase gentamicin-sensitive producer cells with gentamicin for 4 hrs before adding them to gentamicin-resistant indicator cells, again without centrifugation. As with boiled producer cells, no killing was observed. Taken all together, these results support the conclusion that CdzC/D mediate contact-dependent killing.

In some contact-dependent systems, like that mediated by type VI secretion systems, killing occurs primarily on solid substrates, not in culture (Russell et al., 2014b). However, the Cdz

system appeared to drive cell contact-dependent killing even in culture, implying that cells must adhere together at some frequency. The *C. crescentus* strains we used were derived from the strain CB15N, which lacks the adhesive holdfast present in some *Caulobacter* isolates. To test whether the strains we used form stable cell-cell associations, we used a flow cytometry-based

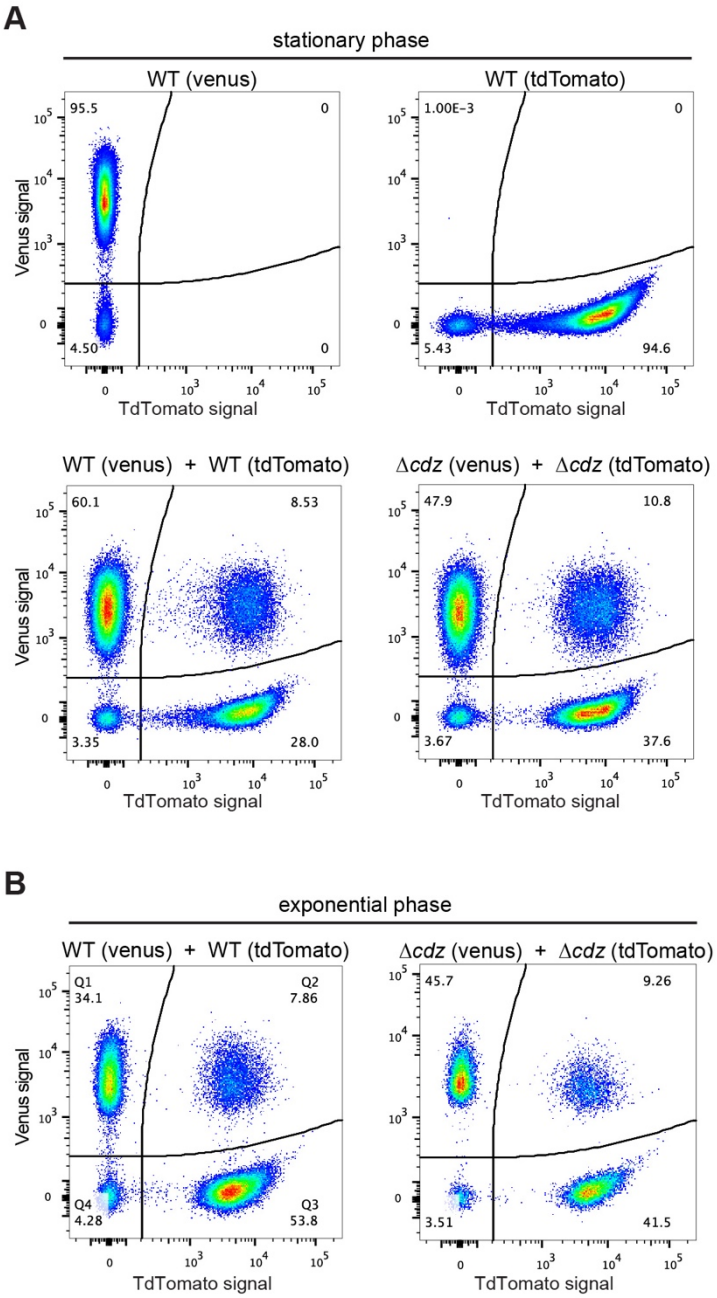

Figure 2.9. Controls for flow cytometry analysis of cell-cell attachment. (A) Flow cytometry analysis of stationary phase cells expressing Venus or TdTomato, as indicated, either in pure culture or mixed at 1:1 ratio and incubated for 2 hours. (B) Same as panel B but for exponential phase cultures.

assay previously developed for studying contact-dependent inhibition in *E. coli* (Ruhe et al., 2015). In brief, stationary phase producer cells producing TdTomato and indicator cells producing Venus were mixed at a 1:1 ratio, and fluorescence measured by flow cytometry (Fig. 2.7C). There were three types of events detected by the flow cytometer: TdTomato$^+$/Venus$^-$, TdTomato$^-$/Venus$^+$, and TdTomato$^+$/Venus$^+$. The latter, detected at a frequency of ~12% in the mixed population, likely represent cases in which at least one producer and at least one indicator cell are closely associated during passage through the flow cytometer. The frequency of such associated cells was not significantly different when examining mixtures of (i) two producers, (ii) an indicator and a producer, or (iii) two indicators (Fig. 2.9A) suggesting that cell-cell contact is not mediated by the *cdz* genes themselves but rather by other genes that the *cdz* system effectively uses to promote killing. Cell-cell attachments were also seen at comparable frequencies in exponential phase cultures (Fig. 2.9B), indicating that whatever mediates attachment is not specifically expressed in stationary phase and so likely does not contribute to stationary phase-specific killing by the Cdz system (Fig. 2.3A).

CdzC and CdzD localize to the outer membrane of producer cells

Our results suggested that CdzC and CdzD are cell associated and mediate contact-dependent killing. To further characterize the subcellular localization of CdzC and CdzD, we performed cell fractionation experiments on cells producing epitope-tagged variants of CdzC, CdzD, and CdzI (Fig. 2.1D, 2.10A-D). Epitope-tagged CdzC and CdzD were fully functional with respect to killing (Fig. 2.11A), while epitope-tagged CdzI was partially functional as an immunity gene (Fig. 2.11B). As controls for the fractionation procedure, we verified by immunoblotting that RpoA, a subunit of RNA polymerase, was found predominantly in the cytoplasmic fraction; the chemoreceptor McpA was found in the total membrane and inner membrane fractions; and $RsaF_a$, a protein involved in S-layer production, was found primarily in the total membrane and outer membrane fractions.

For HA-CdzC, there were two bands in the total membrane fraction (Fig. 2.10A, 2.11C). One was estimated to be ~10 kDa, and likely corresponds to the unprocessed form of CdzC that includes the secretion signal peptide, while the other band likely represents the cleaved, processed form.

Consistent with this interpretation, the full-length form was also seen in the inner membrane fraction, but not the outer membrane fraction, whereas the smaller form had the opposite pattern, appearing predominantly in the outer membrane fraction. Additionally, we noticed that a substantial amount of CdzC was also present in the stacking gel of the total and outer membrane fractions, suggesting that it forms larger aggregates that cannot enter the running

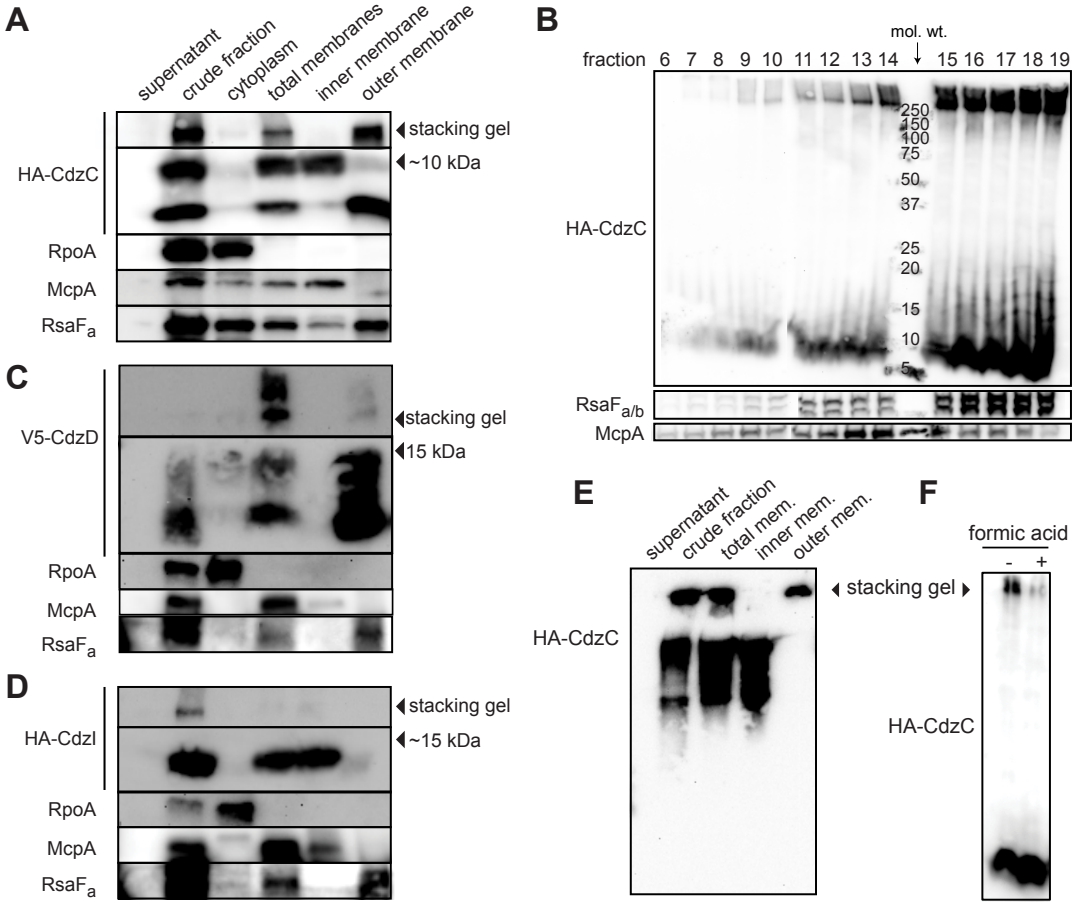

Figure 2.10. CdzC and CdzD localize to the outer membranes of cells, while CdzI is an inner membrane protein. (A) Western blots of the indicated cell fractions from a culture of cells producing HA-tagged CdzC and grown to stationary phase. RpoA, McpA, and RsaF$_a$ serve as controls for cytoplasmic, inner membrane, and outer membrane fractions, respectively. For HA-CdzC, the stacking gel and relevant portion of the running gel are shown. The approximate size of CdzC bands were estimated from a molecular weight ladder run in a non-adjacent lane on the same gel, and confirmed on 16.5% Tris-tricine gels (Fig. 2.11C). (B) Western blot of the indicated fractions from a sucrose gradient (25-60% w/v) based separation of the membrane fractions from a stationary phase culture expressing HA-tagged CdzC. An approximate molecular weight ladder is shown. RsaF$_{a/b}$ and McpA serve as controls for the outer and inner membranes, respectively. (C-D) Same as panel A but for a strain producing (C) V5-CdzD or (D) HA-CdzI. (E) Western blot for HA-CdzC in Triton X-100 based cell fractionation as in panel A, but using native gels instead of SDS-PAGE. (F) Same as panel B, but with outer membrane fractions pooled and either treated or not with formic acid.

gel. The presence of these aggregates did not depend on CdzD as they were still present in a *ΔcdzD* strain (Fig. 2.11D). They were, however, dependent on the CdzAB secretion system. In a *ΔcdzAB* strain, CdzC was found in the cytosolic, total membrane, and inner membrane fractions but not the outer membrane, and no high molecular weight aggregates were seen in the total membrane fraction (Fig. 2.11D). Additionally, in the *ΔcdzAB* strain, only the full-length form was detected.

We confirmed our results for HA-CdzC using a second fractionation method in which cell extracts were run through a sucrose gradient (Fig. 2.10B). Immunoblots of CdzC, along with control blots for McpA and $RsaF_a$, confirmed that CdzC is found in the cell membranes, with the strongest signal seen for fractions corresponding to the outer membrane. Again, strong signal for CdzC was also seen in the stacking gel indicating that CdzC forms large aggregates. Density-based fractionation methods can be misleading as insoluble cytosolic aggregates such as inclusion bodies will migrate with the heaviest fractions, often overlapping with the outer membrane fractions. We ruled out this possibility for CdzC by performing another fractionation experiment with a different range of sucrose concentrations such that outer membrane proteins would separate from the heaviest fractions (Fig. 2.11E). In this experiment, CdzC was still seen in fractions corresponding to the outer membrane, as judged by the location of the control protein RsaF.

Using non-denaturing conditions and native gels, we found that nearly all of the CdzC in outer membranes remained in the stacking gel (Fig. 2.10E), suggesting that CdzC mainly forms large aggregates. These high molecular weight (>220 kDa) aggregates of CdzC were also present in denaturing gels and accounted for much of the CdzC (Fig. 2.10A-B), even though those samples had been resuspended in 2% SDS and 100 mM ß-mercaptoethanol, and then boiled for 30 min. In fact, we could only solubilize these CdzC aggregates by lyophilization and the harsh addition of 90% formic acid (Fig. 2.10F). Taken together, our fractionation studies indicate that CdzC predominantly forms large, insoluble aggregates in the outer membrane compartment of Cdz-producing cells.

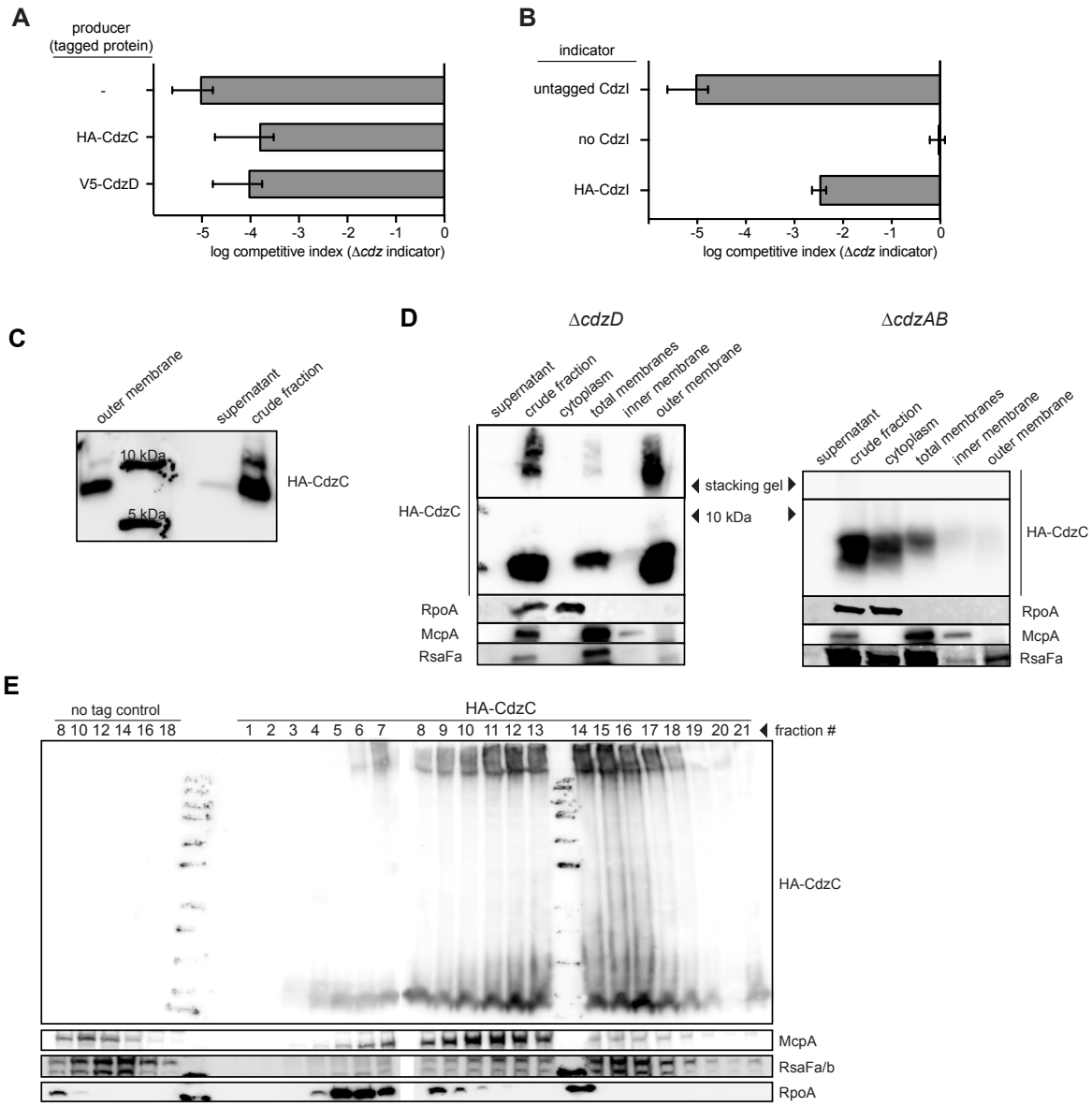

Figure 2.11. Controls for cell-fractionation experiments. (A) Competitions in which the producer strain was *ΔcdzCDI* harboring a low copy number plasmid expressing epitope-tagged CdzC or CdzD, as indicated, with the rest of the operon untagged. The indicator strain in each case was *ΔcdzABCDI*. (B) Competition using wild-type as the producer, and a *ΔcdzCDI* inidicator strain harboring a low copy number plasmid with no CdzD, untagged CdzI, or epitope-tagged CdzI, and with the rest of the operon untagged. In panels A-B, data points represent the mean of at least three independent experiments; error bars indicate S.D. (C) Western blot showing sizes of CdzC bands on a 16.5% tris-trisine gel. (D) Western blot showing Triton X-100 cell fractionation and SDS-PAGE analysis of *ΔcdzD* (left) or *ΔcdzAB* (right) stationary phase producers expressing epitope-tagged CdzC. (E) Sucrose gradient (35-70% w/v) separation of membrane fractions from stationary phase producer cells expressing epitope-tagged CdzC. Inclusion bodies and cytosolic insoluble protein aggregates would be recovered in the heaviest fractions. RpoA (cytosolic), McpA (inner membrane), and $RsaF_a$ (outer membrane) immunoblots are controls for various cell fractions.

We also examined the localization of CdzD and CdzI. Immunoblots for CdzD revealed a similar pattern as for CdzC, with both the unprocessed and mature form present in the total membrane fraction; the mature form was also abundant in the outer membrane fraction (Fig. 2.10C). Like CdzC, there were also high molecular weight aggregates of CdzD in the membrane fractions. However, these aggregates were relatively faint in the outer membrane fraction, suggesting that they had been solubilized during the fractionation procedure. CdzI, the immunity protein, was found in the total membrane fraction, but in contrast to CdzC and CdzD, was primarily in the inner membrane fraction (Fig. 2.10D), similar to the immunity proteins of many pore-forming bacteriocin systems (Cascales et al., 2007; Lagos et al., 1999) and those associated with some membrane-targeting contact-dependent inhibition systems secreted via type V and type VI systems (Ruhe et al., 2013; Russell et al., 2014b).

CdzC forms large aggregates on the surface of producer cells

To assess whether CdzC forms extracellularly-exposed aggregates on the surface of intact cells, we used immunogold labeling and transmission electron microscopy on cells producing epitope-tagged CdzC. Signal from the gold-coupled antibodies was clearly associated with the surface of the cells, usually within a larger matrix of extracellular material that was likely exopolysaccharide (Fig. 2.13A). Importantly, the immunogold signal was absent in exponential phase producer cells (Fig. 2.13B) when CdzC is not produced at high levels and Cdz-producers cannot kill other cells.

To better visualize CdzC on the surface of cells, we also imaged producer strains lacking *manB*, a gene required for exopolysaccharide production (Gandham et al., 2012), and *rsaA*, which encodes the proteinaceous S-layer capsule (Ford et al., 2007). This strain was still competent for killing in a contact-dependent manner (Fig. 2.13C). In this strain, CdzC was more clearly seen within aggregates and fibrils, ranging from 50-250 nm in diameter, that emanated from the cell surface (Fig. 2.10A). Label was also seen directly on the surface of cells embedded in methylcellulose before imaging (Fig. 2.13D). No gold signal was seen on the surface of cells lacking *cdzAB* (Fig. 2.13B), consistent with these genes being required for secretion of CdzC. However, fibrils emanating from the cell were still present in the Δ*cdzAB* strain, suggesting that CdzC associates with these fibrils, but is not their only constituent. Taken together, our cell

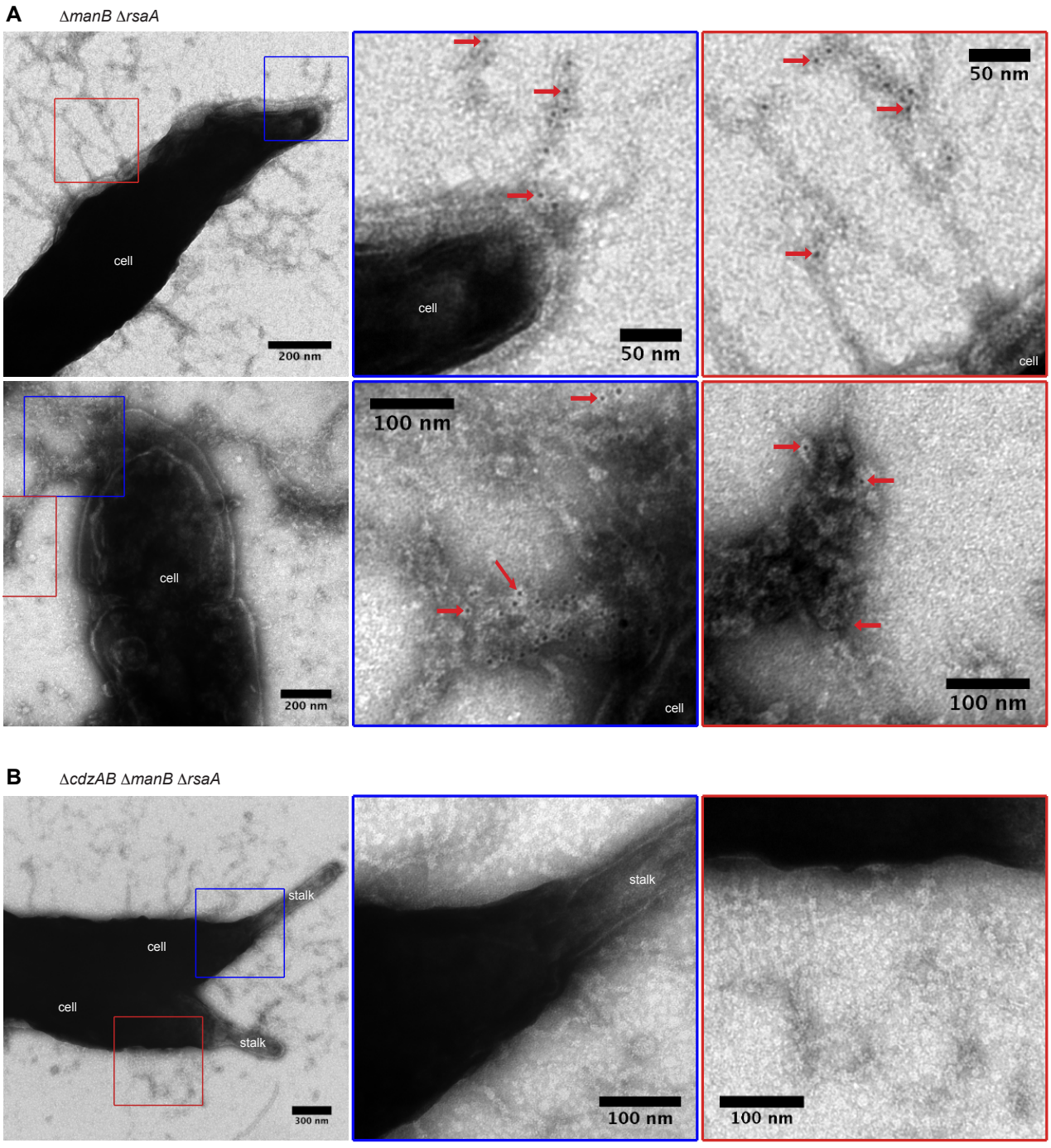

Figure 2.12. CdzC aggregates on the surface of producer cells. Immunogold labelling and transmission electron microscopy of the stationary phase producer cells indicated, each expressing an epitope-tagged CdzC. Middle and right images on each row are zoomed in regions noted on the lower magnification images on the left. Red arrows point at examples of gold particle label. Stationary phase cells of (A) a *ΔmanB ΔrsaA* producer strain and (B) a *ΔcdzAB ΔmanB ΔrsaA* strain.

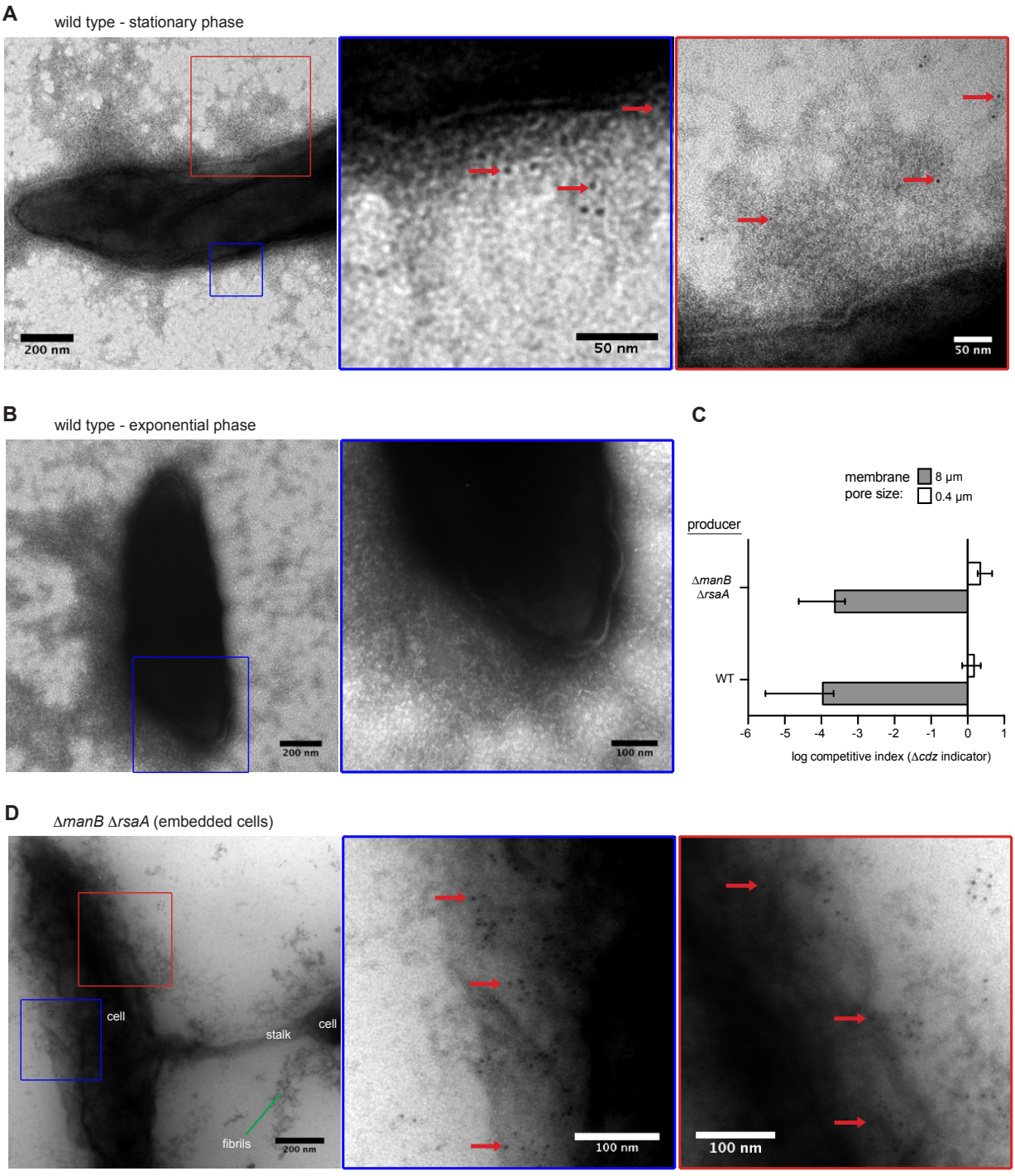

Figure 2.13. Controls for the visualization of Cdz in the surface of producer cells via immunogold labeling and transmission electron microscopy. (A) Immunogold labelling and transmission electron microscopy of stationary phase wild-type producer cells expressing an epitope-tagged CdzC. Middle and right images are zoomed in regions noted on the lower magnification images on the left. Red arrows point at examples of gold particle label. (B) Same as panel A but for exponential phase cells. (C) Split-well competition, like in Fig. 2.7B, between an exopolysaccharide, S-layer deficient producer (*ΔmanB ΔrsaA*) and a *ΔcdzCDI* indicator. (D) Same as panels A-B, but for stationary phase *ΔmanB ΔrsaA* producer cells, embedded in methylcellulose.

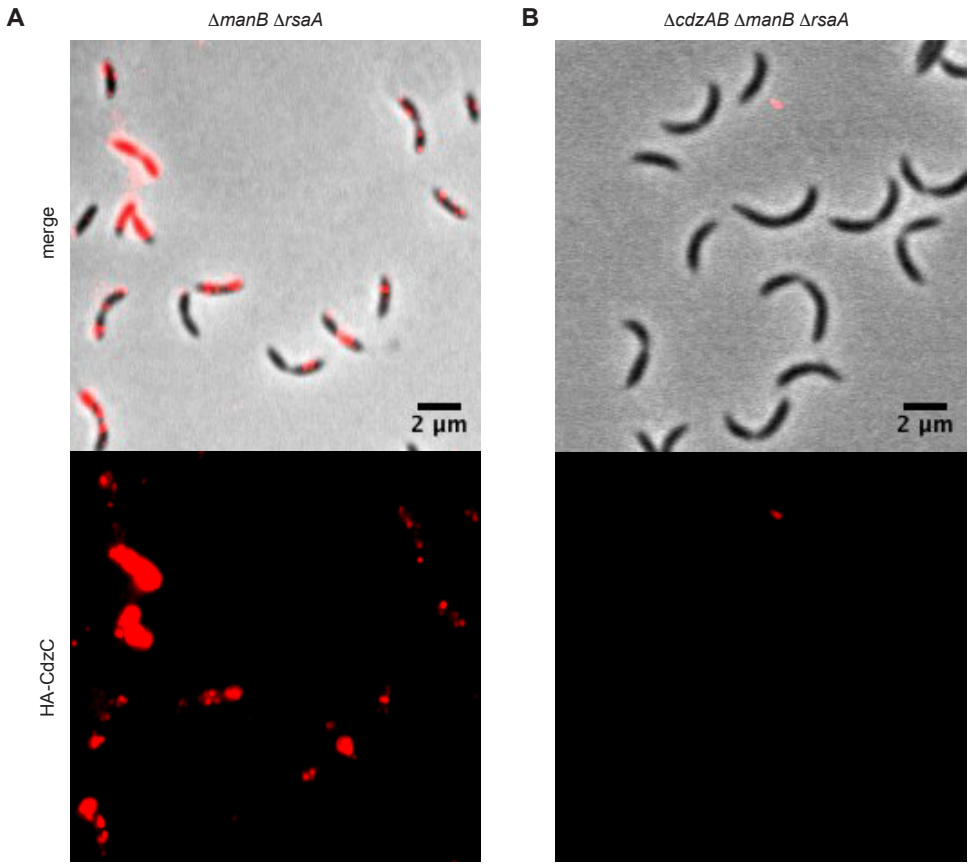

Figure 2.14. CdzC can be detected in the surface of producer cells by immunofluorescence. Immunofluorescence of the producer cells indicated, each expressing an epitope-tagged CdzC. Stationary phase cells of (A) a *ΔmanB ΔrsaA* producer strain and (B) a *ΔcdzAB ΔmanB ΔrsaA* strain.

fractionation experiments and immunogold electron microscopy images support the conclusion that CdzC, and CdzD, localize to the surface of stationary phase cells where they mediate contact-dependent cell killing. We also confirmed localization of CdzC to the cell surface using immunofluorescence microscopy of unpermeabilized cells. Strong signal was seen for a producer strain expressing HA-CdzC, but not for an isogenic Δ*cdzAB* strain lacking the type I secretion system (Fig. 2.14).

To better understand the aggregation propensity of CdzC, we examined the primary sequence of it and CdzD (Fig. 2.15A). One obvious and striking feature was the abundance of glycines and small hydrophobic residues (A, V, I), which together constitute 75% of all residues in the predicted mature form of each protein. A span of 24 and 25 amino acids in CdzC and CdzD, respectively, was predicted to have high aggregation propensity (see Methods). These regions of CdzC and

CdzD harbor extended GxxxGxxxG motifs, or “glycine zippers”. GxxxG motifs are found in many class IIb bacteriocins that are thought to be secreted from cells, forming transmembrane helices in target cells (Nissen-Meyer et al., 2011). Glycine zippers are also found in some transmembrane proteins (Kim et al., 2005) and they are also thought to drive the oligomerization of certain prions and amyloid-forming proteins, such as the Aß amyloid peptide in Alzheimer’s disease (Decock et al., 2016; Fonte et al., 2011) and the human prion protein PrP (Kim et al., 2005). In other proteins with glycine zipper motifs, the x in GxxxG can be any residue, with an enrichment for hydrophobic residues (Senes et al., 2000). In the case of CdzC and CdzD they were exclusively small hydrophobic residues. These sequence characteristics are consistent with the aggregation propensity noted for CdzC, and also suggest that CdzC, and perhaps CdzD, insert into, and disrupt the integrity of, the membranes of target cells (Fig. 2.5).

Cdz can drive interspecies killing and Cdz-like systems are widespread in bacteria

To determine if Cdz can inhibit other species, we carried out competitions of *C. crescentus* producers against three members of the *Caulobacteraceae* family: *Caulobacter segnis*, *Brevundimonas subvibrioides* sp. Poindexter, and *Asticcacaulis exentricus* (Abraham et al., 2014). We also tested the ability of *C. crescentus* to inhibit three more distantly related members of the α-proteobacteria and *Escherichia coli* (Fig. 2.16), none of which encode a homolog of the CdzI immunity protein. *C. segnis* was killed by a wild-type *C. crescentus* producer, but not by a *Δcdz* strain. The inhibitory effect, however, was ~3 orders of magnitude weaker than that observed with a *ΔcdzABCDI C. crescentus* indicator competed against the same producer. *B. subvibrioides* was also killed by a wild-type *C. crescentus* producer, but not by a *Δcdz* strain. In contrast, *A. excentricus* was not inhibited by *C. crescentus*, and neither were the α-proteobacteria *Rhodobacter sphaeroides*, *Sinorhizobium meliloti* and A*grobacterium tumefaciens.* Similarly, the γ-proteobacterium *E. coli* was not killed by *C. crescentus*. The Cdz-resistant species that do not encode an obvious CdzI ortholog may avoid killing because they lack a receptor or membrane composition required for the CdzC/D bacteriocin to act, or because they somehow avoid the cell-cell contact required for CdzC/D to kill.

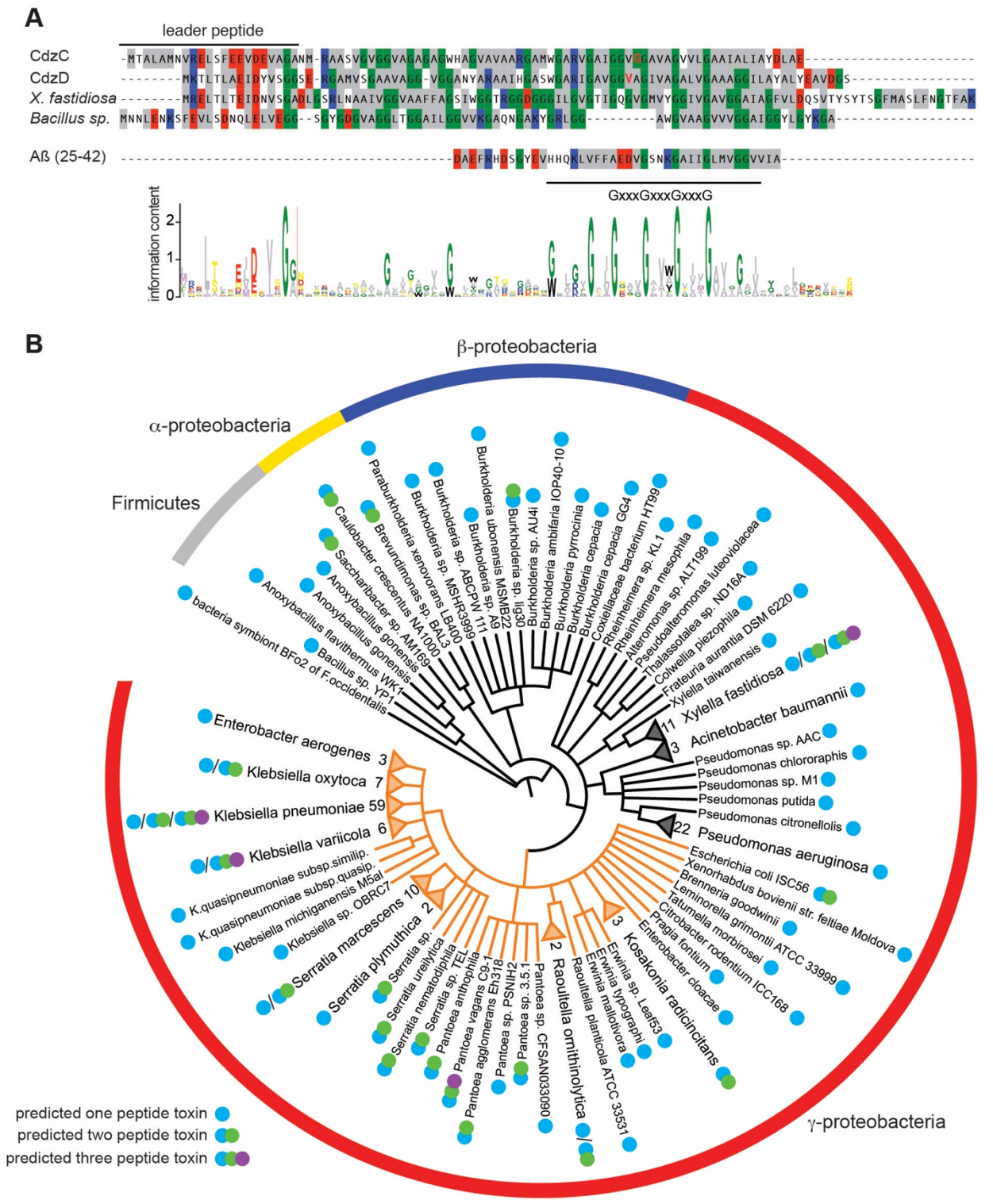

Figure 2.15. Phylogenetic distribution of putative Cdz-like systems in bacteria. (A) Multiple sequence alignment used as the seed in an iterative computational search for Cdz-like systems (see Methods). The presumed leader peptide of each sequence is indicated. Amino acid composition is represented with colors as follows: grey, hydrophobic; glycine, green; positively charged, red; negatively charged, blue. The location of the conserved glycine zipper region is indicated below the alignment. The Aβ peptide, which also contains a glycine zipper is shown for

Figure 2.15 continued on next page

Figure 2.15 continued
comparison. The sequence logo generated from all 239 Cdz-like proteins identified is shown at the bottom. (B) Phylogenetic distribution of Cdz-like systems identified in UniProtKB. Each branch corresponds to a unique sequence. Numbers at the tips of collapsed branches indicate the number of strains for a given species harboring a Cdz-like system. Orange branches correspond to the Enterobacteriaceae. Predicted number of Cdz-like proteins is indicated based on the legend at the bottom left.

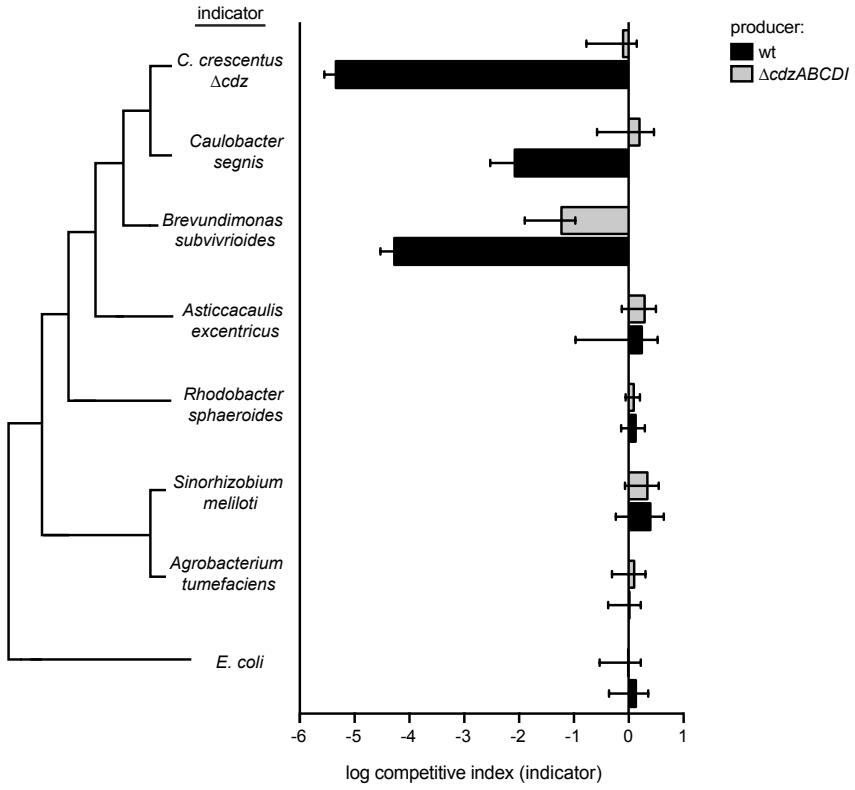

Figure 2.16. Cdz can mediate killing of closely related species. Competitions between a wild-type or *ΔcdzABCDI Caulobacter crescentus* producer and the indicator species shown: *Δcdz Caulobacter crescentus, Caulobacter segnis*, *Brevundimonas subvibrioides*, *Asticcacaulis excentricus, Rhodobacter sphaeroides, Sinorhizobium meliloti, Agrobacterium tumefaciens,* or *E. coli*. In each panel, data points represent the mean of at least three independent experiments; error bars indicate S.D. Tree on the left illustrates phylogenetic relationship between groups, branch lengths are not representative of phylogenetic distance.

We hypothesized the Cdz-like contact-dependent killing system is not unique to *Caulobacter*. However, BLAST searches using CdzC and CdzD as query sequences did not identify any hits, so we screened for potential Cdz-like systems in bacterial genomes using an algorithm based on gene cluster architecture and hidden Markov models (HMM) of the toxin sequences. In brief, we constructed a database of chromosomal regions that included type I secretion systems homologous to CdzAB. We then evaluated all possible small proteins within ~10 kb of the

secretion system for similarity to CdzC and CdzD, using an HMM profile built from a multiple sequence alignment of CdzC, CdzD, and two Cdz-like proteins identified manually in *Bacillus sp*. YP1 and *Xylella fastidiosa* 9a5c (Fig. 2.15). The best three hits for CdzC/D-like proteins were added to the sequence alignment, which was then used as the seed to conduct an iterative search of UniProtKB using *jackhmmer* (Eddy, 2011). Two iterations produced a multiple sequence alignment of 239 unique hits, each exhibiting several of the key features of CdzC and CdzD: (i) 60-151 residues long, (ii) a predicted secretion leader peptide ending in G[G/A/S], (iii) one or two glycine-zipper motifs

flanked, but not interrupted, by a proline or charged residue, and (iv) a short, charged or polar C-terminal region. Further iterations of this analysis began to identify proteins annotated as type IIb bacteriocins, so their results were not taken into consideration.

The phylogenetic distribution of the candidate Cdz-like systems identified (Fig. 2.15, Appendix 1) suggested that this type of contact-dependent inhibition system is widespread in bacteria, particularly in γ-proteobacteria. Notably, we identified several potential Cdz-like systems in clinical isolates of human pathogens such as *Klebsiella pneumoniae*, *Pseudomonas aeruginosa, Serratia marcescens,* and *Burkholderia cepacia.* Some plant pathogens of important agricultural crops also carry Cdz-like clusters, including *Xylella fastidiosa* and *Erwinia sp.*

Unlike in *Caulobacter crescentus,* most of these putative contact-dependent systems were predicted to encode a single Cdz-like toxin protein, with 14% having two adjacent proteins as in *Caulobacter*, and 5% encoding three potential toxins. The identification of immunity proteins was more difficult than the CdzC and CdzD-like proteins, although small, predicted transmembrane proteins were sometimes encoded near the Cdz-like systems identified bioinformatically. Many of the Cdz-like systems identified were likely to have been horizontally acquired as they were often flanked by transposase genes, and most were present in only some isolates of a given species. Interestingly, many of the genomic regions identified, though not the *cdz* cluster in *C. crescentus*, also include genes involved in cell-cell adhesion such as thin aggregative fimbriae (Tafi), which could facilitate contact-dependent delivery of the toxins.

DISCUSSION

A novel contact-dependent killing system

Our results suggest that the Cdz system in *C. crescentus* represents a new type of two-peptide bacteriocin that differs substantially from the previously described, canonical systems involving secreted, diffusible toxins. The small proteins CdzC and CdzD, which are both required for killing (Fig. 2.3), were found almost exclusively in cell pellets, not cell-free supernatants. Our cell fractionation experiments indicated that CdzC and CdzD were located primarily in the outer membrane of cells, with CdzC forming large aggregates visible by electron microscopy on the surface of cells. Consistent with CdzC and CdzD remaining cell-associated, we found that these proteins only promoted the killing of other cells through direct physical contact; in a split-well set-up where indicator and producer cells shared the same growth medium but could not directly interact, no killing was observed (Fig. 2.7B).

There have been other reports of possible, cell-associated bacteriocins (Banerjee et al., 2013; Barbour and Philip, 2014; Burmolle et al., 2006; Daba et al., 1994; Dang and Lovell, 2016; Tahara and Kanatani, 1997; Yang et al., 1992), but these prior cases are unlikely to represent contact-dependent killing systems. In most of these cases, significant killing activity was also found in cell-free supernatants and the bacteriocins were typically easily detected in supernatants, suggesting they are primarily secreted into the environment and not exclusively cell-associated as with CdzC and CdzD. Additionally, to the best of our knowledge, there has not been a direct demonstration that these previously described bacteriocins localize to the outer membranes of producing cells, or a test of whether their activity requires, or is enhanced by, cell-cell contact.

The Cdz system is very strongly upregulated upon entry to stationary phase and appears to be active only during this stage of growth as an indicator strain could be maintained at a 1:1 ratio with a producer strain throughout exponential phase, but was rapidly killed in stationary phase (Fig. 2.3A). These observations suggest that *Caulobacter* cells may produce and use the Cdz system to kill neighboring cells as a means of scavenging for nutrients when they become scarce. The Cdz system was capable of killing other *Caulobacter* cells lacking the CdzI immunity protein

and at least two other members of the *Caulobacteraceae* family, but not more distantly related α-proteobacteria or the γ-proteobacterium *E. coli*. A narrow spectrum of action is common for bacteriocins and may enable targeting of the most similar competitors within a given niche (Riley, 2011). Producing a toxin that remains cell-associated may be critical to an aquatic, oligotrophic bacterium like *Caulobacter* as a fully secreted, diffusible toxin would be quickly flushed away, providing no benefit to a producer cell. We speculate that CdzC/D, and possibly all contact-dependent inhibition systems, represent a means of ensuring benefit to producer cells, preventing the futile release of potentially costly toxins. Contact-dependent systems may also help avoid exploitation by "cheater" cells in a population that do not pay the cost of producing a toxin while benefitting from a secreted, public good (McNally et al., 2017).

Mechanism of secretion and toxin delivery

To the best of our knowledge, the Cdz system is the first contact-dependent inhibition system described involving a type I secretion system, as most rely on type V-based systems also known as two-partner secretion systems, or on type VI secretion systems (Russell et al., 2014b; Willett et al., 2015). The type V-based systems are found in the contact-dependent inhibition system first identified in uropathogenic *E. coli* and subsequently found quite broadly in other Gram-negative bacteria (Anderson et al., 2012; Aoki et al., 2005, 2010). In that system, the CdiA and CdiB proteins use the Sec complex for translocation across the inner membrane. CdiB is then inserted into the outer membrane where it promotes the assembly of CdiA proteins on the cell surface, with subsequent delivery of the C-terminal toxin domain of CdiA to target cells (Willett et al., 2015). CdiA also seems to directly promote the cell-cell adhesion needed for contact-dependent inhibition. In the case of Cdz, cell-cell attachment is not mediated by genes encoded within the *cdz* gene cluster, as both WT and *ΔcdzABCDI* strains showed similar frequencies of cell-cell adhesion by flow cytometry (Fig. 2.7, 2.9). Thus, Cdz toxin delivery likely takes advantage of an adhesion system encoded elsewhere in the genome. Transmission electron microscopy with immunogold labeling indicated that CdzC associates with fibrils on the surface of stationary phase cells. What genes encode these fibrils and whether they mediate attachment remains to be determined. Also of note is that type I systems usually partner with an outer membrane TolC-like

channel to mediate the secretion of proteins into the extracellular milieu (Kanonenberg et al., 2013). How the CdzA/B system manages to retain CdzC/D in the outer membrane following secretion is not yet clear and will require future studies.

Mechanism of killing by CdzC and CdzD

Our fluorescence microscopy studies (Figure 3) suggest that CdzC/D kill cells lacking the immunity protein CdzI by forming pores in the membrane of target cells, a common mechanism of action for bacteriocins (Rebuffat, 2011). When killed, indicator cells became permeable to propidium iodide, a strong indicator that inner membrane integrity had been compromised. These cells eventually lost their characteristic rod-shape, suggesting a complete loss in cell envelope integrity. Consistent with CdzC/D being a membrane pore-forming toxin, the immunity protein CdzI was found primarily in the inner membrane, where it may directly antagonize CdzC/D function. Whether CdzC and CdzD are transferred to a target cell or whether they kill while remaining associated with the producer cell is not yet clear.

CdzC forms large aggregates that appear critical to its toxic activity. These aggregates are stable against SDS and heat, dissolvable only through harsh formic acid treatment. This propensity to aggregate likely stems from the extensive hydrophobicity of CdzC, including an extended glycine zipper region with almost entirely hydrophobic residues within each repeat (Fig. 2.15A). Glycine zippers are often found in amyloid proteins (Chang et al., 2010; Kim et al., 2005) that form insoluble aggregates like those seen for CdzC. The GxxxG motif in CdzC and CdzD have also been seen in bacteriocins thought to kill target cells by inserting into their membranes (Kim et al., 2005). Thus, the extended glycine zipper region of CdzC may mediate both its aggregation on the surface of producer cells and its insertion into the membrane of target cells. In this vein, we note that some annotated type IIb bacteriocins harbor GxxxG motifs (Nissen-Meyer et al., 2011) and may, like CdzC, form large aggregates on the surface of producing cells to drive contact-dependent killing; however, as noted earlier, no such analyses have been reported for bacteriocins, to the best of our knowledge. The Cdz system may represent a special sub-class of type IIb bacteriocins or a new class.

CdzD has a similar set of sequence characteristics as CdzC, including the glycine zipper repeats with almost entirely hydrophobic residues. However, CdzD aggregates appear to be less stable as they were easily solubilized in our cell fractionation studies. However, CdzD and CdzC were both fully required for killing (Fig. 2.3). CdzD could help promote CdzC secretion or it may seed CdzC aggregates, although CdzC still formed very high molecular weight aggregates in a Δ*cdzD* strain (Fig. 2.11D). Alternatively, CdzD may participate only in the 'warhead', or pore-forming element, of a CdzC-driven aggregate, creating a pore alone or in combination with CdzC. Notably, CdzC and CdzD need to be secreted to be active as a strain lacking the secretion system, CdzAB, was fully viable. It is possible that CdzC and/or CdzD must be modified upon secretion. Although the *cdz* gene cluster does not encode any obvious modification enzymes, as is often the case for bacteriocin gene clusters (James et al., 1992; Nissen-Meyer et al., 2011), CdzC and CdzD may at least need to have their leader peptides removed for full activity as toxins or possibly to aggregate, with only aggregates being active.

CdzC was associated with fibrils on the surface of fixed cells, although CdzC is likely not the only, or even primary, component of these fibrils. As already noted, these fibrils may mediate cell adhesion, with the Cdz system effectively using them for toxin delivery. Associations between bacteriocins and fibrils have been reported previously. The pore-forming microcin MccE492 from *Klebsiella pneumoniae* RYC492 is thought to form amyloid-like, but non-toxic fibrils on the surface of cells in stationary phase (Bieler et al., 2005). The toxic form of MccE492 is non-aggregated and diffusible, such that its inhibitory activity is seen only in the supernatants of exponential phase cells. In *Staphylococcus aureus*, phenol soluble modulins (PSM), which share some similarity to eukaryotic anti-microbial peptides, form amyloid-like fibrils required for biofilm stabilization. When purified, some PSM variants have antibacterial activity (Cogen et al., 2010; Schwartz et al., 2012).

An association between small antimicrobial proteins and amyloid formation has also been described in the case of several eukaryotic peptides. En route to forming mature fibers, many amyloid proteins pass through a toxic oligomeric stage that forms pores in membranes (DePas and Chapman, 2012). The most notable examples are the human major prion protein PrP and the

amyloid-beta (Aß) peptide that accumulates in Alzheimer's disease, which has a glycine zipper region similar to those in CdzC and CdzD (Fig. 2.15A). The small hydrophobic residues in the zipper region of the Aß peptide are thought to promote ß-aggregation by creating a "steric-zipper" (Chang et al., 2010). A leucine substitution in one of the glycine residues is sufficient to significantly alter cytotoxicity and oligomer formation by the Aß peptide (Decock et al., 2016; Fonte et al., 2011).

Cdz-like bacteriocins may be widespread in proteobacteria

Collectively, our studies point to the existence of a new family of contact-dependent bacteriocins, secreted via a type I secretion system. This family appears to be relatively widespread, particularly in proteobacteria, with each system containing one to three small (~5-10 kDa) glycine zipper-based toxins. Many of these systems appear to have been horizontally acquired as even closely related species sometimes lack an orthologous copy. Additionally, many of these putative Cdz-like systems are part of, or adjacent to, genomic islands that include genes often associated with recent lateral transfers, such as transposases, CaaX proteases, and fimbrial adhesins.

In some cases, closely related species or strains do have orthologous Cdz-like systems, although the similarity is usually highest for the secretion systems, with substantial variation between the Cdz-like proteins. This type of inter-strain variation has been observed in other types of contact-dependent systems where they may impact self/non-self recognition, thereby playing a critical role in shaping community structure (Alcoforado Diniz and Coulthurst, 2015; Anderson et al., 2012; Russell et al., 2014a, 2014b).

The Cdz-like systems we identified bioinformatically are not restricted to organisms from a specific ecological niche and instead appear to be present in a range of bacteria with diverse lifestyles. Of particular interest are the Cdz-like systems present in clinical isolates of human pathogens. The importance of outcompeting commensal bacteria to establish or maintain an infection has been postulated for several pathogens (Hecht et al., 2016; Russell et al., 2014b) and the Cdz-like systems identified in pathogens (Fig. 2.15) could play such a role. Characterizing

these systems and showing whether they indeed mediate contact-dependent inhibition is an important future goal.

Final Perspective

Caulobacter is a well established model for understanding cell-cycle regulation in bacteria. Considerably less attention has been placed on understanding how it thrives in nutrient-poor aquatic conditions, and no social behaviors or quorum-sensing systems have been described to date. Here, we identified an atypical, but potentially widespread bacteriocin-like system that likely enables *Caulobacter* to compete with other strains and some other species, by killing nearby cells lacking the Cdz system. The Cdz contact-dependent inhibition system presumably also allows *Caulobacter* to avoid the dilemma of producing an expensive common good that could get easily washed away in aquatic environments or that would render a population susceptible to cheaters. Finally, the discovery of the Cdz system, which uses a type I secretion system, expands the repertoire of contact-dependent inhibition mechanisms and suggests that such systems may be even more widespread than previously appreciated.

MATERIALS AND METHODS

Bacterial strains and growth conditions

All oligonucleotides, strains and plasmids used in this study are listed in Supplementary Files 2, 3, and 4, respectively, along with details of how each strain was constructed. *E. coli* strains were grown at 37 °C in LB medium. *A. excentricus* was grown in PYE at 24 ºC. *A. tumefaciens*, *S. meliloti*, and *R. sphaeroides* were grown in LB at 30 ºC for propagation and plating experiments, and in PYE for competitions with *C. crescentus*. *C. crescentus, C. segnis and B. subvibrioides* strains were grown at 30 °C in PYE. Except when specified otherwise, stationary phase cells and culture supernatants were harvested 4 hours after reaching an OD_{600} of 0.85. Media were supplemented, as necessary, with a final concentration of 500 µM vanillate (pH 7.5 stock in water), 1 µM IPTG, or 100 µM cumate (4-isopropylbenzoic acid, stock in 100% ethanol) to induce expression from the P_{van}, P_{lac}, and P_{PQ5} promoters, respectively. Antibiotics were used at the following concentrations (liquid/solid media for *E. coli*; liquid/solid media for *C. crescentus*; in µg/ml): oxytretracycline (12/12; 1/2), kanamycin (30/50; 5/25), gentamycin (15/20; NA/5). For *C. segnis* and *A. tumefaciens*, plates were supplemented with 50 µg/ml kanamycin. For *S. meliloti*, plates were supplemented with 200 µg/ml neomycin.

Competition experiments

For time courses of competitions between different strains (Fig. 2.3A), exponential phase cultures of each strain were diluted to OD_{600} = 0.025 and incubated at 30 ºC for 30 minutes (min) before mixing at a 1:1 ratio by volume. Every hour aliquots were taken and 10-fold serial dilutions (10 µL each) spotted on PYE plates containing antibiotics appropriate for selection of each competitor; colony forming units (CFU) were counted after 2 days. For end-point competitions (Fig. 2.3C-F), each competitor was grown separately to an OD_{600} = 0.85, at which point they were mixed at a 1:1 ratio by volume. For strains harboring P_{van} constructs, vanillate was added 5 hours prior to mixing strains. CFUs for each competitor were quantified as described above at the time of mixing, and then 4 and 16 hours in competition. The competitive index was calculated by taking the ratio of the two strains at the final time point, normalized by the ratio of the two strains at

t=0 (see Fig. 2.3B). To test the effect of growth phase on killing, each competitor strain was grown separately until exponential phase (OD_{600} = 0.2) or stationary phase (OD_{600} = 1). For competitions, 10 mL of the exponential phase culture were pelleted (6000 x g, 2 min) and cells were resuspended in 1 mL of the stationary phase culture.

Testing for inhibitory activity in culture supernatants

To test the effects of cell-free supernatant on an indicator strain, the supernatant from a stationary phase culture of a producer strain was recovered by pelleting cells twice in succession at 13,000 x g for 2 min and filtering through a low protein binding 0.45 µm HT Tuffryn membrane (Pall Life Sciences). This filtered supernatant was used to resuspend stationary phase indicator cells pelleted by centrifugation, and their survival was quantified after incubation at 30 ºC for 4 or 16 hours. As a control, supernatant from an indicator strain was tested, allowing us to quantify background rates of cell death in stationary phase under the experimental conditions used.

To concentrate supernatants from stationary phase cultures of producer strains, we used trichloroacetic acid (TCA) precipitation of total protein in culture supernatants using an adaptation of a published protocol (Koontz, 2014). In brief, 2 L of culture supernatant was centrifuged twice at 13,000 x g for 10 min to remove cells. Samples were then resuspended to a final concentration of 10% (w/v) TCA and incubated at room temperature for 20 min followed by incubation at -20 ºC overnight. Samples were then centrifuged at 15,000 x g for 20 min. Pellets were washed three times with 7 mL of -20 ºC acetone, vortexing to resuspend and incubating 2 hours (first wash) or 30 min (second and third wash) at -20 ºC, and then centrifuging at 15,000 x g and incubating at 4 ºC for 10 min. The final pellet was air-dried and resuspended in PYE, and tested by immunoblotting. To test the activity of the TCA-precipitated proteins in liquid culture, the bulk protein pellet was resuspended in 2 mL of supernatant from a stationary phase indicator culture in PYE and mixed with indicator cells to test their survival.

Bulk precipitation of proteins in culture supernatants using ammonium sulfate was done following a procedure outlined previously (Simpson, 2006). The starting sample was 50 mL of stationary phase culture supernatant, which was filtered using a 0.22 µm Steriflip PES vacuum

filter (EMD Millipore). After ammonium sulfate addition up to 85% saturation at 0 ºC and 1 hour equilibration, samples were pelleted at 17,000 x g for 1 hour. Pellets were then resuspended in 500 µL of 10 mM Tris-HCl pH 7.4 and desalted using an Illustra NAP-5 column (GE Healthcare) following the manufacturer's protocol. Eluate was concentrated to 150 µL using an Amicon Ultra-4 3K centrifugal filter (EMD Millipore) spun at 7,500 x g for 10 min.

To rule out the possibility that large diffusible aggregates present in the supernatant were pelleting with the cells during centrifugation steps, we performed competitions in which the stationary phase producer cells were killed by heating for 5 min at 98 ºC, or 4 hours of treatment with 4 µg/ml gentamicin, prior to mixing without centrifugation to an equal volume of stationary phase indicator carrying a gentamicin resistance cassette. Indicator survival was quantified after incubation for 16 hours at 30ºC.

Split-well competition experiments

Sterile single-well Millicell hanging inserts with a PET membrane (Millipore, 0.4 or 8 µm pore size) were placed into 6-well polystyrene plates to split the well into upper and lower chambers. Only 3 wells per plate were used to prevent cross-contamination between adjacent wells. Each competitor strain was grown separately to OD_{600} = 0.85 and 3 mL added to the top or bottom of the split-well. Plates were covered with a lid and incubated at 30 ºC with shaking (90 rpm to prevent splashing between top and bottom of the well) and the competition evaluated as above. For each pair of strains, independent competitions were done with strains swapped between upper and lower chambers, to rule out effects due to position within the well.

RNA-seq and transcriptional reporters

Exponential phase RNA-seq data (PYE) were taken from GEO sample GSM1326109 (Schrader et al., 2014). For stationary phase, RNA-seq was performed as previously described, with a few modifications (Guo et al., 2014). *Caulobacter* cells were grown in PYE to OD_{600}=1.4 and 2 mL of cells were harvested in the presence of 1 mL 95% ethanol/5% phenol and frozen in liquid nitrogen. The cell pellet was extracted by hot phenol method (Masse et al., 2003) and ribosomal RNA removed with the MICROBExpress kit (Life Technologies). tRNAs were not removed to

ensure recovery of small RNAs. Samples were converted to a sequencing library by lightly fragmenting the RNA with RNA fragmentation reagents (Ambion), isolating and dephosphorylating 25-50 mers with T4 PNK (New England Biolabs), ligating linker-1 (Integrated DNA Technologies) to fragments with T4 RNA ligase II (Epicentre). After reverse transcription was performed with Superscript III (Invitrogen) and RT_oligo, the RNA was hydrolyzed with NaOH, and the ssDNA cDNA was circularized with CircLigase (Epicentre). Final sequencing libraries were PCR amplified with Phusion polymerase and adapter oligos (o231 and o230). Single-end sequencing was performed on Illumina HiSeq2000 (BioMicroCenter MIT) and aligned to NC011916.1 (NA1000) with bowtie (Langmead et al., 2009) allowing for 1 mismatch. Mapped reads were normalized by total number of reads (RPM) and displayed with IGV_2.3.40 software using the "mean" windowing function. Gene expression data are available in the Gene Expression Omnibus: GSE96582.

For time-courses of the *cdzC* transcriptional reporter, an overnight culture was diluted to OD_{600} = 0.025 in PYE. For three replicate cultures, cells were harvested every hour and spotted into 1.5% agarose pads for imaging and fluorescence quantification with MicrobeJ (Ducret et al., 2016). Fold induction was calculated relative to the fluorescence density at OD_{600} = 0.025.

Immunoblotting

Cells were pelleted by centrifugation and resuspended in 2X SDS sample buffer, heated to 95 °C for 30 min and equivalent OD_{600} amounts separated on Mini-PROTEAN TGX 15-well Any kD™ Tris-HCl gels (Bio-Rad) at 150 V using the Laemmli buffer system (Laemmli, 1970). For 16.5% tris-trisine gels (Mini-PROTEAN, Bio-Rad), glycine was replaced in the running buffer with 0.1M tricine. Transfer was done at 100 V for 100 min using a 0.2 µm Immuno-Blot PVDF membrane (Bio-Rad), Towbin buffer and the Mini Trans-Blot Module (Bio-Rad). The following antibodies were used at a 1:5,000 dilution: anti-RpoA (Neoclone #W0003, mouse), anti-McpA ((Iniesta et al., 2006), rabbit), anti-RsaF ((Ford et al., 2007), rabbit), anti-HA (Cell Signaling Technology C29F4, rabbit), anti-V5 (Cell Signaling Technology D3H8Q, rabbit), HRP-conjugated goat anti-rabbit (ThermoFisher), and HRP-conjugated goat anti-mouse (ThermoFisher). Membranes were exposed to SuperSignal West Femto Maximum Sensitivity Substrate (ThermoFisher) and imaged

with a FluorChem M Imager (ProteinSimple).

For non-denaturing gels, the following modifications were done: samples were resuspended in 1X sample buffer (62.5 mM Tris-HCl, pH 6.8, 20% glycerol, 0.005% bromophenol blue) and directly loaded without heating; running buffer was 25 mM Tris, 192 mM glycine. Transfer was done in two steps, using running buffer: 1 hour at room temperature (with ice block) with constant current 400 mA, followed by replacement of running buffer with ice-cold fresh buffer and transfer for 2 more hours at a constant voltage of 100 V at 4ºC.

Fluorescence microscopy of competitions

For time-course imaging of competition experiments, cultures were set up as described above, with the addition of IPTG to the starting overnight culture and to the competition flasks to induce fluorescent reporter expression. At each time point, cells were harvested, diluted in one volume PYE and propidium iodide added to a final concentration of 15 µM. Cells were incubated in the dark for 15 min, spotted onto PYE 1.5% agarose pads and imaged immediately. Phase contrast and fluorescent images were taken on a Zeiss Axiovert 200M microscope with a 63× phase or αFluar 100×/1.45 oil immersion objective, using a digital camera (Orca-II ER; Hamamatsu Photonics) and Metamorph software (Universal Imaging, PA). The following emission/excitation filters were used: YFP, 500/25 and 535/30m; CFP, 436/25 and 480/40; mCherry, 560/40 and 630/75. Image analysis to quantify fluorescent signals for each cell was calculated using MicrobeJ (Ducret et al., 2016). Three independent replicates were analyzed, with a minimum of 250 cells per frame. Fold induction for the P_{cdzC}–YFP transcriptional reporter was calculated relative to fluorescence density at OD_{600} = 0.025. Image overlays were generated using Fiji (Schindelin et al., 2012).

Immunogold labeling and transmission electron microscopy

Cells from a PYE culture were treated with 0.1% paraformaldehyde for 15 min and allowed to sediment for 15 min into formvar/carbon-coated nickel electron microscopy grids freshly treated with 0.2% paraformaldehyde. After 15 min blocking in 1% (w/v) BSA in PBS, grids were moved to anti-HA antibody (1:50 dilution in blocking buffer) for 2 hours, followed by 1 hour in 6 nm

Colloidal Gold secondary antibody (Donkey Anti-Rabbit IgG from Jackson ImmunoResearch, 1:30 dilution in blocking buffer), and then three 1 min washes in PBS. After a brief water wash, negative staining was performed using 1% uranyl acetate. Grids were blot-dried and imaged on a FEI Technai Spirit Transmission Electron Microscope at 80 kV. For methylcellulose embedded samples, after the final water wash, grids were incubated for 10 min in 1% neutral uranyl acetate, briefly washed in water and floated on a 0.2%methylcellulose/3%Polyvinyl alcohol solution containing 1% uranyl acetate. Excess embedding solution was drawn off and grids were air-dried.

Immunofluorescence

Cells were labeled with anti-HA antibodies as described previously (Nomellini et al., 2010), with the following modifications: 1 hour fixation with 2.5% paraformaldehyde at room temperature, 1 hour incubation on ice in primary antibody (2 µL antibody to 200 µL final volume, anti-HA Cell Signaling Technology C29F4), 40 minutes on ice in secondary antibody (1 µL antibody to 100 µL final volume, Life Technologies Alexa Fluor 555 goat anti-rabbit IgG), and two additional wash steps after primary and secondary antibody incubations (done by centrifugation and resuspension in 1.5 ml PYE). After the final wash, cells were resuspended in 100 µL Slowfade Diamond Antifade (Life Technologies) and spotted onto 1.5% agarose pads for imaging.

Flow cytometry

Cultures were grown to OD_{600} = 0.6 (stationary phase) or OD_{600} = 0.025 (exponential phase), supplemented with cumate to induce the expression of Venus or tdTomato, and incubated for 5 hours at 30 ºC with shaking. Exponential phase cells were diluted to OD_{600}=0.04, and the cells expressing Venus or tdTomato were mixed at a 1:1 ratio and cultured for 2 hours or immediately analyzed. Cells were diluted 1:50 into PBS, homogenized by inversion, and flow cytometry performed for 50,000 cells per strain mixture, with an event rate of ~12,000 events/µL. The following settings were used on an BD LSR-II cytometer: FITC voltage 500; PE YG voltage 500; SSC 300; FSC 324. Venus and tdTomato were excited using 488 nm or 561 nm lasers and detected using 515/20 nm or 582/42 nm filters, respectively. Data were visualized using FlowJo software.

Subcellular fractionation

The spheroplasting and Triton X-100 cell fractionation protocol was adapted from Gray et al., 2011. The initial cell pellet was washed once in an equal volume of PYE by resuspension and centrifugation to remove supernatant protein contamination. Lysozyme was used at a final concentration of 100 μg/ml and 10 freeze-thaw cycles were carried out, alternating between liquid N_2 and 50ºC. Lysates were treated with 5 μg/mL DNase I with 25 mM $MgCl_2$. Incubation in 2% (w/v) Triton X solubilization buffer was done overnight at 37 ºC with mixing. All cell fractions were mixed 3:1 with 4X SDS or native sample buffer, and the final insoluble fraction was resuspended in 1X sample buffer.

Cell lysis and sucrose gradient separation of membrane proteins was conducted as previously described (Anwari et al., 2010), supplementing the lysis buffer with 25 μg/mL DNase I and 10 mM $MgCl_2$. Total membranes were resuspended in 25 or 35% (w/v) sucrose in 5 mM EDTA, and separated on either of two different six step sucrose gradients set up on Beckman ultra-clear tubes (14 x 89 mm): 35:40:45:50:55:60% or 45:50:55:60:65:70% (w/v) sucrose in 5 mM EDTA. 500 μL fractions were collected using a BioComp Piston Gradient Fractionator and mixed with 4X SDS sample buffer for immunoblot analysis.

For formic acid extractions of CdzC aggregates, outer membrane fractions determined by immunoblotting to contain CdzC were pooled together, mixed with 5 volumes of TEM buffer (10 mM Tris pH 7.5, 1 mM EDTA, 10 mM $MgCl_2$,10% glycerol) and pelleted at 221,000 x g and 4 °C for 1.5 hours with an ultracentrifuge containing a SW41 rotor. Pellets were resuspended in 90% formic acid, frozen in liquid N_2, lyophilized and resuspended 1X SDS sample buffer for immunoblot analysis.

Computational prediction of aggregation and searches for Cdz-like systems

The protein aggregation propensity and amylogenic regions of CdzC, CdzD and CdzI were predicted based on amino acid sequence using AmylPred 2 (Tsolis et al., 2013), WALZ (high specificity threshold) (Oliveberg, 2010), MetAmyl (with high specificity threshold) (Emily et al.,

2013) and PASTA 2.0 (with peptides threshold) (Walsh et al., 2014). A sequence region was considered aggregation prone if at least three of the above algorithms were in accordance.

To identify CdzC/D-like proteins in other organisms, a multiple sequence alignment was done using CLUSTALW with CdzC, CdzD, and two Cdz-like proteins identified by the GFIT function of KEGG: *Bacillus sp*. YP1 (QF06_18395) and *Xylella fastidiosa* 9a5c (XF_0262). The alignment was used to generate a Hidden Markov Model (HMM) profile using the hmmbuild function in HMMER3 (Eddy, 2011). Separately, a *blastp* search was done against bacterial (taxid:2) sequences in the NCBI non-redundant nucleotide (nr) database to identify homologs of CdzB. For 639 hits obtained, flanking regions 10 kb upstream and downstream were downloaded and all possible ORFs between 60 and 200 residues were translated. This ORF list was scanned with *hmmsearch* using the HMM profile built. The best three hits were added to the multiple sequence alignment. This updated alignment was used as an input for an iterative search of the UniProtKB database using *jackhmmer* (Eddy, 2011), with the bias composition filter off. After the first iteration, hits that included proline or cysteine residues interrupting the glycine-zippers or that had spans of polar/charged residues were filtered out before carrying out a second iteration. Results that did not have a type I secretion system in the 10 kb flanking region were also dropped from the final list. For generation of the Cdz-like protein phylogenetic distribution tree, taxonomic information of each hit was downloaded from the NCBI Taxonomy Browser, and the tree generated using iTOL (Letunic and Bork, 2016).

Table 2.1. Oligonucleotides

Name	Sequence
oLG65	CAGGGCAACGAGCCGATCGCTGACGACGGACTATCGTTCCCGGCCA
oLG66	GTGAGAAGGCCGACATCGAGGCCC
oLG67	caccTCGTCCTCGACGACGCCGGC
oLG68	CGTTGAAGGACCGAGAAAGGGTGACGATTGAATGACCAGGGCGACGCGGCG
oLG69	CGGTATCGATAAGCTTGATATCGAATTC
oLG70	CTGCAGGAATTCAAGAAGTTCCTATTC
oLG073	caccGCGCCAACAATATAATTGCCAGCTCAGCCG
oLG074	CTTGCGGGCGTAGGAAGCGGTAGCG
oLG098	AATCGAATTCTTACTAGAAGAGTTTTGGTATATATTCTGTAGCTTTTGAAAGC
oLG120	AATCGAATTCTTACTATTCTGCGAGGTCGTAGGCG
oLG122	AATCGAATTCTTATCATGATCCGTCCACCGCTTC
oLG126	GATTCATATGATGACCATGACAAAAAGGGCAAC
oLG143	ATTCTGCGAGCACGTTCATCGCCAAAGCTGTC
oLG144	GATGAACGTGCTCGCAGAATAGACCGCAAAGACG
oLG145	ATCCGTCCACAGTTAGCGTCTTCATTTGAGTCGTCC
oLG146	GACGCTAACTGTGGACGGATCATGACCATGAC
oLG147	ATCCGTCCACCACGTTCATCGCCAAAGCTGTC
oLG148	GATGAACGTGGTGGACGGATCATGACCATGAC
oLG149	AGAGTTTTGGCACGTTCATCGCCAAAGCTGTC
oLG150	GATGAACGTGCCAAAACTCTTCTAGTTTTTATCTAGATTGCCC
oLG151	AATTGAAGCCGGCTGGCGCCAAGCTTACCCAAGACGCCCAATAGGATAG
oLG152	GCGTCACGGCCGAAGCTAGCGAATTCGATCTGCCGCTCATAGCTCAGC
oLG154	AATTGAAGCCGGCTGGCGCCAAGCTTACATCGGTCCAAGCTGGCCG
oLG155	GCGTCACGGCCGAAGCTAGCGAATTCCATTTCGGAGTACCGCCCTTC
oLG156	GCCCTTGCTCACCATAGCTGTTTCCTGTGTGAAATTGTTATCC
oLG157	CACAGGAAACAGCTATGGTGAGCAAGGGCGAGGAG
oLG158	GTAGAAAAGATCGTTCTTTCCTGCGTTATCCCCTG
oLG159	TTATCGATACCGGTTCTTTCCTGCGTTATCCCCTG
oLG160	CAGGAAAGAACGATCTTTTCTACGGGGTCTGACGC
oLG161	GCAGGAAAGAACCGGTATCGATAAGCTTGATATCGAATTCA
oLG162	ATGAGGGATAGCTTAGGTGGCGGTACTTGGGTCGA
oLG163	AGCATGAGGGATAGCCTGCAGGAATTCAAGAAGTTCCTATTCTC
oLG164	AGTACCGCCACCTAAGCTATCCCTCATGCTGTATCTTTTTGG
oLG165	CTTGAATTCCTGCAGGCTATCCCTCATGCTGTATCTTTTTGG
oLG172	GATTCATATGACAGCTTTGGCGATGAACG
oLG173	TTCATATGAAGACGCTAACTTTGGCAGAGATTGAC
oLG174	TACTGCAGAGGTCGGACAAGAAACAGCTTCAC
oLG177	AATTGAAGCCGGCTGGCGCCAAGCTTCAGAAGGAGACAGACCGGTAGGG
oLG178	CGATGAACTAGTAGACGCTCATGAGAGGTGGGACC
oLG179	TGAGCGTCTACTAGTTCATCGCCAAAGCTGTCATG
oLG180	GCGTCACGGCCGAAGCTAGCGAATTCGATCTGCCGCTCATAGCTCAGC
oLG182	GAAGAGCTCTTACTAGAAGAGTTTTGGTATATATTCTGTAGCTTTTGAAAGC
oLG183	GAAGAGCTCTTATCATGATCCGTCCACCGCTTC
oLG184	GATTCATATGAGGTCGGACAAGAAACAGCTTCAC
oLG187	GGATCATGACCTCTAGATTGCCCAGACCGAGCG
oLG188	GGCAATCTAGAGGTCATGATCCGTCCACAGTTAGC
oLG190	AATTGAAGCCGGCTGGCGCCAAGCTTTCATGATCCGTCCACCGCTTC

oLG191	GCGTCACGGCCGAAGCTAGCGAATTCGTGAGAAGGCCGACATCGAGG
oLG192	CGTTGTCCATGCGGTCTTCTAACGACGGACTATC
oLG193	CGTTAGAAGACCGCATGGACAACGGCCTCTTTTCG
oLG210	GAAGAGCTCTTACTTGTACAGCTCGTCCATGCC
oLG212	TGTCCGACCTCCCAAGGTCTCGAAAAAATGGTTAAG
oLG213	TGCTCACCATGGCTTTCTCCTGATGTTTGAGAGTG
oLG214	GGAGAAAGCCATGGTGAGCAAGGGCGAGG
oLG253	GTTCAAGCGCTGAGTGGAGCATTCGCGCCGACTG
oLG255	GCGAATGCTCCACTCAGCGCTTGAACTTGGCGTAG
oLG257	GTAGAGGAAGGAATTCCTGCAGCCCGGGGGATC
oLG258	CTGCAGGAATTCCTTCCTCTACTAGTTACAAACAGACCAGATTGTC
oLG267	AATTGAAGCCGGCTGGCGCCAAGCTTACGGTCGTTTAAGGACGGCG
oLG268	GCGTCACGGCCGAAGCTAGCGAATTCGTGAGAAGGCCGACATCGAGG
oLG269	GGCAATCTAGCGACGGACTATCGTTCCCGG
oLG270	TAGTCCGTCGCTAGATTGCCCAGACCGAGCG
oLG291	AATCGAATTCATGGTGAGCAAGGGCGAGGAG
oLG327	TCCGGCTACCGCGCCCGGGACCCCGCCGATAGC
oLG328	GGTGCAGTCGGGGGCCCGGCTGGAATTGTCGCC
oLG329	GGCGACAATTCCAGCCGGGCCCCCGACTGCACC
oLG330	TACGCCGGCTCGAGCGCCAACATGCGCGCAGCCTCCGTC
oLG331	GTCCGGGACGTCGTACGGGTAATTAGCGCCGGCGACCTCGTC
oLG334	GTCGTATTGGGCGCAGCAATTGCGTTAATC
oLG365	AATTGAAGCCGGCTGGCGCCAAGCTTCGAGACGATCTTCAACGCCAAG
oLG366	TCAGATTTCCTGATTGGGCGAGGAGAACATTGAAGG
oLG367	ATGTTCTCCTCGCCCAATCAGGAAATCTGAGTGAGCTGAGATG
oLG368	GCGTCACGGCCGAAGCTAGCGAATTCTGATGTTGAAACGCTCCAGCG
oLG371	TTGTTGGGCTTGGACTCGACCTCGTCGTCCGAACGAGGCGCTATGG
oLG372	CGGGTTCGGGATCGGCTTGCCGGAGCCGCCCGACACATAGTCA
oLG373	ACTACGCCGGCTCGAGCGGCACAAAAAGGGCAACCTTGCAATT
oLG374	CCGGGACGTCGTACGGGTACATGGTCATGATCCGTCCACC
Linker-1	5’-rAppCTGTAGGCACCATCAAT/3ddC/-3’
RT_oligo	5phos/GATCGTCGGACTGTAGAACTCTGAACCTGTCGGTGGTCGCCGTATCATT/iSp18/CACTCA/iSp18/CAAGCAGAAGACGGCATACGAATTGATGGTGCCTACAG
O230	AATGATACGGCGACCACCGAGATCGGAAGAGCACACGTCTGAACTCCAGTCACNNNNNNCGACAGGTTCAGAGTTC
O231	CAAGCAGAAGACGGCATACGA

Table 2.2. Strains

Name	Genotype	Construction details	Reference /Source
CB15n	Synchronizable wild-type CB15		(Evinger and Agabian, 1977)
TLS87	CB15n *ΔrsaA*		(Le et al., 2013)
LG68	*ΔCCNA_00716* to *cdzA*::tet^R	Electroporation of pLG52 into CB15n, two-step recombination method using *sacB* as a counter-selection marker (Skerker et al. 2005), using exponential phase culture for counterselection and supplementing counterselection plate with tetracycline.	This study
LG119	P_{lacI}-*lacI*-P_{lac}-*CFP*::tet^R at *hfaA* locus	Electroporation of pLG129 into CB15n, two-step recombination and counter-selection, supplementing counterselection plate with tetracycline.	This study
LG120	P_{lacI}-*lacI*-P_{lac}-YFP::gent^R at *hfaA* locus	Electroporation of pLG130 into CB15n, two-step recombination and counter-selection, supplementing counterselection plate with gentamycin.	This study
LG121	*ΔcdzC*, P_{lacI}-*lacI*-P_{lac}-CFP::tet^R at *hfaA* locus	Electroporation of pLG125 into CB15n, two-step recombination and counter-selection. Transduction of CFP and tetR markers from LG119 using phage øCr30. (Ely, 1991)	This study
LG122	*ΔcdzD*, P_{lacI}-*lacI*-P_{lac}-CFP::tet^R at *hfaA* locus	Electroporation of pLG126 into CB15n, two-step recombination and counter-selection. Transduction of CFP and tetR markers from LG119 using phage øCr30	This study
LG123	*ΔcdzCD*, P_{lacI}-*lacI*-P_{lac}-CFP::tet^R at *hfaA* locus	Electroporation of pLG127 into CB15n, two-step recombination and counter-selection. Transduction of CFP and tetR markers from LG119 using phage øCr30	This study
LG124	*ΔcdzCDI*, P_{lacI}-*lacI*-P_{lac}-CFP::tet^R at *hfaA* locus	Electroporation of pLG128 into CB15n, two-step recombination and counter-selection, using exponential phase culture for counterselection. Transduction of CFP and tetR markers from LG119 using phage øCr30	This study
LG125	*ΔcdzC*, P_{lacI}-*lacI*-P_{lac}-YFP::gent^R at *hfaA* locus	Electroporation of pLG125 intoCB15n, two-step recombination and counter-selection. Transduction of YFP and gentR markers from LG120 using phage øCr30	This study
LG126	*ΔcdzD*, P_{lacI}-*lacI*-P_{lac}-YFP::gent^R at *hfaA* locus	Electroporation of pLG126 into CB15n, two-step recombination and counter-selection. Transduction of YFP and gentR markers from LG120 using phage øCr30	This study

LG127	*ΔcdzCD*, P_{lacI}-*lacI*-P_{lac}-YFP::gent^R at *hfaA* locus	Electroporation of pLG127 intoCB15n, two-step recombination and counter-selection. Transduction of YFP and gentR markers from LG120 using phage øCr30	This study
LG128	*ΔcdzCDI*, P_{lacI}-*lacI*-P_{lac}-YFP::gent^R at *hfaA* locus	Electroporation of pLG128 into LG120, two-step recombination and counter-selection, using exponential phase culture for counterselection. Transduction of YFP and gentR markers from LG120 using phage øCr30	This study
LG147	P_{lacI}-*lacI*-P_{lac}-*CFP*::tet^R at *hfaA* locus , P_{van}-*CFP* in low copy number plasmid	Electroporation of pMT738 into LG119	This study
LG150	*ΔcdzCDI*, P_{lacI}-*lacI*-P_{lac}-CFP::tet^R at *hfaA* locus, P_{van}-CFP in low copy number plasmid	Electroporation of pMT738 into LG124	This study
LG151	*ΔcdzCDI*, P_{lacI}-*lacI*-P_{lac}-CFP::tet^R at *hfaA* locus, P_{van}-*cdzD* in high copy number plasmid	Electroporation of pLG139 into LG124	This study
LG152	*ΔcdzCDI*, P_{lacI}-*lacI*-P_{lac}-CFP::tet^R at *hfaA* locus, P_{van}-*cdzC* in high copy number plasmid	Electroporation of pLG138 into LG124	This study
LG153	*ΔcdzCDI*, P_{lacI}-*lacI*-P_{lac}-CFP::tet^R at *hfaA* locus, P_{van}-*cdzI* in high copy number plasmid	Electroporation of pLG140 into LG124	This study
LG167	*ΔcdzD*, P_{lacI}-*lacI*-P_{lac}-CFP::tet^R at *hfaA* locus , P_{van}-*cdzD* in high copy number plasmid	Electroporation of pLG139 into LG122	This study
LG168	*ΔcdzC*, P_{lacI}-*lacI*-P_{lac}-CFP::tet^R at *hfaA* locus, P_{van}-*cdzC* in high copy number plasmid	Electroporation of pLG138 into LG121	This study
LG169	*ΔcdzCDI*, P_{lacI}-*lacI*-P_{lac}-YFP::gent^R at *hfaA* locus, empty vector (low copy number)	Electroporation of pMT630 into LG128	This study
LG170	P_{lacI}-*lacI*-P_{lac}-*YFP*::gent^R at *hfaA* locus, empty vector (low copy number)	Electroporation of pMT630 into LG120	This study
LG171	*ΔcdzCDI*, P_{lacI}-*lacI*-P_{lac}-CFP::tet^R at *hfaA* locus, empty vector (high copy number)	Electroporation of pMT426 into LG124	This study
LG172	*ΔCCNA_00716* to *cdzC*,P_{lacI}-*lacI*-P_{lac}-CFP::tet^R at *hfaA* locus	Electroporation of pLG141 into LG119, two-step recombination and counter-selection, using exponential phase culture for counterselection and supplementing counterselection plate with tetracycline.	This study
LG173	*ΔCCNA_00716* to *cdzC*, P_{lacI}-*lacI*-P_{lac}-YFP::gent^R at *hfaA* locus	Electroporation of pLG141 into LG120, two-step recombination and counter-selection, using exponential phase culture for counterselection and supplementing counterselection plate with gentamycin.	This study

LG174	P_{lacI}-*lacI*-P_{lac}-YFP::gent^R at *hfaA* locus, P_{van}-*cdzI* in high copy number plasmid	Electroporation of pLG140 into LG120	This study
LG176	*ΔcdzAB*, P_{lacI}-*lacI*-P_{lac}-YFP::gent^R at *hfaA* locus	Electroporation of pLG145 into LG120, two-step recombination and counter-selection, supplementing counterselection plate with gentamycin.	This study
LG178	*ΔcdzC*, P_{lacI}-*lacI*-P_{lac}-YFP::gent^R at *hfaA* locus, P_{cdzC}-*cdzC* in low copy number plasmid	Electroporation of pLG135 into LG125	This study
LG180	*ΔCCNA_00716* to *cdzC*, P_{lacI}-*lacI*-P_{lac}-YFP::gent^R at *hfaA* locus, P_{cdzC}-*cdzCD* in low copy number plasmid	Electroporation of pLG136 into LG173	This study
LG190	*ΔcdzCDI*, P_{lacI}-*lacI*-P_{lac}-CFP::tet^R at *hfaA* locus, P_{cdzC}-*cdzCDI* in low copy number plasmid	Electroporation of pLG137 into LG124	This study
LG191	*ΔcdzCDI*, P_{lacI}-*lacI*-P_{lac}-YFP::gent^R at *hfaA* locus, P_{cdzC}-*cdzCDI* in low copy number plasmid	Electroporation of pLG137 into LG128	This study
LG192	*ΔCCNA_00716* to *cdzC*, P_{lacI}-*lacI*-P_{lac}-CFP::tet^R at *hfaA* locus, P_{cdzC}-*cdzCDI* in low copy number plasmid	Electroporation of pLG137 into LG172	This study
LG193	*ΔCCNA_00716* to *cdzC*, P_{lacI}-*lacI*-P_{lac}-YFP::gent^R at *hfaA* locus, P_{cdzC}-*cdzCDI* in low copy number plasmid	Electroporation of pLG137 into LG173	This study
LG194	*ΔCCNA_00716* to *cdzA*::tet^R, P_{cdzC}-*cdzCDI* in low copy number plasmid	Electroporation of pLG137 into LG68	This study
LG195	*ΔcdzCD*, P_{lacI}-*lacI*-P_{lac}-YFP::gent^R at *hfaA* locus, P_{cdzC}-*cdzCD* in low copy number plasmid	Electroporation of pLG136 into LG127	This study
LG196	*ΔCCNA_00716* to *cdzC*, P_{lacI}-*lacI*-P_{lac}-CFP::tet^R at *hfaA* locus, P_{cdzC}-*cdzCD* in low copy number plasmid	Electroporation of pLG136 into LG172	This study
LG197	*ΔcdzDI*, P_{lacI}-*lacI*-P_{lac}-CFP::tet^R at *hfaA* locus	Electroporation of pLG146 into LG119, two-step recombination and counter-selection, using exponential phase culture for counterselection.	This study
LG198	P_{cdzC}-YFP::gent^R at *hfaA* locus	Electroporation of pLG153 into CB15n, two-step recombination and counter-selection, supplementing counter-selection plate with gentamycin.	This study
LG219	*ΔcdzABCDI*, P_{lacI}-*lacI*-P_{lac}-CFP::tet^R at *hfaA* locus	Electroporation of pLG183 into LG119, two-step recombination and counter-selection.	This study
LG220	*ΔcdzABCDI*, P_{lacI}-*lacI*-P_{lac}-YFP::gent^R at *hfaA* locus	Electroporation of pLG183 into LG120, two-step recombination and counter-selection.	This study
LG223	*ΔcdzABCDI*, P_{lacI}-*lacI*-P_{lac}-CFP::tet^R at *hfaA* locus, P_{van}-*cdzI* in high copy number plasmid	Electroporation of pLG140 into LG219	This study

LG225	*ΔcdzABCDI,* P_{lacI}-*lacI*-P_{lac}-CFP::tet^R at *hfaA* locus, P_{cdzC}-*cdzI* in low copy number plasmid	Electroporation of pLG158 into LG225	This study
LG226	*ΔcdzABCDI*, P_{lacI}-*lacI*-P_{lac}-CFP::tet^R at *hfaA* locus, empty vector (low copy number)	Electroporation of pMT630 into LG219	This study
LG227	*ΔcdzABCDI*, P_{lacI}-*lacI*-P_{lac}-YFP::$gent^R$ at *hfaA* locus, P_{cdzC}-*cdzCDI* in low copy number plasmid	Electroporation of pLG137 into LG220	This study
LG228	*ΔcdzABCDI*, P_{lacI}-*lacI*-P_{lac}-YFP::$gent^R$ at *hfaA* locus, empty vector (low copy number)	Electroporation of pMT630 into LG220	This study
LG229	*ΔcdzCD*, P_{lacI}-*lacI*-P*lac*-YFP::$gent^R$ at *hfaA* locus, P_{cdzC}-*cdzC* in low copy number plasmid	Electroporation of pLG135 into LG127	This study
LG230	*ΔcdzCD*, P_{lacI}-*lacI*-P_{lac}-YFP::$gent^R$ at *hfaA* locus, P_{cdzC}-*cdzD* in low copy number plasmid	Electroporation of pLG157 into LG127	This study
LG235	*ΔCCNA_00716* to *cdzA*::tet^R, P_{Q5}-tdTomato in high copy number plasmid	Electroporation of pLG155 into LG68	This study
LG236	*ΔCCNA_00716* to *cdzA*::tet^R, P_{Q5}-venus in high copy number plasmid	Electroporation of pLG159 into LG68	This study
LG240	P_{Q5}-*tdTomato* in high copy number plasmid	Electroporation of pLG155 into CB15n	This study
LG241	P_{Q5}-*venus* in high copy number plasmid	Electroporation of pLG159 into CB15n	This study
LG268	*ΔcdzABCDI*, P_{lacI}-*lacI*-P_{lac}-CFP::tet^R at *hfaA* locus, P_{cdzC}-*cdzCDI* in low copy number plasmid	Electroporation of pLG158 into LG219	This study
LG284	*ΔcdzCDI*, P_{lacI}-*lacI*-P_{lac}-YFP::$gent^R$ at *hfaA* locus, P_{cdzC}-$cdzC_{HA}$-*cdzDI* in low copy number plasmid	Electroporation of pLG205 into LG128	This study
LG301	*ΔmanB ΔrsaA*	Electroporation of pLG223 into TLS87, two-step recombination and counter-selection.	This study
LG308	*ΔmanB ΔrsaA*, P_{cdzC}-$cdzC_{HA}$-*cdzDI* in low copy number plasmid	Electroporation of pLG205 into LG301	This study
LG318	*ΔcdzCDI*, P_{lacI}-*lacI*-P_{lac}-YFP::$gent^R$ at *hfaA* locus, P_{cdzC}-*cdzC*-$cdzD_{V5}$-*cdzI* in low copy number plasmid	Electroporation of pLG227 into LG128	This study
LG319	*ΔcdzCDI*, P_{lacI}-*lacI*-P_{lac}-CFP::tet^R at *hfaA* locus, P_{cdzC}-*cdzCD*-$cdzI_{HA}$ in low copy number plasmid	Electroporation of pLG228 into LG124	This study
LG330	*ΔcdzAB*, P_{lacI}-*lacI*-P_{lac}-YFP::$gent^R$ at *hfaA* locus, P_{cdzC}-(*cdzC*$_{HA}$)-*cdzDI* in low copy number plasmid	Electroporation of pLG205 into LG176	This study
LG331	*ΔcdzABCDI ΔmanB ΔrsaA*, P_{cdzC}-$cdzC_{HA}$-*cdzDI* in low copy number plasmid	1) Electroporation of pLG183 into LG301, two-step recombination and counter-selection. 2)Electroporation of pLG205	This study

LG332	*ΔcdzD*, P_{lacI}-*lacI*-P_{lac}-YFP::gent^R at *hfaA* locus, P_{cdzC}-*cdzC*$_{HA}$ in low copy number plasmid	Electroporation of pLG204 into LG126	This study
LG339	ΔCCNA_00716 to *cdzA*::tet^R, *cdzABCDI* in low copy number plasmid	Electroporation of pLG238 into LG68	This study
LG345	*Brevundimonas subvivioides Poindexter* ATCC 15264 with kan^R	Conjugation with *E. coli* EZ-Tn5-kan^R delivery strain . 4 Individual clones were tested in competition experiments	This study
LG346	*Caulobacter segnis* ATCC 21756 with kan^R	Conjugation with E. coli Tn5-kan^R delivery strain. 4 Individual clones were tested in competition experiments	This study
LG347	*Asticcacaulis excentricus* with kan^R	Conjugation with E. coli Tn5-kan^R delivery strain. 4 Individual clones were tested in competition experiments	This study
LG348	*Agrobacterium tumefaciens* with kan^R	Conjugation with E. coli Tn5-kan^R delivery strain. 4 Individual clones were tested in competition experiments	This study
LG349	*Sinorhizobium meliloti* strain 1021 with kan^R	Conjugation with E. coli Tn5-kan^R delivery strain. 4 Individual clones were tested in competition experiments	This study
LG350	*Rhodobacter sphaeroides* strain 2.4.1 with kan^R	Conjugation with E. coli Tn5-kan^R delivery strain. 4 Individual clones were tested in competition experiments	This study
ML23	E. coli SM10 (kan^R)		Lab strain collection

Table 2.3. Plasmids

Name	Description	Construction details	Reference /Source
pMT426	High copy number plasmid with vanillate promoter		(Thanbichler et al., 2007)
pMT630	Low copy number plasmid with vanillate promoter		(Thanbichler et al., 2007)
pMT738	Low copy number plasmid with vanillate promoter driving CFP expression		(Thanbichler et al., 2007)
pNPTS138	Integration vector (kanR) with *sacB* counterselection		(Skerker et al., 2005)
pNPTspec	pNPTS138 LR destination derivative modified with spec^R cassette		(Gora et al., 2010)
pLG52	pNPTspec-based plasmid for replacement of *CCNA_00716* to *cdzA* with tet^R	SOE PCR with oLG66+oLG67 to fuse: 1) 800 bp upstream region of CCNA_00716 (PCR oLG67+68) 2)tetR(PCR oLG69+70) 3)800 bp downstream region of cdzA (PCR oLG65+66) ligated into pENTR-D-TOPO and LR reaction into pNPTspec	This study
pLG53	region spanning 3' end of *CCNA_00719* (last 150 bp included) to 5' of *cdzB* (first 150 bp included), cloned into D-TOPO-pENTR	PCR of CB15n DNA, using oLG73+74. Reaction ligated into TOPO-pENTR	
pLG125	pNPTS138-based plasmid for markerless in-frame deletion *ΔcdzC*	SLIC reaction (Li and Elledge, 2007) to fuse: 1)HindIII-HF and EcoRI-HF digested pNPTS138 2) 1400 bp upstream of cdzC (first 8 codons) amplified by PCR (oLG144+151) 3) last 3 codons of cdzC and 800 bp downstream amplified by PCR (oLG143+152)	This study
pLG126	pNPTS138-based plasmid for markerless in-frame deletion *ΔcdzD*	SLIC reaction to fuse: 1)HindIII-HF and EcoRI-HF digested pNPTS138 2) 1100 bp upstream of cdzD (first 5 codons) amplified by PCR (oLG146+151) 3) last 5 codons of cdzD and 1100 bp downstream amplified by PCR (oLG145+152)	This study
pLG127	pNPTS138-based plasmid for markerless in-frame deletion *ΔcdzCD*	SLIC reaction to fuse: 1)HindIII-HF and EcoRI-HF digested pNPTS138 2) 1100 bp upstream of cdzC (first 8 codons) amplified by PCR (oLG148+151) 3) last 5 codons of cdzD and 800 bp downstream amplified by PCR (oLG147+152)	This study

pLG128	pNPTS138-based plasmid for markerless in-frame deletion *ΔcdzCDI*	SLIC reaction to fuse: 1)HindIII-HF and EcoRI-HF digested pNPTS138 2) 800 bp upstream of cdzC (first 8 codons) amplified by PCR (oLG150+151) 3) last 5 codons of cdzI and 800 bp downstream amplified by PCR (oLG149+152)	This study
pLG129	pNPTS138-based plasmid for integration of P_{lacI}-*lacI*-P_{lac}-*CFP* and tet^R at *hfaA* locus	Fragment A made by SOE PCR (oLG154+159) to fuse: 1) *hfaA* upstream region-P_{lacI}-*lacI*-P_{lac} amplified by PCR (oLG154+156) using pCA66 as template 2) *CFP* amplified by PCR (oLG157+159) using pMT738 as template Fragment B made by SOE PCR (oLG155+161) to fuse: 1) tet^R (PCR oLG161+163) 2) *hfaA* (PCR oLG155+165) Fragments A and B were fused by SLIC into pNPTS138 previously digested with HindIII-HF and EcoRI-HF	This study
pLG130	pNPTS138-based plasmid for integration of P_{lacI}-*lacI*-P_{lac}-*YFP* and $gent^R$ at *hfaA* locus	Fragment A: *hfaA* upstream region-P_{lacI}-*lacI*-P_{lac} amplified by PCR (oLG154+156) using pCA66 as template Fragment B made by SOE PCR (oLG155+157) to fuse: 1) Y*FP* amplified by PCR (oLG157+158) using pMT737 as template 2) $gent^R$ (PCR oLG160+162) 3) *hfaA* (PCR oLG155+164) Fragments A and B were fused by SLIC into pNPTS138 previously digested with HindIII-HF and EcoRI-HF	This study
pLG135	pMT630-based plasmid for expression of P_{cdzC}-*cdzC*	Pcdz-cdzC amplified by PCR (oLG120+174), cloned by restriction cloning using PstI and EcoRI to ligate into pMT630	This study
pLG136	pMT630-based plasmid for expression of P_{cdzC}-*cdzCD*	Pcdz-cdzCD amplified by PCR (oLG183+184), cloned by restriction cloning using NdeI and SacI-HF to ligate into pMT630	This study
pLG137	pMT630-based plasmid for expression of P_{cdzC}-*cdzCDI*	Pcdz-cdzCDI amplified by PCR (oLG182+184), cloned by restriction cloning using NdeI and SacI-HF to ligate into pMT630	This study
pLG138	pMT426-based plasmid for expression of P_{van}-*cdzC*	cdzC was amplified by PCR (oLG120+172), cloned by restriction cloning using NdeI and EcoRI-HF to ligate into pMT426	This study
pLG139	pMT426-based plasmid for expression of P_{van}-*cdzD*	cdzD was amplified by PCR (oLG122+173), cloned by restriction cloning using NdeI and EcoRI-HF to ligate into pMT426,	This study
pLG140	pMT426-based plasmid for expression of P_{van}-*cdzI*	cdzD was amplified by PCR (oLG98+126), cloned by restriction cloning using NdeI and EcoRI-HF to ligate into pMT426	This study
pLG141	pNPTS138-based plasmid for markerless deletion of *CCNA_00716* to *cdzC*	SLIC reaction to fuse: 1)HindIII-HF and EcoRI-HF digested pNPTS138 2) 733 bp upstream of CCNA_00716 amplified by PCR (oLG177+178) 3) 796 bp downstream of cdzC amplified by PCR (oLG179+180)	This study

pLG145	pNPTS138-based plasmid for markerless deletion *ΔcdzAB*	SLIC reaction to fuse: 1)HindIII-HF and EcoRI-HF digested pNPTS138 2) 697 bp upstream of cdzB (first 5 codons) amplified by PCR (oLG190+193) 3) 832 bp downstream of cdzA (last 5 codons) amplified by PCR (oLG191+192)	This study
pLG146	pNPTS138-based plasmid for markerless deletion *ΔcdzDI*	SLIC reaction to fuse: 1)HindIII-HF and EcoRI-HF digested pNPTS138 2) 775 bp upstream of cdzD (first 5 codons) amplified by PCR (oLG151+187) 3) 1120 bp downstream of cdzI (last 5 codons) amplified by PCR (oLG152+188)	This study
pLG153	pNPTS138-based plasmid for integration P_{cdzC}-YFP::gent^R at hfa locus	SLIC reaction to fuse: 1)HindIII-HF and EcoRI-HF digested pNPTS138 2) 530 bp upstream of hfaA amplified by PCR (oLG154+212) 3) 126 bp promoter region of cdzC amplified by PCR (oLG211+213) 4) YFP::gentR-hfaA cassette amplified by PCR (oLG155+214) using pLG130 as template	This study
pLG155	pLG174-based plasmid for expression of P_{Q5}-*tdTomato*	*tdTomato* was amplified by PCR (oLG210+291) (Shaner et al., 2004), cloned by restriction cloning using EcoRI-HF and SacI-HF to ligate into pLG174	This study
pLG157	pMT630-based plasmid for expression of P_{cdzC}-*cdzD*	SLIC reaction to fuse: 1) pMT630 digested with SacI-HF and NdeI 2) PcdzC-D amplified by PCR (oLG183+184) using pLG125 as template	This study
pLG158	pMT630-based plasmid for expression of P_{cdzC}-*cdzI*	SLIC reaction to fuse: 1) pMT630 digested with SacI-HF and NdeI 2) PcdzC-E amplified by PCR (oLG182+184) using pLG127 as template	This study
pLG159	pMT426-based plasmid for expression of P_{Q5}-*venus*	*venus* was amplified by PCR (oLG210+291) from pMT648 (Thanbichler et al.,2007), cloned by restriction cloning using EcoRI-HF and SacI-HF to ligate into pLG174	This study
pLG174	pMT426-based plasmid for protein expression of P_{Q5} with multiple cloning site	SLIC reaction to fuse: 1) pMT426 excluding vanillate repressor and P_{van} , amplified by PCR (oLG253+257) 2) P_{Q5} amplified by PCR (oLG255+258) using pQF (Kaczmarczyk et al., 2013)	This study
pLG183	pNPTS138-based plasmid for markerless deletion *ΔcdzABCDI*	SLIC reaction to fuse: 1)HindIII-HF and EcoRI-HF digested pNPTS138 2) 920 bp upstream of cdzI amplified by PCR (oLG267+270) 3) 800 bp downstream of cdzA amplified by PCR (oLG268+269)	This study
pLG204	pMT630-based plasmid for expression of P_{cdzC}-*cdzC*$_{HA}$	1) round-the-horn site-directed mutagenesis to insert HA tag into cdzC after leader peptide, with oLG330+331, using pLG53 as template 3) PCR of Pcdz-C using plasmid from step 2 as template (oLG184+186), cloned by restriction cloning using NdeI and SacI-HF to ligate into pMT630	This study

pLG205	pMT630-based plasmid for expression of P_{cdzC}-*cdzC*$_{HA}$-*cdzDI*	1) round-the-horn site-directed mutagenesis with oLG330+331 using pLG53 as template 3) PCR of Pcdz-CDE using plasmid from step 2 as template (oLG182+184), cloned by restriction cloning using NdeI and SacI-HF to ligate into pMT630	This study
pLG223	pNPTS138-based plasmid for markerless deletion *ΔManB (CCNA_02347)*	SLIC reaction to fuse: 1)HindIII-HF and EcoRI-HF digested pNPTS138 2) 950 bp upstream of *manB* (first 5 codons) amplified by PCR (oLG365+366) 3) last 5 codons of *manB* and 950 bp downstream amplified by PCR (oLG367+368)	This study
pLG227	pMT630-based plasmid for expression of P_{cdzC}-*cdzC-cdzD*$_{V5}$-*cdzI*	1) round-the-horn site-directed mutagenesis to insert V5 tag into cdzD after leader peptide, with oLG371+372 using pLG53 as template 3) PCR of Pcdz-CDE using plasmid from step 2 as template (oLG182+184), cloned by restriction cloning using NdeI and SacI-HF to ligate into pMT630	This study
pLG228	pMT630-based plasmid for expression of P_{cdzC}-*cdzCD*-edtI$_{HA}$	1) round-the-horn site-directed mutagenesis with oLG373+374 using pLG53 as template 3) PCR of Pcdz-CDE using plasmid from step 2 as template (oLG182+184), cloned by restriction cloning using NdeI and SacI-HF to ligate into pMT630	This study
pLG238	pMT630-based plasmid with *cdzABCDI*	1) PCR of cdzABCDI, using oLG410+411. Reaction ligated into TOPO-pENTR 2) Subcloned by Gibson assembly into pMT630 cut with NdeI+SacI-HF	This study

ACKNOWLEDGEMENTS

We thank the labs of T. Le, L. Shapiro, J. Smit, S. Bell, R. Sauer, A. Grossman, and Y. Brun for strains and reagents. We acknowledge G. Paradis at the Koch Institute Flow Cytometry Core at MIT for assistance with flow cytometry and especially N. Watson at the Whitehead Institute Keck Microscopy Facility for help with the electron microscopy. We thank M. LeRoux for helpful discussions and comments on the manuscript. This work was supported by an NIH grant (R01GM082899) to M.T.L., who is also an Investigator of the Howard Hughes Medical Institute, and by an HHMI International Predoctoral Fellowship to L.G.

REFERENCES

Abraham, W.-R., Rohde, M., and Bennasar, A. (2014). The Family Caulobacteraceae. In The Prokaryotes, E. Rosenberg, E.F. DeLong, S. Lory, E. Stackebrandt, and F. Thompson, eds. (Berlin, Heidelberg: Springer Berlin Heidelberg), pp. 179–205.

Aguirre-von-Wobeser, E., Eguiarte, L.E., Souza, V., and Soberon-Chavez, G. (2015). Theoretical analysis of the cost of antagonistic activity for aquatic bacteria in oligotrophic environments. Front. Microbiol. *6*.

Alcoforado Diniz, J., and Coulthurst, S.J. (2015). Intraspecies Competition in Serratia marcescens Is Mediated by Type VI-Secreted Rhs Effectors and a Conserved Effector-Associated Accessory Protein. J. Bacteriol. *197*, 2350–2360.

Anderson, M.S., Garcia, E.C., and Cotter, P.A. (2012). The Burkholderia bcpAIOB Genes Define Unique Classes of Two-Partner Secretion and Contact Dependent Growth Inhibition Systems. PLoS Genet. *8*, e1002877.

Anwari, K., Poggio, S., Perry, A., Gatsos, X., Ramarathinam, S.H., Williamson, N.A., Noinaj, N., Buchanan, S., Gabriel, K., Purcell, A.W., et al. (2010). A Modular BAM Complex in the Outer Membrane of the α-Proteobacterium Caulobacter crescentus. PLoS ONE *5*, e8619.

Aoki, S.K., Pamma, R., Hernday, A.D., Bickham, J.E., Braaten, B.A., and Low, D.A. (2005). Contact-Dependent Inhibition of Growth in Escherichia coli. Science *309*, 1245–1248.

Aoki, S.K., Diner, E.J., de Roodenbeke, C. t'Kint, Burgess, B.R., Poole, S.J., Braaten, B.A., Jones, A.M., Webb, J.S., Hayes, C.S., Cotter, P.A., et al. (2010). A widespread family of polymorphic contact-dependent toxin delivery systems in bacteria. Nature *468*, 439–442.

Banerjee, S.P., Dora, K.C., and Chowdhury, S. (2013). Detection, partial purification and characterization of bacteriocin produced by Lactobacillus brevis FPTLB3 isolated from freshwater fish: Bacteriocin from Lb. brevis FPTLB3. J. Food Sci. Technol. *50*, 17–25.

Barbour, A., and Philip, K. (2014). Variable Characteristics of Bacteriocin-Producing Streptococcus salivarius Strains Isolated from Malaysian Subjects. PLoS ONE *9*, e100541.

Bieler, S., Estrada, L., Lagos, R., Baeza, M., Castilla, J., and Soto, C. (2005). Amyloid Formation Modulates the Biological Activity of a Bacterial Protein. J. Biol. Chem. *280*, 26880–26885.

Burmolle, M., Webb, J.S., Rao, D., Hansen, L.H., Sorensen, S.J., and Kjelleberg, S. (2006). Enhanced Biofilm Formation and Increased Resistance to Antimicrobial Agents and Bacterial Invasion Are Caused by Synergistic Interactions in Multispecies Biofilms. Appl. Environ. Microbiol. *72*, 3916–3923.

Cao, Z., Casabona, M.G., Kneuper, H., Chalmers, J.D., and Palmer, T. (2016). The type VII secretion system of Staphylococcus aureus secretes a nuclease toxin that targets competitor bacteria. Nat. Microbiol. *2*, 16183.

Cascales, E., Buchanan, S.K., Duche, D., Kleanthous, C., Lloubes, R., Postle, K., Riley, M., Slatin, S., and Cavard, D. (2007). Colicin Biology. Microbiol. Mol. Biol. Rev. *71*, 158–229.

Chang, L.-K., Zhao, J.-H., Liu, H.-L., Wu, J.W., Chuang, C.-K., Liu, K.-T., Chen, J.-T., Tsai, W.-B., and Ho, Y. (2010). The Importance of Steric Zipper on the Aggregation of the MVGGVV Peptide Derived from the Amyloid β Peptide. J. Biomol. Struct. Dyn. *28*, 39–50.

Cogen, A.L., Yamasaki, K., Sanchez, K.M., Dorschner, R.A., Lai, Y., MacLeod, D.T., Torpey, J.W., Otto, M., Nizet, V., Kim, J.E., et al. (2010). Selective antimicrobial action is provided by phenol-soluble modulins derived from Staphylococcus epidermidis, a normal resident of the skin. J. Invest. Dermatol. *130*, 192–200.

Cornforth, D.M., and Foster, K.R. (2013). Competition sensing: the social side of bacterial stress responses. Nat. Rev. Microbiol. *11*, 285–293.

Cotter, P.D., Ross, R.P., and Hill, C. (2012). Bacteriocins — a viable alternative to antibiotics? Nat. Rev. Microbiol. *11*, 95–105.

Daba, H., Lacroix, C., Huang, J., Simard, R.E., and Lemieux, L. (1994). Simple method of purification and sequencing of a bacteriocin produced by Pediococcus acidilactici UL5. J. Appl. Bacteriol. *77*, 682–688.

Dang, H., and Lovell, C.R. (2016). Microbial Surface Colonization and Biofilm Development in Marine Environments. Microbiol. Mol. Biol. Rev. *80*, 91–138.

De Kwaadsteniet, M., Fraser, T., Van Reenen, C.A., and Dicks, L.M.T. (2006). Bacteriocin T8, a Novel Class IIa sec-Dependent Bacteriocin Produced by Enterococcus faecium T8, Isolated from

Vaginal Secretions of Children Infected with Human Immunodeficiency Virus. Appl. Environ. Microbiol. *72*, 4761–4766.

Decock, M., Stanga, S., Octave, J.-N., Dewachter, I., Smith, S.O., Constantinescu, S.N., and Kienlen-Campard, P. (2016). Glycines from the APP GXXXG/GXXXA Transmembrane Motifs Promote Formation of Pathogenic Aβ Oligomers in Cells. Front. Aging Neurosci. *8*.

DePas, W.H., and Chapman, M.R. (2012). Microbial manipulation of the amyloid fold. Res. Microbiol. *163*, 592–606.

Ducret, A., Quardokus, E.M., and Brun, Y.V. (2016). MicrobeJ, a tool for high throughput bacterial cell detection and quantitative analysis. Nat. Microbiol. *1*, 16077.

Eddy, S.R. (2011). Accelerated Profile HMM Searches. PLoS Comput. Biol. *7*, e1002195.

Ely, B. (1991). Genetics of Caulobacter crescentus. Methods Enzymol. *204*, 372–384.

Emily, M., Talvas, A., and Delamarche, C. (2013). MetAmyl: A METa-Predictor for AMYLoid Proteins. PLoS ONE *8*, e79722.

Evinger, M., and Agabian, N. (1977). Envelope-associated nucleoid from Caulobacter crescentus stalked and swarmer cells. J. Bacteriol. *132*, 294–301.

Fonte, V., Dostal, V., Roberts, C.M., Gonzales, P., Lacor, P., Magrane, J., Dingwell, N., Fan, E.Y., Silverman, M.A., Stein, G.H., et al. (2011). A glycine zipper motif mediates the formation of toxic β-amyloid oligomers in vitro and in vivo. Mol. Neurodegener. *6*, 61.

Ford, M.J., Nomellini, J.F., and Smit, J. (2007). S-Layer Anchoring and Localization of an S-Layer-Associated Protease in Caulobacter crescentus. J. Bacteriol. *189*, 2226–2237.

Gandham, L., Nomellini, J.F., and Smit, J. (2012). Evaluating secretion and surface attachment of SapA, an S-layer-associated metalloprotease of Caulobacter crescentus. Arch. Microbiol. *194*, 865–877.

Gora, K.G., Tsokos, C.G., Chen, Y.E., Srinivasan, B.S., Perchuk, B.S., and Laub, M.T. (2010). A cell-type-specific protein-protein interaction modulates transcriptional activity of a master regulator in Caulobacter crescentus. Mol. Cell *39*, 455–467.

Gray, A.N., Henderson-Frost, J.M., Boyd, D., Shirafi, S., Niki, H., and Goldberg, M.B. (2011). Unbalanced Charge Distribution as a Determinant for Dependence of a Subset of Escherichia coli Membrane Proteins on the Membrane Insertase YidC. mBio *2*, e00238-11-e00238-11.

Guo, M.S., Updegrove, T.B., Gogol, E.B., Shabalina, S.A., Gross, C.A., and Storz, G. (2014). MicL, a new E-dependent sRNA, combats envelope stress by repressing synthesis of Lpp, the major outer membrane lipoprotein. Genes Dev. *28*, 1620–1634.

Hecht, A.L., Casterline, B.W., Earley, Z.M., Goo, Y.A., Goodlett, D.R., and Bubeck Wardenburg, J. (2016). Strain competition restricts colonization of an enteric pathogen and prevents colitis. EMBO Rep. *17*, 1281–1291.

Hibbing, M.E., Fuqua, C., Parsek, M.R., and Peterson, S.B. (2010). Bacterial competition: surviving and thriving in the microbial jungle. Nat. Rev. Microbiol. *8*, 15–25.

Hood, R.D., Singh, P., Hsu, F., Güvener, T., Carl, M.A., Trinidad, R.R.S., Silverman, J.M., Ohlson, B.B., Hicks, K.G., Plemel, R.L., et al. (2010). A Type VI Secretion System of Pseudomonas aeruginosa Targets a Toxin to Bacteria. Cell Host Microbe *7*, 25–37.

Iniesta, A.A., McGrath, P.T., Reisenauer, A., McAdams, H.H., and Shapiro, L. (2006). A phospho-signaling pathway controls the localization and activity of a protease complex critical for bacterial cell cycle progression. Proc. Natl. Acad. Sci. *103*, 10935–10940.

James, R., Lazdunski, C., and Pattus, F. (1992). Bacteriocins, microcins and lantibiotics (Berlin ; New York: Springer-Verlag).

Kaczmarczyk, A., Vorholt, J.A., and Francez-Charlot, A. (2013). Cumate-inducible gene expression system for sphingomonads and other Alphaproteobacteria. Appl. Environ. Microbiol. *79*, 6795–6802.

Kanonenberg, K., Schwarz, C.K.W., and Schmitt, L. (2013). Type I secretion systems – a story of appendices. Res. Microbiol. *164*, 596–604.

Kim, S., Jeon, T.-J., Oberai, A., Yang, D., Schmidt, J.J., and Bowie, J.U. (2005). Transmembrane glycine zippers: Physiological and pathological roles in membrane proteins. Proc. Natl. Acad. Sci. *102*, 14278–14283.

Koontz, L. (2014). TCA Precipitation. In Methods in Enzymology, (Elsevier), pp. 3–10.

Laemmli, U.K. (1970). Cleavage of Structural Proteins during the Assembly of the Head of Bacteriophage T4. Nature *227*, 680–685.

Lagos, R., Villanueva, J.E., and Monasterio, O. (1999). Identification and properties of the genes encoding microcin E492 and its immunity protein. J. Bacteriol. *181*, 212–217.

Langmead, B., Trapnell, C., Pop, M., and Salzberg, S.L. (2009). Ultrafast and memory-efficient alignment of short DNA sequences to the human genome. Genome Biol. *10*, R25.

Le, T.B.K., Imakaev, M.V., Mirny, L.A., and Laub, M.T. (2013). High-resolution mapping of the spatial organization of a bacterial chromosome. Science *342*, 731–734.

Letunic, I., and Bork, P. (2016). Interactive tree of life (iTOL) v3: an online tool for the display and annotation of phylogenetic and other trees. Nucleic Acids Res. *44*, W242–W245.

Li, M.Z., and Elledge, S.J. (2007). Harnessing homologous recombination in vitro to generate recombinant DNA via SLIC. Nat. Methods *4*, 251–256.

Marks, M.E., Castro-Rojas, C.M., Teiling, C., Du, L., Kapatral, V., Walunas, T.L., and Crosson, S. (2010). The Genetic Basis of Laboratory Adaptation in Caulobacter crescentus. J. Bacteriol. *192*, 3678–3688.

Masse, E., Escorcia, F.E., and Gottesman, S. (2003). Coupled degradation of a small regulatory RNA and its mRNA targets in Escherichia coli. Genes Dev. *17*, 2374–2383.

McNally, L., Bernardy, E., Thomas, J., Kalziqi, A., Pentz, J., Brown, S.P., Hammer, B.K., Yunker, P.J., and Ratcliff, W.C. (2017). Killing by Type VI secretion drives genetic phase separation and correlates with increased cooperation. Nat. Commun. *8*, 14371.

Nissen-Meyer, J., Oppegård, C., Rogne, P., Haugen, H.S., and Kristiansen, P.E. (2011). The Two-Peptide (Class-IIb) Bacteriocins: Genetics, Biosynthesis, Structure, and Mode of Action. In Prokaryotic Antimicrobial Peptides, D. Drider, and S. Rebuffat, eds. (New York, NY: Springer New York), pp. 197–212.

Nomellini, J.F., Li, C., Lavallee, D., Shanina, I., Cavacini, L.A., Horwitz, M.S., and Smit, J. (2010). Development of an HIV-1 Specific Microbicide Using Caulobacter crescentus S-Layer Mediated Display of CD4 and MIP1α. PLoS ONE *5*, e10366.

Oliveberg, M. (2010). Waltz, an exciting new move in amyloid prediction. Nat. Methods *7*, 187–188.

Poindexter, J. (1981). The caulobacters: ubiquitous unusual bacteria. Microbiol. Rev. *45*, 123–179.

Rebuffat, S. (2011). Microcins from Enterobacteria: On the Edge Between Gram-Positive Bacteriocins and Colicins. In Prokaryotic Antimicrobial Peptides, D. Drider, and S. Rebuffat, eds. (New York, NY: Springer New York), pp. 333–349.

Riley, M.A. (2011). Bacteriocin-Mediated Competitive Interactions of Bacterial Populations and Communities. In Prokaryotic Antimicrobial Peptides, D. Drider, and S. Rebuffat, eds. (New York, NY: Springer New York), pp. 13–26.

Riley, M.A., and Gordon, D.M. (1999). The ecological role of bacteriocins in bacterial competition. Trends Microbiol. *7*, 129–133.

Riley, M.A., and Wertz, J.E. (2002). Bacteriocins: Evolution, Ecology, and Application. Annu. Rev. Microbiol. *56*, 117–137.

Ruhe, Z.C., Low, D.A., and Hayes, C.S. (2013). Bacterial contact-dependent growth inhibition. Trends Microbiol. *21*, 230–237.

Ruhe, Z.C., Hayes, C.S., and Low, D.A. (2015). Measuring Cell–Cell Binding Using Flow-Cytometry. In The BAM Complex, S. Buchanan, and N. Noinaj, eds. (New York, NY: Springer New York), pp. 127–136.

Russell, A.B., Wexler, A.G., Harding, B.N., Whitney, J.C., Bohn, A.J., Goo, Y.A., Tran, B.Q., Barry, N.A., Zheng, H., Peterson, S.B., et al. (2014a). A Type VI Secretion-Related Pathway in Bacteroidetes Mediates Interbacterial Antagonism. Cell Host Microbe *16*, 227–236.

Russell, A.B., Peterson, S.B., and Mougous, J.D. (2014b). Type VI secretion system effectors: poisons with a purpose. Nat. Rev. Microbiol. *12*, 137–148.

Schindelin, J., Arganda-Carreras, I., Frise, E., Kaynig, V., Longair, M., Pietzsch, T., Preibisch, S., Rueden, C., Saalfeld, S., Schmid, B., et al. (2012). Fiji: an open-source platform for biological-image analysis. Nat. Methods *9*, 676–682.

Schrader, J.M., Zhou, B., Li, G.-W., Lasker, K., Childers, W.S., Williams, B., Long, T., Crosson, S., McAdams, H.H., Weissman, J.S., et al. (2014). The coding and noncoding architecture of the Caulobacter crescentus genome. PLoS Genet. *10*, e1004463.

Schwartz, K., Syed, A.K., Stephenson, R.E., Rickard, A.H., and Boles, B.R. (2012). Functional Amyloids Composed of Phenol Soluble Modulins Stabilize Staphylococcus aureus Biofilms. PLoS Pathog. *8*, e1002744.

Senes, A., Gerstein, M., and Engelman, D.M. (2000). Statistical analysis of amino acid patterns in transmembrane helices: the GxxxG motif occurs frequently and in association with β-branched residues at neighboring positions. J. Mol. Biol. *296*, 921–936.

Shaner, N.C., Campbell, R.E., Steinbach, P.A., Giepmans, B.N.G., Palmer, A.E., and Tsien, R.Y. (2004). Improved monomeric red, orange and yellow fluorescent proteins derived from Discosoma sp. red fluorescent protein. Nat. Biotechnol. *22*, 1567–1572.

Simpson, R.J. (2006). Bulk Precipitation of Proteins by Ammonium Sulfate. Cold Spring Harb. Protoc. *2006*, pdb.prot4308.

Skerker, J.M., Prasol, M.S., Perchuk, B.S., Biondi, E.G., and Laub, M.T. (2005). Two-component signal transduction pathways regulating growth and cell cycle progression in a bacterium: a system-level analysis. PLoS Biol. *3*, e334.

Tahara, T., and Kanatani, K. (1997). Isolation and partial characterization of crispacin A, a cell-associated bacteriocin produced by Lactobacillus crispatus JCM 2009. FEMS Microbiol. Lett. *147*, 287–290.

Thanbichler, M., Iniesta, A.A., and Shapiro, L. (2007). A comprehensive set of plasmids for vanillate- and xylose-inducible gene expression in Caulobacter crescentus. Nucleic Acids Res. *35*, e137.

Travisano, M., and Velicer, G.J. (2004). Strategies of microbial cheater control. Trends Microbiol. *12*, 72–78.

Tsolis, A.C., Papandreou, N.C., Iconomidou, V.A., and Hamodrakas, S.J. (2013). A Consensus Method for the Prediction of "Aggregation-Prone" Peptides in Globular Proteins. PLoS ONE *8*, e54175.

Vassiliadis, G., Destoumieux-Garzón, D., and Peduzzi, J. (2011). Class II Microcins. In Prokaryotic Antimicrobial Peptides, D. Drider, and S. Rebuffat, eds. (New York, NY: Springer New York), pp. 309–332.

Walsh, I., Seno, F., Tosatto, S.C.E., and Trovato, A. (2014). PASTA 2.0: an improved server for protein aggregation prediction. Nucleic Acids Res. *42*, W301–W307.

Willett, J.L.E., Ruhe, Z.C., Goulding, C.W., Low, D.A., and Hayes, C.S. (2015). Contact-Dependent Growth Inhibition (CDI) and CdiB/CdiA Two-Partner Secretion Proteins. J. Mol. Biol. *427*, 3754–3765.

Yang, R., Johnson, M.C., and Ray, B. (1992). Novel method to extract large amounts of bacteriocins from lactic acid bacteria. Appl. Environ. Microbiol. *58*, 3355–3359.

Chapter 3
Mechanisms of resistance to Cdz-mediated killing

This work is in preparation for submission as García-Bayona L and Laub MT. Resistance mechanisms to the Cdz contact-dependent bacteriocin from *Caulobacter crescentus*, which disrupts membrane integrity in target cells.

ABSTRACT

The Cdz system is an atypical contact-dependent bacteriocin system that allows the aquatic oligotrophic bacterium *Caulobacter crescentus* to kill closely related species. The toxin is composed of two small hydrophobic proteins bearing an extended glycine-zipper motif that may disrupt the membrane integrity of target cells. Whether Cdz toxins must bind a specific receptor protein in target cells to initiate killing, as with other contact-dependent toxins, is unknown. Here, we identify and characterize suppressor mutations in a target strain that allow it to escape Cdz-mediated killing. Our results suggest that a primary receptor for the Cdz toxins is PerA, an envelope-associated protein harboring several pentapeptide-repeat motifs thought to adopt a quadrilateral β-helical fold. Although required for normal growth in rich medium, our genetic screen identified alleles of *perA* that retain viability, but rescue cells against killing by the Cdz system. Additionally, we identified suppressor mutations in the *zerRAB* operon, which appears to play a role in modulating cell envelope composition. These mutations likely produce changes in the cell envelope that somehow renders cells less susceptible to killing by Cdz toxins, supporting a model in which these toxins inhibit cells by disrupting cell envelope integrity. These results are also consistent with the observation that target cells experience rapid membrane depolarization after being put in competition with a Cdz producer.

INTRODUCTION

Recently, we described a new type of bacteriocin in the aquatic oligotrophic α-proteobacterium *Caulobacter crescentus*. The Cdz toxin (contact-dependent inhibition by glycine zipper proteins) is composed of two small hydrophobic proteins, CdzC and CdzD, that harbor extended glycine-zipper motifs. These proteins are secreted via a type I secretion system and aggregate on the surface of producer cells to mediate contact-dependent killing of target cells. The mechanism of CdzC/D aggregation has not been characterized, but is thought to share some similarities with other toxins bearing glycine-zippers, such as the amyloid β peptide in Alzheimer's disease. The exact means of toxin delivery into the target cell also remains elusive (García-Bayona et al., 2017).

The initial evidence suggests that the Cdz toxins may target the inner membrane, similar to other membrane-acting bacteriocins. The latter can increase membrane permeability to ions by directly forming pores in the membrane (Cotter et al., 2012), or by associating with integral membrane proteins, altering their structure to cause leakage of cellular contents (Bieler et al., 2006; Diep et al., 2007). CdzC and CdzD are expected to be active in the inner membrane or the periplasm of target cells, as the immunity protein CdzI that protects the producer cells from self-intoxication is a small, integral inner membrane protein (García-Bayona et al., 2017). Additionally, both CdzC and CdzD bear some weak sequence similarity to the diffusible pore-forming small bacteriocins Thermophilin 13 from *Streptococcus thermophilus* (Marciset et al., 1997) and microcin MccE492 from *K. pneumoniae* (de Lorenzo and Pugsley, 1985). However, these and other pore-forming bacteriocins are typically amphipathic (Rea et al., 2011), whereas, CdzC and CdzD are comprised almost entirely of hydrophobic residues in their predicted transmembrane regions.

In competition with a Cdz producer, target cells become permeable to the viability dye propidium iodide (PI), indicating compromised membrane integrity (García-Bayona et al., 2017; Sträuber and Müller, 2010). However, the observed permeabilization could be an indirect effect of cell death by a toxin with a different direct cellular target (Shi et al., 2007). Other common cellular targets of small bacteriocins include the peptidoglycan, nucleic acids and tRNAs, DNA gyrase, and RNA polymerase (Rea et al., 2011; Rebuffat, 2011).

To investigate the mechanism(s) by which Cdz toxins target and kill cells lacking the CdzI immunity protein, we conducted a genetic screen to identify mutations that allow *ΔcdzCDI* target cells to escape Cdz-mediated killing. The mutants identified may disrupt any one of the several steps that a toxin needs to complete in order to kill cells. First, the producer cell needs to be in direct contact with the target cell, which is likely mediated by an as-yet unidentified cell surface adhesin. Second, the toxin may directly bind a cell-surface receptor, and it may need an integral outer membrane protein to import it into the periplasm (or, if the ultimate target is cytoplasmic, an inner membrane transporter is required). Finally, the toxin binds its cellular target and can exert its inhibitory activity. This last step could be suppressed by mutations that alter the target molecule so that it is no longer bound. Additionally, if the toxin carries out an enzymatic activity that leads to growth inhibition, this type of action could be suppressed by increasing the compensatory enzymatic activity in the target cell. For example, the effect of a peptidoglycan amidase toxin can be suppressed by upregulation of peptidoglycan synthesis and cross-linking enzymes (Cotter et al., 2012).

We identified three loci involved in resistance to killing by a Cdz producer. One encodes a TonB-dependent receptor, which Cdz may require for import across the outer membrane into the periplasm (or cytoplasm) of the target cell. We also found mutations in a three gene operon, *zerRAB* (zipper envelope resistance), which appears to play a role in modulating cell envelope composition under certain stress conditions. The mutations identified lead to an upregulation of ZerA and ZerB, which encode inner membrane proteins that likely also each contain periplasmic domains. Modest upregulation leads to resistance to Cdz-mediated killing, whereas stronger upregulation causes significant alterations in cell growth and inhibited cell division suggesting that *zerAB* expression counteracts the effects of Cdz toxins by altering cell envelope properties.

Finally, we identify loss-of-function mutations in an envelope-associated pentapeptide-repeat protein (PPR) that may be a cell surface receptor for the Cdz toxins. The PPR protein family is characterized by the occurrence of multiple tandem repeats of the [STAV][D/N][L/F]XX motif, where X can be any amino acid (Ni et al., 2009; Vetting et al., 2006). Crystal structures show that these repeats adopt a regular right-handed quadrilateral β-helix fold (Rfr fold) with few

excursions from the main structural element (Shah and Heddle, 2014; Vetting et al., 2007). This protein family is ubiquitous in bacteria and particularly abundant in cyanobacteria, which carry up to 40 variants per genome (Ni et al., 2009). However, their functions remain largely obscure, with few characterized members (Hegde et al., 2011; Vetting et al., 2007). PPRs from cyanobacteria have been shown to be involved in heterocyst differentiation, glycolipid localization in the cell envelope, and regulation of manganese uptake (Anwari et al., 2010; Black et al., 1995; Chandler et al., 2003). Interestingly, some γ-proteobacteria and Gram-positive bacteria harbor PPRs that reduce susceptibility to antibiotics from the quinolone family (gyrase inhibitors). They are proposed to act as structural DNA mimics, competitively binding DNA gyrase (Gibello et al., 2014; Montero et al., 2001; Shah and Heddle, 2014). Likewise, some PPRs confer immunity to modified peptide bacteriocins that inhibit gyrase. Such PPRs are required in the bacteriocin producer cell to prevent self-intoxication (Cociancich et al., 2015; Garrido et al., 1988; Scholz et al., 2011). In contrast, in *C. crescentus*, the surface-exposed PPR protein PerA (pentapeptide envelope resistance A) is likely to act as the Cdz receptor, thereby conferring susceptibility rather than resistance. PerA normally plays a key role in maintaining envelope homeostasis under normal growth conditions, as mutants lacking this gene show significantly impaired fitness.

RESULTS

A suppressor screen to identify mutations that render target cells resistant to Cdz-mediated killing

When a *ΔcdzCDI* target strain is co-cultured with a wild-type *C. crescentus* producer for 20 hours, the target population loses up to 7 logs of viability by cfu counts, with ~1000 cfu/ml surviving. When those surviving colonies are re-streaked and competed again against the wild-type, roughly half have become resistant to Cdz-mediated killing and retain full viability in co-culture. We took advantage of this observation to identify spontaneous mutations in the target strain that render it resistant to Cdz. The genetic screen used, outlined in Fig 3.1A, used an indicator and producer strain that each harbored two different markers, one a fluorescent protein and one an antibiotic resistance cassette. After two rounds of competition, target strain isolates that were still tet^R and CFP+ were submitted for whole genome sequencing. Reads were mapped to the reference parental genome and mutations identified using the software package breseq, which can detect single nucleotide variants (SNVs), small insertions or deletions (indels), and larger chromosomal rearrangements (structural variants). We then verified mutations by Sanger sequencing.

Figure 3.1B summarizes the four resistance loci identified in this screen, along with the specific mutations obtained for each one. An early stop codon was identified in gene CCNA_03680, which encodes a putative membrane-associated aminopeptidase of unknown function. This gene is predicted to be co-translated with downstream gene CCNA_03681, a putative thioesterase. We did not investigate this operon further. Two independent single nucleotide substitutions in the gene CCNA_03108, which encodes a TonB-dependent receptor, are predicted to produce a premature stop codon at residue 28 of an otherwise 1,112 residue protein or a non-synonymous mutation. Thus, this mutations are likely to produce resistance through the loss of function of this TonB-dependent receptor, but we have not yet examined whether a complete deletion of CCNA_03108 confers Cdz resistance or whether the sensitivity of the strain harboring a nonsense mutation is restored by producing a full-length copy of the gene *in trans*.

A

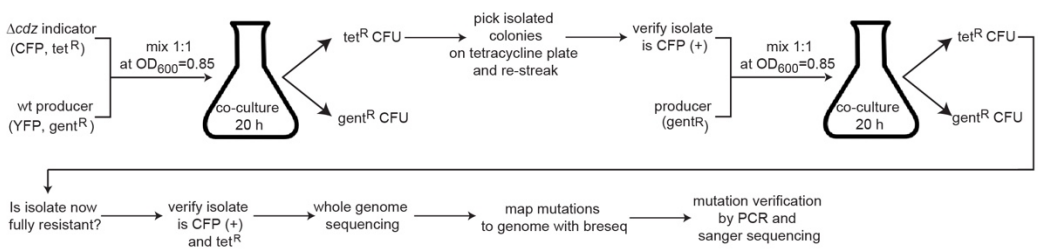

B

locus	Size (residues)	Description	Essential by Tn-seq	Gene cluster?	Predicted localization	Type of mutation (gene → protein)
CCNA_01968 (*perA*)	289	Pentapeptide-repeats containing protein	Yes	Pentapeptide-repeat containing protein upstream	Outer membrane or cell surface	• Δ309 bp in promoter and 5' region → no protein • Δ15 bp →Δresidues 103-107 • Δ105 bp → Δresidues 150-18 • Δ1 bp → Protein with modified C-terminus (residues 234 to 288)
CCNA_03108	1112	TonB-dependent outer membrane receptor	No	No	Outer membrane	• Q28* • F174S
CCNA_03519 (*zerRAB*)	108	PadR-family transcriptional regulator	No	Regulator of two putative envelope-associated proteins	Cytosolic	• T(-59)C in promoter region++ • L59P
CCNA_03680	1196	Aminopeptidase N	No	PaaI thioestherase and ABC transporter ATP-binding protein	Inner membrane	• Q834*

* = stop codon

C

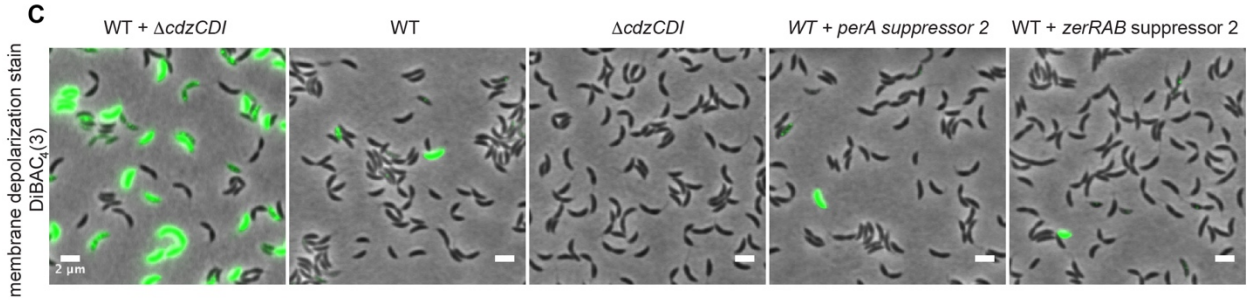

Figure 3.1. Identification of mutations that confer resistance to Cdz-mediated killing. A. Experimental design of the suppressor screen. CFU = colony forming units**. B.** Suppressor mutations identified in the screen. ++= relative to the start codon, * = stop codon. **C.** $DiBAC_4(3)$ staining of a competition of the indicated strains, 30 minutes after strains were mixed.

TonB-dependent receptors are outer membrane channels that facilitate the import of specific substrates, powered by the TonB complex that couples the import process with the proton gradient across the inner membrane (Krewulak and Vogel, 2011), suggesting that Cdz toxins could be using this TonB-dependent receptor, encoded by CCNA_03108, for import into and access to the periplasm or cytoplasm of target cells.

Previously, using propidium iodide staining, we showed that cdz-mediated killing leads to disruption of cell membrane integrity after several hours in competition (García-Bayona et al., 2017). Remarkably, all the suppressor mutations identified in the screen corresponded to

putative envelope-associated genes, further suggesting that the Cdz toxins kill the target cell by disrupting the cell envelope. We therefore directly tested the effect of Cdz on membrane potential by using the fluorescent anionic lipophilic dye $DiBAC_4(3)$, which can only enter cells with depolarized membranes (Fig. 3.1C). When stationary phase wild-type producer cells where mixed at an equal ratio with a *ΔcdzCDI* indicator, half of the cells were DiBAC-positive 30 minutes after mixing, indicating that Cdz causes rapid membrane depolarization (loss of the proton gradient across the inner membrane). In contrast, when each strain was grown separately, most cells remained DiBAC-negative. Finally, we selected 2 of the suppressor strains identified in the screen (one for each of the two characterized suppressor genes described below), to carry out competitions against a wild-type Cdz-producer strain. In both cases, the cells remained DiBAC negative, indicating that they are resistant to Cdz-mediated membrane depolarization. These suppressors also retained full viability by Colony Forming Unit counts.

Increased expression of the envelope-associated *zerRAB* operon confers resistance to Cdz

Three suppressor isolates had mutations mapping to the CCNA_03519/20/21 locus, predicted to be a three gene operon based on RNA-seq data (Schrader et al., 2014). We named these genes *zerRAB* for zipper envelope resistance. Two of the suppressors had the same mutation, which arose independently in separate competition experiments. This single nucleotide substitution falls within the promoter region of the three gene operon, 38 bp upstream of the annotated transcription start site (Schrader et al., 2014). The other mutation is a non-synonymous L59P substitution in ZerR, a predicted transcriptional repressor of the PadR family. To determine the effect of these mutations on expression of the *zerRAB* operon, we used a transcriptional reporter construct where the promoter region and coding sequence of *zerR* were placed upstream of the coding sequence for Venus fluorescent protein (Fig 3.2A). When cells were grown to exponential or stationary phase and their individual fluorescence was evaluated by epi-fluorescence microscopy, fluorescence was substantially higher in the strains harboring the Cdz suppressor mutations compared to an isogenic wild-type reporter strain, indicating that these mutations led to an upregulation of the *zerRAB* operon in exponential and stationary phase.

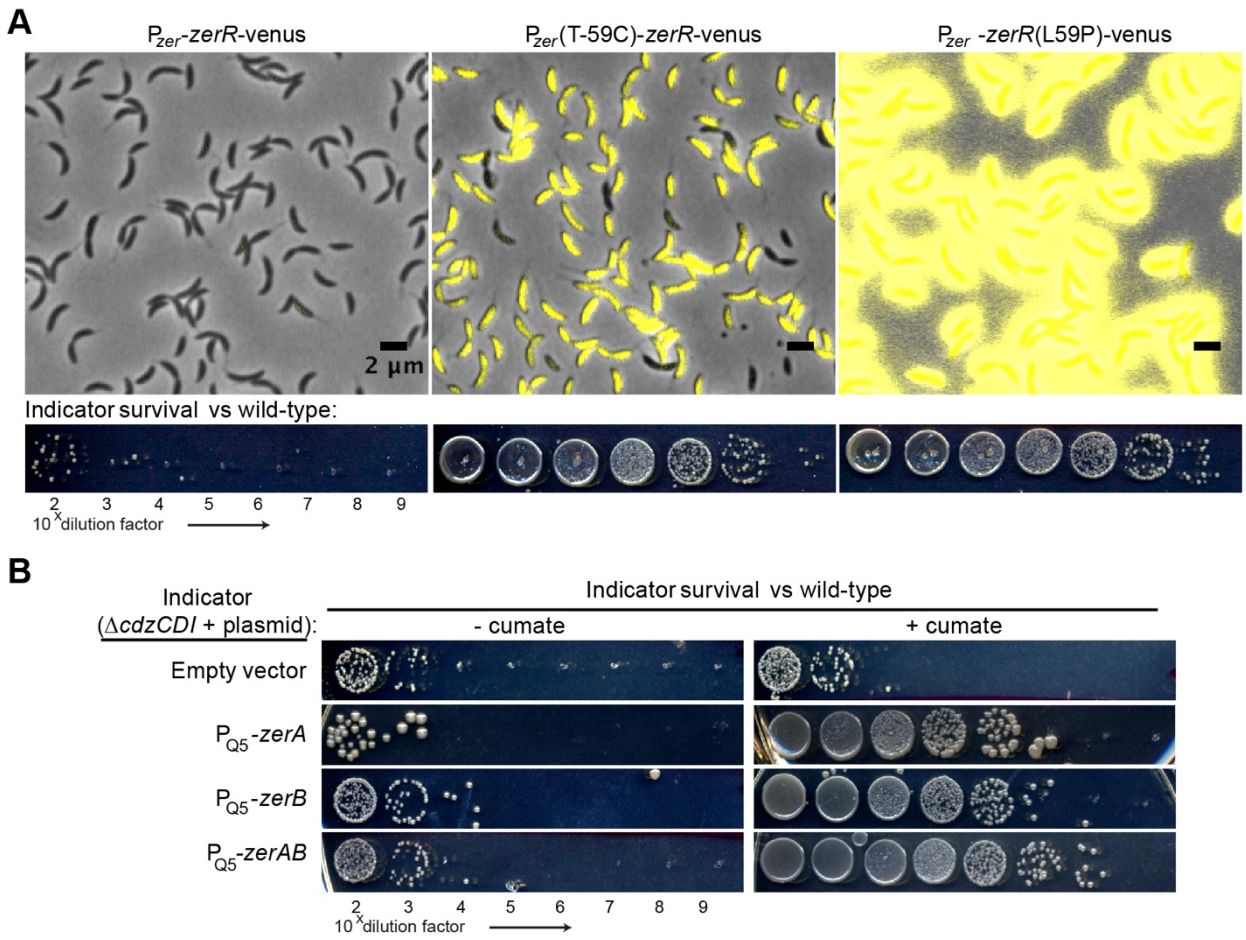

Figure 3.2. Increased expression of the *zerRAB* operon leads to Cdz resistance. A. Venus transcriptional reporter of the wild-type or mutated versions of P_{zerR}-zerR. Underneath is the survival of each mutant in a competition with a Cdz producer. **B.** Survival of an indicator strain expressing the indicated construct under the cumate promoter (P_{Q5}), in competition with a wild-type Cdz producer.

To pinpoint which of the genes in the *zerRAB* operon was responsible for the resistance to Cdz toxins, we made strains in which each gene was individually overexpressed or with *zerAB* both overexpressed. Each construct was controlled by a cumate-inducible promoter (Kaczmarczyk et al., 2013) on a chromosomal integration and was expressed in a Δ*cdzCDI* background. Expression was induced in early-log phase for 12h prior to mixing with the Cdz producer. Production of *zerA* as well as *zerB* alone led to a 4-log increase in survival in competition with a wild-type producer strain, while the overexpression of *zerAB* together was sufficient to reduce Cdz-mediated killing by almost 5 logs (Fig 3.2B). These results suggest that production of either ZerA or ZerB, or both can protect cells. The fact that expressing ZerA or ZerB alone did not provide as much resistance

as expressing ZerAB together suggests that the relative stoichiometry of ZerA and ZerB may be important for full protection, or that both carry complementary biological activities.

To understand the role of *zerRAB* in Cdz toxin resistance, we sought to better characterize their physiological roles. ZerA and ZerB are predicted to have one and three transmembrane spans, respectively, with each also containing a predicted periplasmic domain of unknown function (Fig. 3.3A). For ZerB this periplasmic domain is predicted to be a trimeric auto-transporter adhesin (TAA) head domain. This family of proteins adopts a β-roll fold and has characteristic repeats centered around GSG motifs that allow a tight β turn. This family of proteins may have a role in cell-cell adhesion (autoagglutination) and in attachment to host cells, like classic auto-transporter adhesins. However, previously characterized auto-transporter adhesins are large extracellular proteins that also include an outer membrane β-barrel anchor and a long stalk (Nummelin et al., 2004), whereas ZerB has only the adhesin head domain and is predicted to be anchored to the inner membrane. The head domain of auto-transporters usually bind to high molecular weight extracellular matrix components such as collagen or fibronectin (Nummelin et al., 2004). We speculate that ZerB may interact with other structural components of the cell envelope, such as peptidoglycan or MreC filaments (Dye et al., 2005). This hypothesis is consistent with the observation that both *zerRAB* suppressors identified have significantly decreased cell curvature (Fig 3.3C).

Figure 3.3. Expression of the *zerRAB* causes cell-envelope and morphology alterations. A. Schematic representation of the predicted topology of ZerA and ZerB. TM = transmembrane domain predicted by TMHMM. **B.** Western blots of the indicated cell fractions from a culture of cells producing HA-tagged ZerA or ZerB from a chromosomal insertion under the cumate promoter and grown to stationary phase. RpoA, McpA, and $RsaF_a$ serve as controls for cytoplasmic, inner membrane, and outer membrane fractions, respectively. **C.** Phase microscopy of the parental strain Δ*cdzCDI* and the suppressor strains with mutated versions of P_{zerR}-zerR. **D.** Phase microscopy of *ΔcdzCDI* cells overexpressing the indicated construct under the cumate promoter (P_{Q5}). Red arrows indicate bent stalks, white arrow indicates lysing cell. **E.** Transmission electron micrographs of a normal stalk (empty vector control strain) or abnormal stalks from a strain overexpressing ZerB.

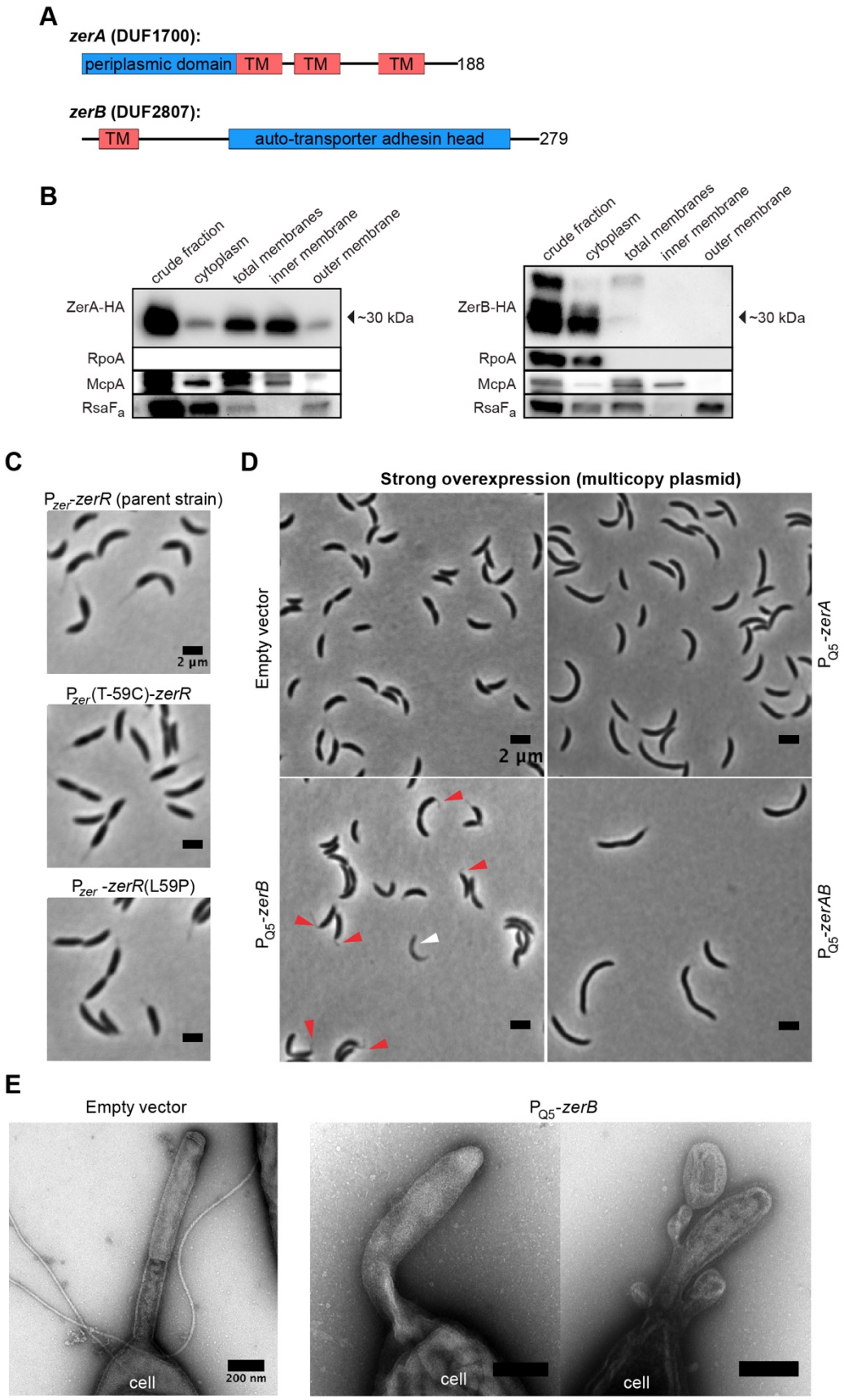
A
zerA (DUF1700):
periplasmic domain
TM
TM
TM
188
zerB (DUF2807):
TM
auto-transporter adhesin head
279
B
crude fraction
cytoplasm
total membranes
inner membrane
outer membrane
ZerA-HA
~30 kDa
RpoA
McpA
RsaFa
ZerB-HA
~30 kDa
C
Pzer-zerR (parent strain)
2 µm
Pzer(T-59C)-zerR
Pzer -zerR(L59P)
D
Strong overexpression (multicopy plasmid)
Empty vector
PQ5-zerA
PQ5-zerB
PQ5-zerAB
2 µm
E
Empty vector
PQ5-zerB
cell
200 nm
cell
cell

To further characterize the subcellular localization of ZerA and ZerB, we performed cell fractionation experiments on cells producing HA-tagged variants (Fig 3.3B). These epitope-tagged ZerA and ZerB were fully functional with respect to conferring immunity to a Cdz producer. The fractionation experiments confirmed that ZerA primarily localized to the inner membrane. In contrast, the full length ZerB could only be detected as a faint band in the total membrane fraction, while the most abundant species appeared to be a cytosolic smaller processed version. The fact that the full length ZerB could not be detected in the inner membrane is probably due to the loss of protein during the fractionation procedure. As controls for the fractionation procedure, we verified by immunoblotting that RpoA, a subunit of RNA polymerase, was found predominantly in the cytoplasmic fraction; the chemoreceptor McpA was found in the total membrane and inner membrane fractions; and $RsaF_a$, a protein involved in S-layer production, was found primarily in the total membrane and outer membrane fractions.

To probe the role of ZerA and ZerB in *Caulobacter*, we evaluated the effect of their overexpression from a multi-copy plasmid on growth and morphology (Fig. 3.3D). Strains carrying individual overexpression constructs or producing both genes were grown to mid-exponential phase, supplemented with inducer and diluted back to early exponential phase to evaluate their growth rate (Fig 3.4). For all three constructs, induction lead to impaired growth, indicating that the overexpression levels achieved were harmful for the cells. After 4 hours of induction, cells overexpressing *zerA* were somewhat elongated and filamentous (Fig. 3.3D), indicating that cell division was impaired. The phenotype of a *zerB* overexpression strain was more subtle, with polar stalks often shorter than normal or bent (Fig. 3.3D). When visualized by transmission electron microscopy and negative staining, the stalks of this strain frequently appeared bent or showed severe blebbing (Fig 3.3E). The *zerB* overexpression strain also exhibited some evidence of lysis, with a small frequency of "ghost" cells (Fig. 3.3D). The co-expression of both *zerA* and *zerB* led to a significant growth defect, with cellular filamentation and altered cell shape. Instead of appearing strictly crescent shaped, these cells also displayed an irregular morphology, with strong kinks in the contour of cells rather that a gradual curvature. These changes in cellular morphology could reflect changes in cell envelope composition or structure, possibly explaining the increased resistance to Cdz toxin-dependent killing when ZerA and ZerB are overproduced.

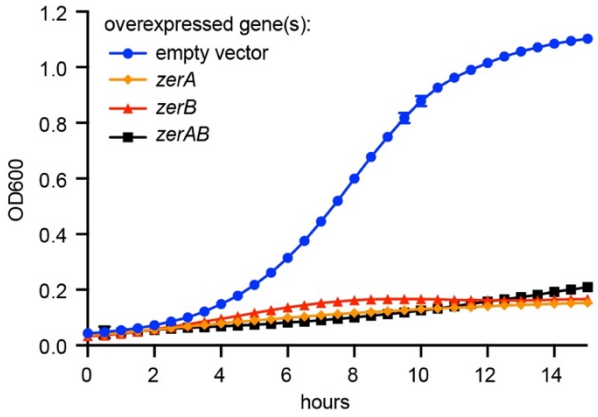

Figure 3.4. *zerA/B* overexpression inhibits growth. Growth curves in rich medium with cumate to induce overexpression of the indicated genes, in a *ΔcdzCDI* strain. Data points are mean of four independent cultures; error bars indicate standard deviation (S.D.), not shown when smaller than the symbol.

Consistent with the notion that the upregulation of *zerRAB* protects cells against Cdz toxins by leading to changes in cell surface composition, we noted that *zerRAB* was previously reported to be up-regulated ~14-fold by the UzcRS two-component system, and has a UzcR binding box in its promoter region. The UzcRS system regulates a metal-induced (UO_2^{2+}, Zn^{2+}, Cu^{2+}) extracytoplasmic stress response independent of the canonical cell envelope stress response. The signal that activates the system is likely not to be the metals themselves, but cell envelope damage caused when they are at toxic concentrations (Park et al., 2017).

The pentapeptide-repeat protein PerA probably acts as the CdzC/D surface receptor

We obtained four independent suppressors with mutations mapping to the gene CCNA_01968, which is a hypothetical pentapeptide-repeat protein of unknown function. We named this gene *perA* (pentapeptide envelope resistance A). One of the suppressor mutations was a deletion of the whole promoter region and 5' region of the *perA* gene. The other mutations were smaller in-frame deletions (5 or 35 residues) in the core of the protein or a frameshift leading to a truncation at the C-terminus (missing residues 234 to 238). To determine if the suppressors identified were loss-of-function mutations, we introduced an ectopic copy of the wild-type *perA* gene into each of the suppressor strains and tested them in competition with a wild-type producer (Fig 3.5A). In each case, the presence of a wild-type copy of *perA* restored sensitivity to the wild-type producer.

To test if a *perA* null strain also conferred resistance to killing by Cdz toxins, we constructed a strain in which the entire *perA* coding region was deleted. The *perA* gene was previously suggested to be essential for viability based on a saturating transposon insertion screen in rich medium (Christen et al., 2011). However, we were able to make a viable *ΔperA* deletion strain, although this strain caused a significant growth defect discussed below. Despite this growth defect, *ΔperA ΔcdzCDI* cells showed nearly complete survival in competition with a Cdz producer. Expression of a full-length copy of *perA* resensitized the Δ*perA* strain to killing (Fig 3.5A). These results confirm that the loss of PerA function leads to resistance against Cdz toxins.

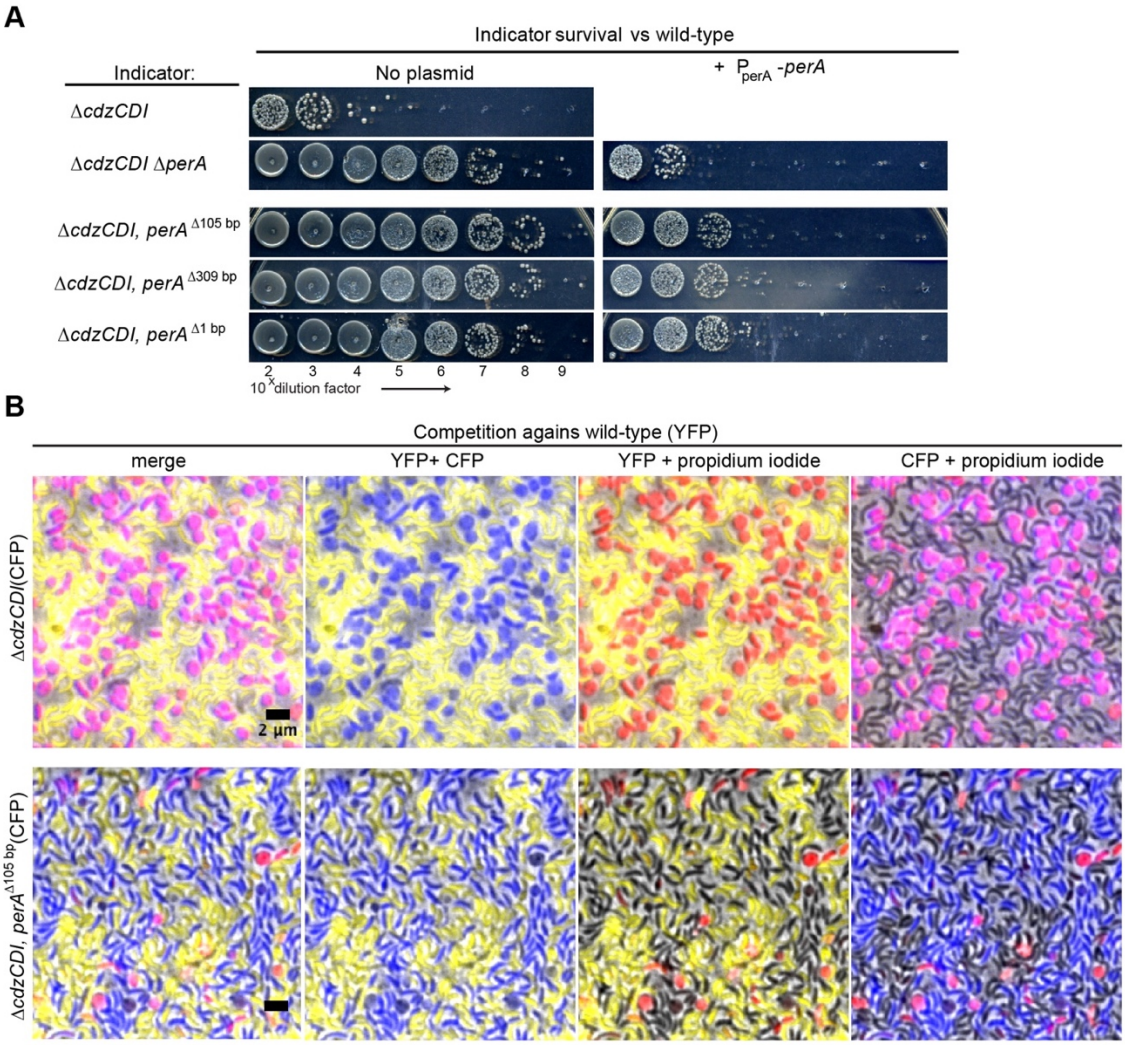

Figure 3.5. PerA acts as a receptor for Cdz. A. Survival of the indicated strains in competition with a wild-type Cdz producer. **B.** Competition of the indicated strains (expressing CFP) against a wild-type Cdz producer expressing YFP, in agarose pads with propidium iodide (PI). Images correspond to day 3.

PerA has a predicted secretion leader sequence and, according to an outer-membrane proteomics study, is associated with the outer membrane (Cao et al., 2012). To further probe the subcellular localization of PerA, we performed cell fractionation of a strain expressing an HA-tagged perA, which confirmed that PerA localizes to the outer membrane (Fig 3.6A). To determine its specific localization along the cell, we made a translational fusion of PerA to mCherry, driven by the native *perA* promoter. This fusion protein was functional, as it restored normal cell morphology to a *ΔperA* deletion strain. PerA appeared primarily envelope-associated in a mostly homogeneous manner (Fig. 3.6B) and did not localize to specific parts of the cells such as the poles or mid-cell.

To determine whether PerA is surface-exposed, we used immunofluorescence in a strain expressing HA-tagged PerA and lacking *manB*, a gene required for exopolysaccharide production (Gandham et al., 2012), and *rsaA*, which encodes the proteinaceous S-layer capsule (Ford et al., 2007). In this background, we could detect PerA in the surface of unpermeabilized cells (Fig. 3.6C), indicating that PerA associates with the outer-leaflet of the outer membrane, facing the extracellular environment. In contrast, no signal was detected in a control without addition of the anti-HA antibody. Additionally, we used a strain expressing HA-tagged CdzI, which localizes to the inner membrane, as a control that the cells were not being accidentally permeabilized during the immunofluorescence procedure.

As noted above, pentapeptide repeat proteins are predicted to form β-helix structures. Notably, the CdiA toxins in *E. coli* and related species also form right-handed β-helical proteins that can promote adhesion to target cells to mediate contact-dependent inhibition (Nummelin et al., 2004; Ruhe et al., 2015a). We therefore hypothesized that PerA may mediate cell-cell attachment in *C. crescentus*. To test this hypothesis, we forced cell-cell contact between producer and target cells by conducting the competition experiments in agarose pads, where the cells form a dense multi-layer lawn. If the main mechanism by which PerA confers Cdz-sensitivity is to promote cell-cell attachment, this experimental set-up would by-pass the requirement for perA, *i.e.* a perA mutation should no longer confer protection against killing when cells are in direct contact in the pad.

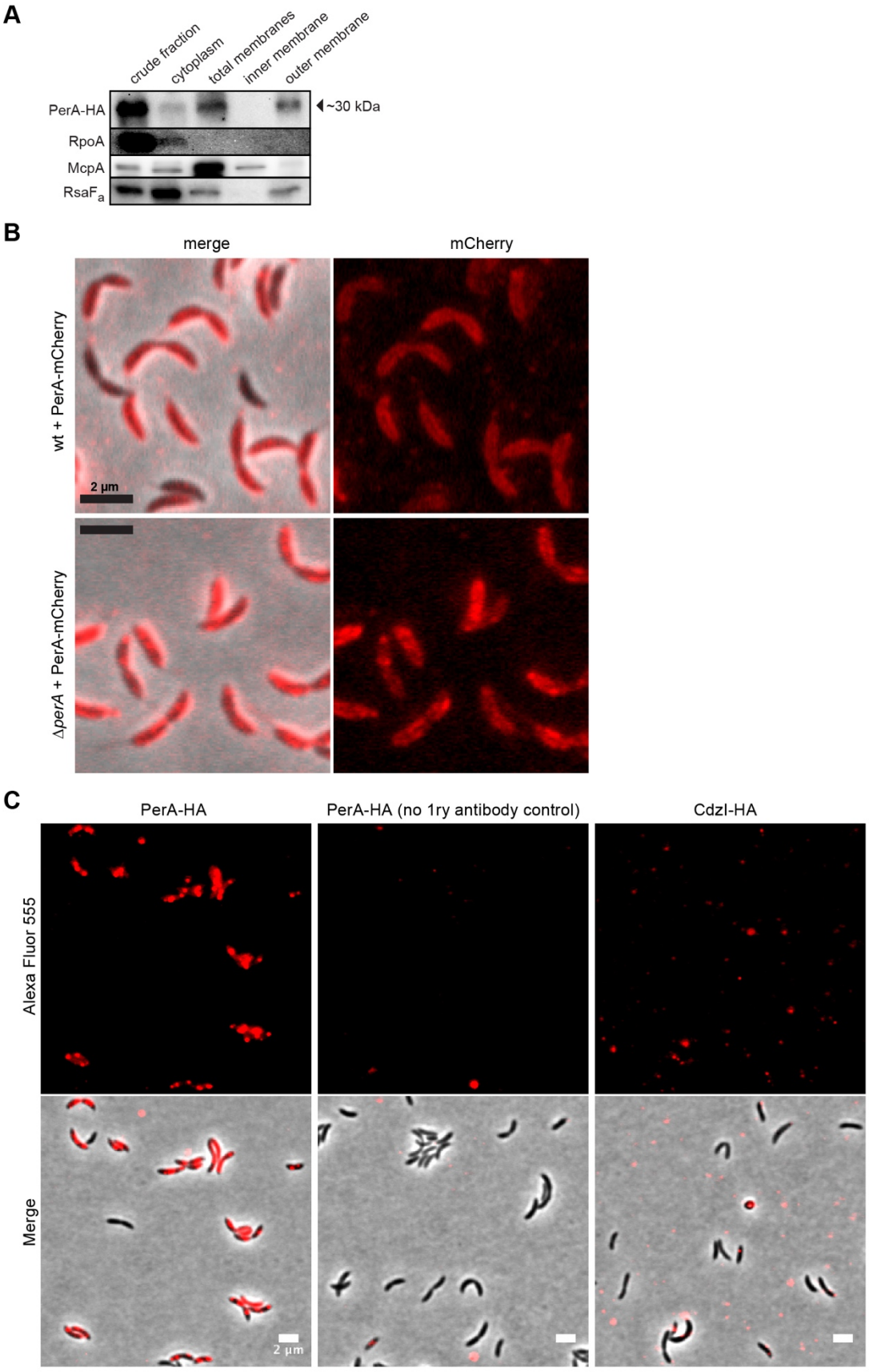
A
crude fraction
cytoplasm
total membranes
inner membrane
outer membrane
PerA-HA
RpoA
McpA
RsaF$_a$
~30 kDa
B
merge
mCherry
wt + PerA-mCherry
2 µm
ΔperA + PerA-mCherry
C
PerA-HA
PerA-HA (no 1ry antibody control)
CdzI-HA
Alexa Fluor 555
Merge
2 µm

Figure 3.6. PerA is a surface-exposed outer membrane protein. A. Western blots of the indicated cell fractions from a culture of cells producing HA-tagged PerA. RpoA, McpA, and $RsaF_a$ serve as controls for cytoplasmic, inner membrane, and outer membrane fractions, respectively. **B.** Cellular localization of PerA-mCherry in a wild-type or *ΔperA* background**. C.** Immunofluorescence of *ΔmanB ΔrsaA* cells, expressing an HA-tagged PerA or CdzI.

We used fluorescent protein markers to identify the two strains, and conducted the competition in the presence of propidium iodide (PI) as a marker for cell death. After three days in co-culture, the cells were blotted onto a coverslip and observed under the microscope. In a competition between a wild-type producer (YFP) and a *ΔcdzCDI* indicator (CFP), the vast majority of target cells had been killed by day three (Fig 3.5B). In contrast, a competition of the suppressor strain harboring the $PerA^{\Delta 105\ bp}$ allele did not show any evidence of killing despite the enforced cell-cell contact. This result suggests that PerA is not mediating cell-cell adhesion as a means of promoting killing by Cdz toxins. Instead, PerA may contribute to Cdz-dependent killing by serving as a receptor for the Cdz toxins or by promoting a cell envelope structure or composition that is compatible with killing.

PerA is required for normal cell envelope homeostasis

To test whether the mutations identified in *perA* render cells resistant to Cdz toxins by altering the cell envelope, as suggested for *zerRAB*, we sought to characterize the PerA protein and its molecular function. As noted, *perA* is an envelope-associated gene but its function is uncharacterized. Fig. 3.7A highlights the main sequence features of this pentapeptide-repeat protein in *C. crescentus* and some of its close relatives. This gene is fairly conserved in many of the close *Caulobacter* relatives, and its more distant homologs are ubiquitous in α-proteobacteria. The protein has 25 repeats of the [ASV][DEN][AFILM]XX motif, where X is any amino acid. Each occurrence of the repeat is thought to represent one of the sides of the right-handed quadrilateral β-helix fold that the protein is predicted to assume (Fig. 3.7B). PerA is predicted to have a highly regular structure with one excursion, a small protruding loop. The predicted core of the helix is mostly composed of hydrophobic residues, while the outside surface has polar and charged residues. The other striking feature of PerA is that, in contrast to other PPRs, it has a proline-rich and positively charged C-terminus.

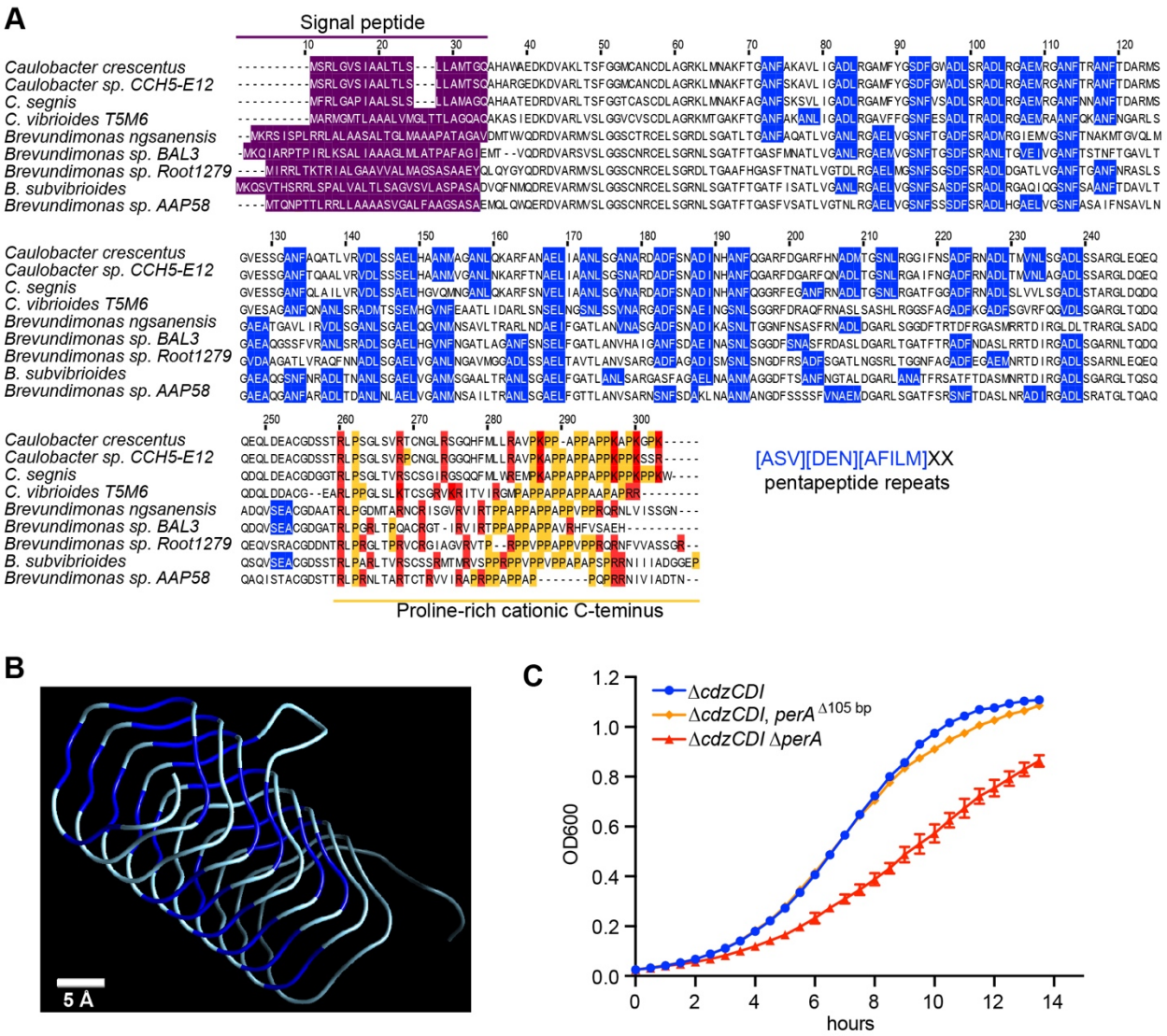

Figure 3.7. PerA is a pentapeptide-repeat protein required for normal cell growth. A. Multiple sequence alignment of PerA homologs from *C. crescentus* and other close relatives. Blue boxes represent instances of the first 3 residues of the pentapeptide-repeat motif. Prolines are indicated in yellow and positively charged residues at the C-terminus in red. **B**. Representation of the predicted 3D structure for the PPR domain (excluding the secretion leader and the C-terminus), made using threading on structure 4YFOA. **C.** Growth curves of the indicated strains in rich medium. Data points are mean of three independent cultures; error bars indicate standard deviation (S.D.)

A strain harboring a deletion of *perA* exhibited a significant growth defect in rich medium (Fig. 3.7C), with slower forming colonies on plates (3 days instead of 2) and a 29% slower growth rate in liquid culture in exponential phase, which can be corrected to normal by introduction of an ectopic copy of *perA*. The *perA* deletion strain also exhibited significant morphological aberrations (Fig. 3.8A). The surface of the cells appeared irregular, with some evidence of blebbing and regions of increased cell width. Additionally, rather than being crescent-shaped, the

cells were straight, and some cells were filamentous, often with several constriction sites (Fig 3.8A).

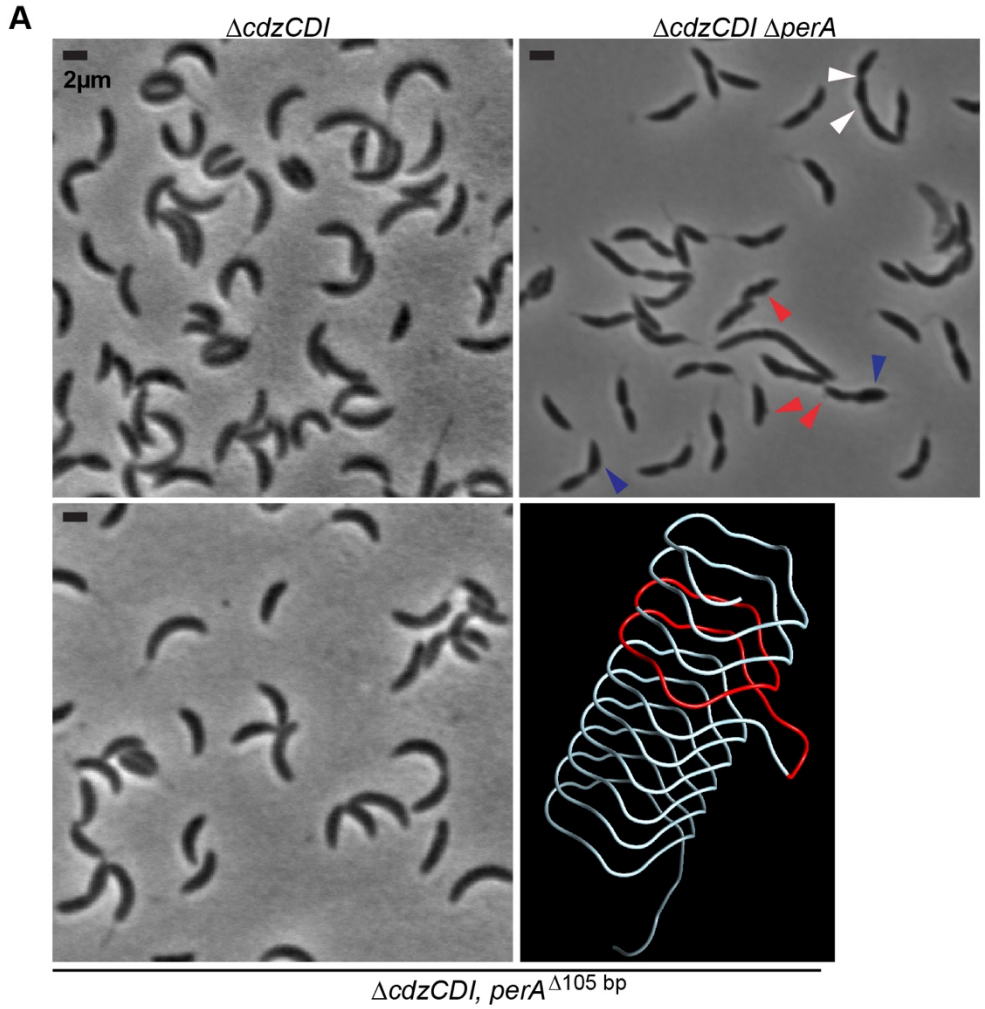

Figure 3.8. Altered cell morphology caused by a perA deletion. A. Phase micrographs of the indicated strains. For the *ΔcdzCDIΔperA* image, red arrows point at membrane blebs, blue arrows indicate cells with increased cell width and white arrows show pinching sites in a filamentous cell. Depletion image corresponds to 2 days without inducer, keeping the cells in exponential phase. The 3D structure (see Fig. 3.6A legend) illustrates in red the region that is deleted in the $perA^{\Delta 105\ bp}$ allele. **B.** Cell length of the indicated strains. A minimum of 200 cells in 3 independent frames were analyzed. Mean of the populations differs with $p<0.0001$ in an unpaired t-test.

The morphological defects of the *perA* deletion strain may reflect changes in the cell envelope, which could explain the Cdz-resistance of cells harboring loss-of-function mutations in *perA*. However, notably, the suppressor strain carrying the $perA^{\Delta 105\ bp}$ allele did not exhibit the same growth defects (Fig. 3.7C) or morphological anomalies (Fig. 3.8A) as the *perA* deletion strain. The $perA^{\Delta 105\ bp}$ cells had a slightly increased average cell length (11%, Fig. 3.8B), indicating that cell division may be somewhat delayed. These results indicate that this allele, which corresponds to roughly two turns of the β-helix and part of the protruding loop (Fig 3.8A), leads to a mostly functional protein. Additionally, this allele generally uncouples the role of PerA in cellular morphology from its role in Cdz. Thus, we conclude that PerA may serve as the direct surface receptor for Cdz toxins.

DISCUSSION

Use of spontaneous suppressor mutations and deep sequencing to identify genes involved in bacteriocin sensitivity

Suppressor screens to identify bacteriocin receptors and/or targets are often based on the use of transposon mutagenesis (Bieler et al., 2006; Roelofs et al., 2016). More recently, some studies have successfully used the same experimental setup used in this report, based on selection of spontaneous suppressor mutations and whole genome sequencing, to identify the surface receptor of two two-peptide bacteriocins and a lectin binding pyocin (Kjos et al., 2014; McCaughey et al., 2014; Oppegard et al., 2016). Although arguably more expensive than a transposon insertion library, this approach has the advantage of allowing other types of mutations in addition to loss-of-function mutations. One obvious advantage of this is that it permits the identification of mutations in essential genes that would not be found otherwise. Indeed, many bacteriocins target essential genes such as gyrase or RNA-polymerase and some bacteriocin receptors are also essential genes (Cotter et al., 2012; Rea et al., 2011; Rebuffat, 2011). Therefore, in cases where a good reference genome is available, whole genome sequencing may provide more discovery power. Using this approach, we were able to identify the putative receptor and likely outer membrane transporter that are required for import of the Cdz toxin into target cells of *C. crescentus*. The screen, using a new type of envelope-acting bacteriocin, also led to the discovery of three genes with domains of unknown function that appear to have important roles in envelope remodeling either in normal growth conditions or under specific types of envelope stress.

Considering that two of the loci with a suppressor mutations were only observed on one strain, we believe that more genes may remain undiscovered that affect sensitivity or resistance to Cdz. For instance, we were not able to identify the gene(s) that mediates the cell-cell attachment previously observed by flow cytometry and required for contact-dependent killing (García-Bayona et al., 2017). In order to increase the chances of obtaining mutations in the adhesion genes, a new screen could be conducted where the target strain has two *perA* copies and a *zerRAB* deletion so as to avoid re-sequencing of the already identified mutations. Additionally,

the competitions could be conducted in diluted growth medium where the cells reach up to 10-fold less cell density yet are still subject to Cdz-mediated killing. However, this observation suggests that adhesion may require a mutation in the producer cell rather than the target cell, or a mutation may be required in both target and producer cells simultaneously. In this case, a screen of producer cells that can't kill would be more likely to be successful.

A new type of receptor for a new type of toxin

The recently described Cdz system from the oligotrophic aquatic bacterium *Caulobacter crescentus* differs from other characterized bacteriocins in terms of sequence (hydrophobic core with an extended glycine zipper) and ability to aggregate and kill in a contact-dependent manner (García-Bayona et al., 2017). However, similar to many characterized bacteriocins, the main mechanism by which Cdz kills target cells is likely through membrane permeabilization leading to loss of the proton gradient across the inner membrane. This effect is likely to be somewhat specific to small cations, as the membrane of the producer cells become depolarized almost immediately after contact with a Cdz-producer, whereas general permeability to propidium iodide takes place at a longer time scale (several hours) (García-Bayona et al., 2017).

The putative Cdz-receptor, PerA, is different to the receptors of any other characterized bacteriocin, usually integral outer membrane proteins or lipopolysaccharide (LPS) (Cotter et al., 2012; McCaughey et al., 2014; de Zamaroczy and Chauleau, 2011). This pentapeptide-repeat gene is expected to associate with the outer leaflet of the outer-membrane and allow anchoring of the Cdz toxins to the target cell, likely prior to import across the outer membrane via a TonB-dependent receptor. These results need to be validated further by showing that there is a direct interaction between CdzC/D and PerA, since it is formally possible that PerA may be upstream in a regulatory cascade of the real Cdz receptor. Although unlikely, PerA could also act as a direct target of the Cdz toxins. This possibility can be ruled out by making an endogenous expression construct of the mature Cdz toxin pair, which should now be toxic in a *ΔperA* strain if this protein acts as surface receptor.

Similarly, TonB mediated import through CCNA_03108 has only been suggested by the identification of a suppressor mutation, but needs to be properly confirmed. An alternative explanation is that this outer membrane protein could be used as an anchor by the cryptic adhesin, akin to the role of BamA in mediating attachment to the adhesion regions of CdiA in the Cdi contact-dependent killing system (Ruhe et al., 2015b).

A newly identified member of the pentapeptide-repeat family has a role in envelope homeostasis

Few members of the ubiquitous pentapeptide repeat family have been characterized to date, and most are cytosolic (Knodler et al., 2004; Ni et al., 2009; Strahilevitz et al., 2009). PerA, in contrast appears to be envelope-associated and to play an important role in envelope maintenance. The repeat motif in PerA, [ASV][DEN][AFILM]XX, indicates that a glutamate can also be tolerated in the second position, in addition to the previously described aspartate and asparagine. Based on the polar/charged exposed surface of PerA, it is unlikely that it is an integral outer membrane protein. We hypothesize that the proline-rich cationic C-terminus may mediate anchoring PerA to the negatively charged LPS surface, or could play a role in protein-protein interactions.

How an extracellular protein could affect cell shape and envelope integrity remains an open question. The phenotype of a *perA* deletion is suggestive of outer membrane alterations, and although viable, this strain has a significant growth defect. However, the absence of PerA does not generally alter outer membrane permeability. We speculate that PerA may play a role in regulation of other membrane properties such as membrane fluidity or distribution of other membrane proteins. The cells lose their characteristic crescent shape, becoming straight or bent at sharper angles than normal. In *C. crescentus* curvature is mainly determined by crescentin filaments which associate to the inner membrane on the cytosolic side, and regulate incorporation of new glycan strands into the peptidoglycan (Cabeen et al., 2009). It has been previously shown that an altered form of O-antigen on LPS leads to loss of cell curvature, although the mechanism remains unclear (Cabeen et al., 2010). In order to identify the connection between the shape determining inner-membrane/periplasmic proteins and the likely surface

protein PerA, a genetic screen could be conducted for mutations that rescue a *perA* deletion under conditions that are lethal for this strain (e.g. in the presence of PI). We are also currently conducting a pull-down experiment to identify potential interaction partners.

Although PerA is very important for normal growth in rich medium, RNAseq experiments and our PerA-mCherry microscopy indicate that the gene is expressed at low levels under these conditions. In contrast, under cationic metal stress (Cu^{2+}, Zn^{2+}, UO_2^{2+}), *perA* expression is upregulated as part of the putative envelope stress response mediated by the two-component system UzcRS (Park et al., 2017). Therefore, although not strictly essential under optimal growth conditions, PerA is expected to be crucial for survival under more challenging conditions. From an evolutionary perspective, a bacteriocin that preys on a receptor that is essential to the target cell is less likely to lead to the emergence of resistance, as most mutations in the receptor will incur a significant fitness cost. Therefore, producer cells would be expected to have a fitness advantage over resistant cells, despite the energetic cost of producing the toxin. Likewise, resistant alleles would be unlikely to remain in the population in the absence of bacteriocin.

Newly identified envelope remodeling genes in *C. crescentus*

Interestingly, upregulation of another operon of inner-membrane/periplasmic genes from the UzcRS response also leads to resistance to Cdz-mediated killing. The *zerAB* genes are also thought to play an envelope remodeling role, as hinted by the morphological alterations in the suppressor and the overexpression strains. Several types of envelope stress responses, mediated by different types of regulators have been described in *E. coli,* to respond to different types of stress such as osmotic challenge (EnvZ/OmpR two-component system) and LPS/OM damage caused by cationic antimicrobial peptides (σ^E, CpxAR). In the latter case, cells respond by inducing extracellular polysaccharide production and LPS-modifying enzymes (Dalebroux and Miller, 2014; Egger et al., 1997; Konovalova et al., 2016). We postulate that *zerAB* suppression of Cdz-mediated killing may occur through a similar mechanism, albeit in the periplasm and/or inner membrane. It is possible that ZerA/B may have physiological effects that counteract the toxic activity of CdzA/B or decrease permeability to it and may be indicative that the Cdz toxins are not merely disrupting the inner membrane in a detergent-like fashion. Indeed, for pore-forming bacteriocins,

mechanisms of resistance often involve changes in the membrane (composition, charge or fluidity) or peptidoglycan layer properties (thickness, charge, degree of cross-linking) (Dicks et al., 2011).

MATERIALS AND METHODS

Bacterial strains and growth conditions

All oligonucleotides, strains and plasmids used in this study are listed in Tables 3.1, 3.2 and 3.3, respectively, along with details of how each strain was constructed. *E. coli* strains were grown at 37°C in LB medium. *C. crescentus* strains were grown at 30°C in PYE. Media were supplemented, as necessary, with a final concentration of 1 mM IPTG, or 50 µM cumate (4- isopropylbenzoic acid, stock in 100% ethanol) to induce expression from the P_{lac}, and P_{Q5} promoters, respectively. Antibiotics were used at the following concentrations (liquid/solid media for *E. coli*; liquid/solid media for *C. crescentus*; in mg/ml): oxytetracycline (12/12; 1/2), kanamycin (30/50; 5/25), gentamycin (15/20; NA/5).

Competition experiments

Co-culture competition experiments in liquid culture were conducted as described previously (García-Bayona et al., 2017). For competitions with indicator strains expressing *zerA*, *zerB* or *zerAB*, we used strains carrying a chromosomal insertion at the vanillate locus of *zerA*/*B*/*AB* under the cumate promoter PQ_5 along with its repressor (Kaczmarczyk et al., 2013). Each strain was grown to exponential phase, diluted to an OD_{600} of 0.01 and the culture was supplemented with 50 µM cumate. Cells were mixed with the producer strain after 13 hours of induction.

For competitions in agarose pads, cells were grown in medium supplemented with IPTG. At 0.9 OD, indicator and producer strains were mixed at a 1:1 volume ratio, diluted 1:3 in PYE and 10 µL and spread on a 24 x 24 mm 1.5% low melt agarose pad of 900 µL PYE supplemented with IPTG and 1 µM PI. After drying of the cell droplet, pads were incubated in a humid chamber at 30°C for 3 days in the dark. At time zero and at every 24 hour interval, cells were imaged. For time points after 24h, pads were blotted several times against a 24 x 60 mm coverslip to remove excess cells, and the coverslip blots were imaged, choosing frames were a monolayer of cells was visible.

Suppressor screening and mapping

Competition experiments were conducted in liquid culture as specified, but plating on selective media was done after 20 hours. Isolated indicator colonies were re-streaked in selective plates. These isolates were subjected to a second round of competition, and those that exhibited full resistance were imaged as described below after IPTG induction in liquid medium to verify presence of the expected fluorescent protein marker. Whole genome sequencing of the parental and suppressor strains was conducted using Illumina as previously described (Jonas et al., 2013). Mutations were mapped to the reference genome using breseq (Deatherage and Barrick, 2014). Genomic regions corresponding to the mapped mutations were amplified by PCR and sequenced by Sanger sequencing.

Membrane depolarization staining

Each strain was grown separately to stationary phase and they were mixed at an equal volume ratio. A 200 µL aliquot was collected 30 minutes after mixing, and stained with bis-[1,3-dibutylbarbiturate] trimethine oxonol ($DiBAC_4(3)$) as described by (Smit et al., 2000), with modifications. Briefly, cells were collected by centrifugation and re-suspended in 200 µL M2 salts medium, followed by centrifugation and resuspension in 200 µL M2 salts with 1µg/ml $DiBAC_4(3)$. After incubation with shaking at 30ºC for 10 minutes, cells were collected by centrifugation and re-suspended in 400 µL M2 salts medium and spotted on agarose pads for fluorescence microscopy on the GFP channel.

Fluorescence and transmission electron microscopy

For evaluation of morphology of the overexpresion of *zerA* and *zerB* alone or together, we used strains carrying the respective construct under the cumate promoter on a multicopy plasmid. Cells were grown to 0.2 OD, supplemented with cumate and incubated for 4 hours prior to imaging.

Phase and fluorescence microscopy were carried out as previously described (García-Bayona et al., 2017). The following emission/excitation filters were used: YFP, 500/25 and 535/30m; CFP, 436/25 and 480/40; mCherry, 560/40 and 630/75; GFP, S470/40 and 520/40. Image analysis to quantify cell length was calculated using MicrobeJ (Ducret et al., 2016).

Samples for electron microscopy were grown to 0.2 OD, supplemented with cumate and incubated for 8 hours prior to imaging. Negative staining with 2% uranyl acetate and transmission electron microscopy were done as specified in (García-Bayona et al., 2017).

Triton X-100 fractionation and western blotting

Induction of the HA-tagged ZerA or ZerB was carried out in the same way as for competition experiments. Samples for fractionation were collected after 13 hours. Induction of HA-tagged PerA was done by supplementing an exponential phase culture at OD_{600} 0.15 with 10 µM cumate and samples were collected after 6 hours. Triton X-100 cell fractionation and immunoblotting were carried out as described in (García-Bayona et al., 2017).

Immunofluorescence

For immunofluorescence, cells were grown to an OD_{600} of 0.2 and supplemented with 10 µM cumate to induce the expression of HA-tagged PerA. Samples were collected after 7 hours of induction and immunofluorescence was carried out as described previously (García-Bayona et al., 2017). In order to reduce background, one additional wash step with fresh PYE was added after incubation in primary antibody, and two additional wash steps with fresh PYE after incubation in secondary antibody.

Alignment visualization and 3D model prediction

Protein structures were predicted by threading using RaptorX (Kallberg et al., 2012) and visualized using Chimera (Pettersen et al., 2004). Multiple sequence alignments were conducted using ClustalW (Thompson et al., 2002) and visualized using Jalview (Waterhouse et al., 2009).

Table 3.1. Oligonucleotides

Name	Sequence
oLG294	TTCGGGCGCGGAGATGGATC (PCR *perA* for sequencing)
oLG295	GCTTCGCAGGCCATTACAGGTG (PCR perA for sequencing)
oLG296	GCTGAGCATGGGAACAGCC (PCR zerR and promoter region for sequencing)
oLG297	TCGTGATCGGCGATGATGTC (PCR zerR and promoter region for sequencing)
oLG298	GATTCATATGTAAGTGGTCTCTGGCCCTCCG
oLG299	GAAGAGCTCTGGCCTACTAGCGACCTTACTTGG
oLG302	AATTGAAGCCGGCTGGCGCCAAGCTTGACAATCTGGTGTTCGCCAGC
oLG303	TATCGATACCTTGCGGTAATGACGGGGATTTAAC
oLG304	ATTACCGCAAGGTATCGATAAGCTTGATATCGAATTCATG
oLG305	CTTACTTGGGCTGCAGGAATTCAAGAAGTTCCTATTCTC
oLG306	ATTCCTGCAGCCCAAGTAAGGTCGCTAGTAGGCC
oLG307	GCGTCACGGCCGAAGCTAGCGAATTCCTGCGACCGTATGAACAGCTG
oLG393	CACGATGCGAGGAAACGCATATCCCTCACGGCCCGTTTCG
oLG394	CTTGCTCACCATGCGGCGGCTCCCACGATG
oLG395	GGGAGCCGCCGCATGGTGAGCAAGGGCGAGG
oLG396	CACCGGTACGTAGATCTTAAGAGCTTTACTTGTACAGCTCGTCCATGCC
oLG450	GACTACAAGGATGACGATGACAAGTAAGGTCGCTAGTAGGCCAGAGCTC
oLG451	GCCGGCGCTCGACCCGCCCTTGGGGCCTTTGGGGGC
oLG458	GCCGGCGCTCGACCCGCCCTTGGGGCCTTTGGGGGCC
oLG459	GGCGGGTCGAGCGCCGGCATGGTGAGCAAGGGCGAGG
oLG464	TTGTAACTAGTAGAGGAAGGAATTCATGACCCGCGCCGAGTTCATC
oLG468	TTGTAACTAGTAGAGGAAGGAATTCATGAGCCGAGAGGAGGGGACC
oLG469	ACTCACTATAGGGCGAATTGGAGCTCTCAAGCTTGTTCCAGGGCCG
oLG470	ACTCACTATAGGGCGAATTGGAGCTCATCAGTACTCGCGGCGGACC
oLG479	CACGATGCGAGGAAACGCATTAAGTGGTCTCTGGCCCTCCG
oLG482	CACCGGTACGTGTATCTTAAGAGCTTTACTTGTACAGCTCGTCCATGCC
oLG483	TTGTAACTAGTAGAGGAAGGAATTCTAAGTGGTCTCTGGCCCTCCG
oLG484	ACTCACTATAGGGCGAATTGGAGCTCTGGCCTACTAGCGACCTTACTTGG
oLG487	TCGCGAGACGTCCAATTGCACAGAACGCAGCTTCTATCGGATC
oLG488	GCGCCGACTGAAGCTGGGCCTTCGTCGTTTAAAGATCC
oLG489	AAACGACGAAGGCCCAGCTTCAGTCGGCGCGAATG
oLG490	ACGTTCGAATTCTCCGGAGCTCATCAGTACTCGCGGCGGACC
oLG504	TACGACGTCCCGGACTACGCCTGATGAGCTCCGGAGAATTCG
oLG505	CGGGTAGGCGCTCGAGCCGTACTCGCGGCGGACCTCG
oLG522	CCCGGACTACGCCTGATGAGGTCGCTAGTAGGCCAGAGCTCC
oLG523	ACGTCGTACGGGTAGCCGGCGCTCGACCCGCC
oLG524	TGAGCTCCGGAGAATTCGAACG
oLG525	TCAAGCTTGTTCCAGGGCCG

Table 3.2. Strains

Name	Genotype	Construction details	Reference/Source
CB15n	Synchronizable wild-type CB15		Evinger, M. and Agabian, N. (1977)
LG120	P_{lacI}-*lacI*-P_{lac}-YFP-gent^R at *hfaA* locus		García-Bayona et al., 2017
LG124	*ΔcdzCDI*, P_{lacI}-*lacI*-P_{lac}-CFP-tet^R at *hfaA* locus		García-Bayona et al., 2017
LG150	*ΔcdzCDI*, P_{lacI}-*lacI*-P_{lac}-CFP-tet^R at *hfaA* locus, P_{van}-CFP in low copy number plasmid		García-Bayona et al., 2017
LG170	P_{lacI}-*lacI*-P_{lac}-*YFP*-gent^R at *hfaA* locus, empty vector (low copy number)		García-Bayona et al., 2017
LG116	*ΔcdzCDI*	Electroporation of pLG128 into CB15n, two-step recombination and counter-selection, using exponential phase culture for counter-selection.	This study
LG124-S1	LG124 with *perA* Δbases 307-321	Suppressor screen	This study
LG124-S2	LG124 with *perA* Δbases 455-559	Suppressor screen	This study
LG124-S6	LG124 with Δ309 bp in promoter and 5' region of *perA*	Suppressor screen	This study
LG124-S8	LG124 with *perA* Δbase 697	Suppressor screen	This study
LG124-S5	LG124 with point mutation in CCNA_03108 (Q24*)	Suppressor screen	This study
LG124-S11	LG124 with point mutation in CCNA_03108 (F174S)	Suppressor screen	This study
LG124-S3	LG124 with point mutation *zerR*(L59P)	Suppressor screen	This study
LG124-S9	LG124 with point mutation in *zerR* promoter region T(-59)C	Suppressor screen	This study
LG124-S7	LG124 with Q834stop in CCNA_03680	Suppressor screen	This study
LG244	LG124-S2 with low copy plasmid carrying *perA* under native promoter	Electroporation of pLG191 into LG124-S2	This study
LG245	LG124-S6 with low copy plasmid carrying *perA* under native promoter	Electroporation of pLG191 into LG124-S6	This study
LG246	LG124-S8 with low copy plasmid carrying *perA* under native promoter	Electroporation of pLG191 into LG124-S8	This study

LG267	Δ*perA, perA* gene replaced with tet^R cassette	Electroporation of pLG190 into CB15n, two-step recombination method using *sacB* as a counter-selection marker (Skerker et al. 2005), supplementing counter-selection plate with tetracycline. Transduction using phage øCr30 (Ely 1991) of this deletion into a clean CB15n, to avoid mutations that may have occurred during two-step deletion process.	This study
LG300	Δc*dzCDI*, Δ*perA, perA* gene replaced with tet^R cassette	Transduction of ΔperA::tetR marker from LG267 using phage øCr30 (Ely 1991), into LG116	This study
LG322	P_{zerR}-zerR-venus in low copy number plasmid	Electroporation of pLG230 into CB15n	This study
LG323	$P_{zerR(T-59C)}$-zerR-venus in low copy number plasmid in LG124-S9	Electroporation of pLG231 into LG124-S9	This study
LG324	P_{zerR}-zerR(L59P)-venus in low copy number plasmid in LG124-S3	Electroporation of pLG232 into LG124-S3	This study
LG353	high copy number plasmid with P_{Q5}-*zerA*, Δc*dzCDI*, P_{lacI}-*lacI*-P_{lac}-CFP-tet^R at *hfaA* locus	Electroporation of pLG247 into LG124	This study
LG354	high copy number plasmid with P_{Q5}-*zerB*, Δc*dzCDI*, P_{lacI}-*lacI*-P_{lac}-CFP-tet^R at *hfaA* locus	Electroporation of pLG248 into LG124	This study
LG355	high copy number plasmid with P_{Q5}-*zerAB*, Δc*dzCDI*, P_{lacI}-*lacI*-P_{lac}-CFP-tet^R at *hfaA* locus	Electroporation of pLG249 into LG124	This study
LG373	P_{perA}-*perA*-mCherry translational fusion in low copy number plasmid, Δc*dzCDI*, Δ*perA, perA* gene replaced with tet^R cassette	Electroporation of pLG242 into LG300	This study
LG374	P_{perA}-*perA*-mCherry translational fusion in low copy number plasmid, Δc*dzCDI*	Electroporation of pLG242 into LG116	This study
LG375	Δc*dzCDI*, Δ*perA, perA* gene replaced with tet^R cassette, with low copy plasmid carrying perA under native promoter	Electroporation of pLG191 into LG300	This study
LG388	Integration at *vanB* locus of kan^R plasmid carrying P_{Q5}-*zerAB*, Δc*dzCDI*, P_{lacI}-*lacI*-P_{lac}-CFP-tet^R at *hfaA* locus	Electroporation of pLG256 into LG124	This study

LG389	Integration at *vanB* locus of kan^R plasmid carrying P_{Q5}-*zerB*, Δ*cdzCDI*, P_{lacI}-*lacI*-P_{lac}-CFP-tet^R at *hfaA* locus	Electroporation of pLG257 into LG124	This study
LG398	P_{perA}-perA with HA tag at the C-terminus, after a GGSSAG linker, in multi-copy plasmid pLG174, *ΔmanB ΔrsaA*	Electroporation of pLG266 into LG301	This study
LG399	P_{cdz}-*cdzCD-cdzI*$_{HA}$ in low copy number plasmid, *ΔmanB ΔrsaA*	Electroporation of pLG217 into LG301	This study
LG400	P_{perA}-perA with HA tag at the C-terminus, after a GGSSAG linker, in multi-copy plasmid pLG174, P_{lacI}-*lacI*-P_{lac}-YFP-gent^R at *hfaA* locus	Electroporation of pLG266 into LG120	This study
LG401	P_{perA}-perA with HA tag at the C-terminus, after a GGSSAG linker, in multi-copy plasmid pLG174, Δc*dzCDI*, Δ*perA, perA* gene replaced with tet^R cassette	Electroporation of pLG266 into LG300	This study
LG402	Integration at *vanB* locus of kan^R plasmid carrying P_{Q5}-*zerA*, Δ*cdzCDI,* P_{lacI}-*lacI*-P_{lac}-CFP-tet^R at *hfaA* locus	Electroporation of pLG267 into LG124	This study
LG403	Integration at *vanB* locus of kan^R plasmid carrying P_{Q5}-*zerAB* where ZerA has a c-terminal HA tag after a GGSSAG linker, Δ*cdzCDI*, P_{lacI}-*lacI*-P_{lac}-CFP-tet^R at *hfaA* locus	Electroporation of pLG269 into LG124	This study
LG404	Integration at *vanB* locus of kan^R plasmid carrying P_{Q5}-*zerAB* where ZerA has a c-terminal HA tag after a GGSSAG linker, P_{lacI}-*lacI*-P_{lac}-YFP-gent^R at *hfaA* locus	Electroporation of pLG269 into LG120	This study
LG405	Integration at *vanB* locus of kan^R plasmid carrying P_{Q5}-*zerB* where ZerB has a c-terminal HA tag after a GGSSAG linker, Δ*cdzCDI*, P_{lacI}-*lacI*-P_{lac}-CFP-tet^R at *hfaA* locus	Electroporation of pLG268 into LG124	This study
LG406	Integration at *vanB* locus of kan^R plasmid carrying P_{Q5}-*zerB* where ZerB has a c-terminal HA tag after a GGSSAG linker, P_{lacI}-*lacI*-P_{lac}-YFP-gent^R at *hfaA* locus	Electroporation of pLG268 into LG120	This study

Table 3.3. Plasmids

Name	Description	Construction details	Reference /Source
pMT630	Low copy number plasmid with vanillate promoter		Thanbichler et al., 2007
pMT634	Integration vector with kan^R		Thanbichler et al., 2007
pLG174	pMT426-based plasmid for protein expression of P_{Q5} with multiple cloning site		García-Bayona et al., 2017
pNPTS138	Integration vector (kanR) with *sacB* counterselection		Skerker at al., 2005
pLG190	For deletion of *perA* and replacement with tet^R cassette	SLIC reaction (Li and Elledge, 2007) to fuse: 1)HindIII-HF and EcoRI-HF digested pNPTS138 2) 800 bp upstream of *perA* amplified by PCR from genomic DNA (oLG302+303) 3) tet^R cassette amplified by PCR (oLG304+305) from pLG129 4) 800 bp downstream of perA amplified by PCR from genomic DNA (oLG306+307)	This study
pLG191	P_{perA}-*perA* in low copy number plasmid	P_{perA}-*perA* amplified by PCR from genomic DNA (oLG298+299), cloned by restriction cloning using NdeI and SacI-HF to ligate into pMT630	This study
pLG217	P_{cdz}-*cdzCD-cdzI*$_{HA}$ in low copy number plasmid		García-Bayona et al., 2017
pLG230	P_{zerR}-zerR-venus in low copy number plasmid	Gibson reaction to fuse: 1)NdeI and SacI-HF digested pMT630 2) *zerR* with promoter region, amplified from CB15n genomic DNA (oLG393+394) 3) venus amplified by PCR (oLG395+396) from pLG159 (García Bayona et al., 2017)	This study
pLG231	$P_{zerR(T-59C)}$-zerR-venus in low copy number plasmid	Gibson reaction to fuse: 1)NdeI and SacI-HF digested pMT630 2) *zerR* with promoter region, amplified from LG124-S9 genomic DNA (oLG393+394) 3) venus amplified by PCR (oLG395+396) from pLG159 (García Bayona et al., 2017)	This study
pLG232	P_{zerR}-zerR(L59P)-venus in low copy number plasmid	Gibson reaction to fuse: 1)NdeI and SacI-HF digested pMT630 2) *zerR* with promoter region, amplified from LG124-S3 genomic DNA (oLG393+394) 3) venus amplified by PCR (oLG395+396) from pLG159 (García Bayona et al., 2017)	This study
pLG242	P_{perA}-*perA*-GSSAGG-mCherry translational fusion in low copy number plasmid	Gibson reaction to fuse: 1)NdeI and SacI-HF digested pMT630 2) *perA* with promoter region, amplified from CN15n genomic DNA (oLG479+458) 3) venus amplified by PCR (oLG459+482) from pRVCHYC-2 (Thanbichler et al., 2007)	This study

pLG247	high copy number plasmid with P_{Q5}-*zerA*	Gibson reaction to fuse: 1)EcoRI-HF and SacI-HF digested pLG174 2) *zerA* with promoter region, amplified from CN15n genomic DNA (oLG464+469)	This study
pLG248	high copy number plasmid with P_{Q5}-*zerB*	Gibson reaction to fuse: 1)EcoRI-HF and SacI-HF digested pLG174 2) *zerB* with promoter region, amplified from CN15n genomic DNA (oLG468+470)	This study
pLG249	high copy number plasmid with P_{Q5}-*zerAB*	Gibson reaction to fuse: 1) EcoRI-HF and SacI-HF digested pLG174 2) *zerAB* with promoter region, amplified from CN15n genomic DNA (oLG464+470)	This study
pLG256	kan^R plasmid for Integration at *vanB* locus, carrying P_{Q5}-*zerAB*	Gibson reaction to fuse: 1) NdeI and SacI-HF digested pMT634 2) 800 bp *vanB* homology region, amplified from CN15n genomic DNA (oLG487+488) 3) P_{Q5}-*zerAB*, amplified from pLG249(oLG489+490)	This study
pLG257	kan^R plasmid for Integration at *vanB* locus, carrying P_{Q5}-*zerB*	Gibson reaction to fuse: 1) NdeI and SacI-HF digested pMT634 2) 800 bp *vanB* homology region, amplified from CN15n genomic DNA (oLG487+488) 3) P_{Q5}-zerB, amplified from pLG248 (oLG489+490)	This study
pLG266	P_{perA}-perA with HA tag at the C-terminus, after a GGSSAG linker, in multi-copy plasmid pLG174	1) Gibson reaction to fuse A) EcoRI-HF and SacI-HF digested pLG174 B) *perA* with promoter region, amplified from CB15n genomic DNA using oLG483+484 2) round-the-horn site-directed mutagenesis with oLG450+451 using pLG240 as template = pLG245 3) round-the-horn site-directed mutagenesis with oLG522+523 using pLG245 as template	This study
pLG267	kan^R plasmid for Integration at *vanB* locus, carrying P_{Q5}-*zerA*	round-the-horn site-directed mutagenesis with oLG524+525, using pLG256 as template	This study
pLG268	kan^R plasmid for Integration at *vanB* locus, carrying P_{Q5}-*zerB,* where ZerB has a c-terminal HA tag after a GGSSAG linker	round-the-horn site-directed mutagenesis with oLG504+505, using pLG257 as template	This study
pLG269	kan^R plasmid for Integration at *vanB* locus, carrying P_{Q5}-*zerAB,* where ZerA has a c-terminal HA tag after a GGSSAG linker	round-the-horn site-directed mutagenesis with oLG506+507, using pLG256 as template	This study

ACKNOWLEDGEMENTS

We thank the labs of R Sauer and A Grossman for reagents. We acknowledge S Levine at the MIT BioMicroCenter for guidance with Illumina sequencing and N Watson from the Keck Microscopy Facility at the Whitehead Institute for assistance with electron microscopy. This work was supported by an NIH grant (R01GM082899) to MTL, who is also an Investigator of the Howard Hughes Medical Institute, and by an HHMI International Predoctoral Fellowship to LG.

REFERENCES

Anwari, K., Poggio, S., Perry, A., Gatsos, X., Ramarathinam, S.H., Williamson, N.A., Noinaj, N., Buchanan, S., Gabriel, K., Purcell, A.W., et al. (2010). A Modular BAM Complex in the Outer Membrane of the α-Proteobacterium Caulobacter crescentus. PLoS ONE *5*, e8619.

Bieler, S., Silva, F., Soto, C., and Belin, D. (2006). Bactericidal Activity of both Secreted and Nonsecreted Microcin E492 Requires the Mannose Permease. J. Bacteriol. *188*, 7049–7061.

Black, K., Buikema, W.J., and Haselkorn, R. (1995). The hglK gene is required for localization of heterocyst-specific glycolipids in the cyanobacterium Anabaena sp. strain PCC 7120. J. Bacteriol. *177*, 6440–6448.

Cabeen, M.T., Charbon, G., Vollmer, W., Born, P., Ausmees, N., Weibel, D.B., and Jacobs-Wagner, C. (2009). Bacterial cell curvature through mechanical control of cell growth. EMBO J. *28*, 1208–1219.

Cabeen, M.T., Murolo, M.A., Briegel, A., Bui, N.K., Vollmer, W., Ausmees, N., Jensen, G.J., and Jacobs-Wagner, C. (2010). Mutations in the Lipopolysaccharide Biosynthesis Pathway Interfere with Crescentin-Mediated Cell Curvature in Caulobacter crescentus. J. Bacteriol. *192*, 3368–3378.

Cao, Y., Johnson, H.M., and Bazemore-Walker, C.R. (2012). Improved enrichment and proteomic identification of outer membrane proteins from a Gram-negative bacterium: Focus on Caulobacter crescentus. PROTEOMICS *12*, 251–262.

Chandler, L.E., Bartsevich, V.V., and Pakrasi, H.B. (2003). Regulation of manganese uptake in Synechocystis 6803 by RfrA, a member of a novel family of proteins containing a repeated five-residues domain. Biochemistry (Mosc.) *42*, 5508–5514.

Christen, B., Abeliuk, E., Collier, J.M., Kalogeraki, V.S., Passarelli, B., Coller, J.A., Fero, M.J., McAdams, H.H., and Shapiro, L. (2011). The essential genome of a bacterium. Mol. Syst. Biol. *7*, 528.

Cociancich, S., Pesic, A., Petras, D., Uhlmann, S., Kretz, J., Schubert, V., Vieweg, L., Duplan, S., Marguerettaz, M., Noëll, J., et al. (2015). The gyrase inhibitor albicidin consists of p-aminobenzoic acids and cyanoalanine. Nat. Chem. Biol. *11*, 195–197.

Cotter, P.D., Ross, R.P., and Hill, C. (2012). Bacteriocins — a viable alternative to antibiotics? Nat. Rev. Microbiol. *11*, 95–105.

Dalebroux, Z.D., and Miller, S.I. (2014). Salmonellae PhoPQ regulation of the outer membrane to resist innate immunity. Curr. Opin. Microbiol. *17*, 106–113.

Deatherage, D.E., and Barrick, J.E. (2014). Identification of Mutations in Laboratory-Evolved Microbes from Next-Generation Sequencing Data Using breseq. In Engineering and Analyzing Multicellular Systems, L. Sun, and W. Shou, eds. (New York, NY: Springer New York), pp. 165–188.

Dicks, L.M.T., Heunis, T.D.J., van Staden, D.A., Brand, A., Noll, K.S., and Chikindas, M.L. (2011). Medical and Personal Care Applications of Bacteriocins Produced by Lactic Acid Bacteria. In Prokaryotic Antimicrobial Peptides, D. Drider, and S. Rebuffat, eds. (New York, NY: Springer New York), pp. 391–421.

Diep, D.B., Skaugen, M., Salehian, Z., Holo, H., and Nes, I.F. (2007). Common mechanisms of target cell recognition and immunity for class II bacteriocins. Proc. Natl. Acad. Sci. *104*, 2384–2389.

Ducret, A., Quardokus, E.M., and Brun, Y.V. (2016). MicrobeJ, a tool for high throughput bacterial cell detection and quantitative analysis. Nat. Microbiol. *1*, 16077.

Dye, N.A., Pincus, Z., Theriot, J.A., Shapiro, L., and Gitai, Z. (2005). Two independent spiral structures control cell shape in Caulobacter. Proc. Natl. Acad. Sci. *102*, 18608–18613.

Egger, L.A., Park, H., and Inouye, M. (1997). Signal transduction via the histidyl-aspartyl phosphorelay. Genes Cells Devoted Mol. Cell. Mech. *2*, 167–184.

Ford, M.J., Nomellini, J.F., and Smit, J. (2007). S-Layer Anchoring and Localization of an S-Layer-Associated Protease in Caulobacter crescentus. J. Bacteriol. *189*, 2226–2237.

Gandham, L., Nomellini, J.F., and Smit, J. (2012). Evaluating secretion and surface attachment of SapA, an S-layer-associated metalloprotease of Caulobacter crescentus. Arch. Microbiol. *194*, 865–877.

García-Bayona, L., Guo, M.S., and Laub, M.T. (2017). Contact-dependent killing by *Caulobacter crescentus* via cell surface-associated, glycine zipper proteins. eLife *6:e24869*.

Garrido, M., Herrero, M., Kolter, R., and Moreno, F. (1988). The export of the DNA replication inhibitor Microcin B17 provides immunity for the host cell. EMBO J. *7*, 1853.

Gibello, A., Díaz de Alba, P., Blanco, M.M., Machuca, J., Cutuli, M.T., and Rodríguez-Martínez, J.M. (2014). Lactococcus garvieae carries a chromosomally encoded pentapeptide repeat protein that confers reduced susceptibility to quinolones in Escherichia coli producing a cytotoxic effect. Res. Microbiol. *165*, 590–599.

Hegde, S.S., Vetting, M.W., Mitchenall, L.A., Maxwell, A., and Blanchard, J.S. (2011). Structural and Biochemical Analysis of the Pentapeptide Repeat Protein EfsQnr, a Potent DNA Gyrase Inhibitor. Antimicrob. Agents Chemother. *55*, 110–117.

Jonas, K., Liu, J., Chien, P., and Laub, M. (2013). Proteotoxic Stress Induces a Cell-Cycle Arrest by Stimulating Lon to Degrade the Replication Initiator DnaA. Cell *154*, 623–636.

Kaczmarczyk, A., Vorholt, J.A., and Francez-Charlot, A. (2013). Cumate-inducible gene expression system for sphingomonads and other Alphaproteobacteria. Appl. Environ. Microbiol. *79*, 6795–6802.

Kallberg, M., Wang, H., Wang, S., Peng, J., Wang, Z., Lu, H., and Xu, J. (2012). Template-based protein structure modeling using the RaptorX web server. Nat. Protoc. *7*, 1511–1522.

Kjos, M., Oppegård, C., Diep, D.B., Nes, I.F., Veening, J.-W., Nissen-Meyer, J., and Kristensen, T. (2014). Sensitivity to the two-peptide bacteriocin lactococcin G is dependent on UppP, an enzyme involved in cell-wall synthesis: Lactococcin G receptor. Mol. Microbiol. *92*, 1177–1187.

Knodler, L.A., Vallance, B.A., Hensel, M., Jäckel, D., Finlay, B.B., and Steele-Mortimer, O. (2004). Salmonella type III effectors PipB and PipB2 are targeted to detergent-resistant microdomains on internal host cell membranes: Association of SPI-2 effectors with DRMs. Mol. Microbiol. *49*, 685–704.

Konovalova, A., Mitchell, A.M., and Silhavy, T.J. (2016). A lipoprotein/?-barrel complex monitors lipopolysaccharide integrity transducing information across the outer membrane. eLife *5*.

Krewulak, K.D., and Vogel, H.J. (2011). TonB or not TonB: is that the question?This paper is one of a selection of papers published in a Special Issue entitled CSBMCB 53rd Annual Meeting — Membrane Proteins in Health and Disease, and has undergone the Journal's usual peer review process. Biochem. Cell Biol. *89*, 87–97.

de Lorenzo, V., and Pugsley, A.P. (1985). Microcin E492, a low-molecular-weight peptide antibiotic which causes depolarization of the Escherichia coli cytoplasmic membrane. Antimicrob. Agents Chemother. *27*, 666–669.

Marciset, O., Jeronimus-Stratingh, M.C., Mollet, B., and Poolman, B. (1997). Thermophilin 13, a nontypical antilisterial poration complex bacteriocin, that functions without a receptor. J. Biol. Chem. *272*, 14277–14284.

McCaughey, L.C., Grinter, R., Josts, I., Roszak, A.W., Wal?en, K.I., Cogdell, R.J., Milner, J., Evans, T., Kelly, S., Tucker, N.P., et al. (2014). Lectin-Like Bacteriocins from Pseudomonas spp. Utilise D-Rhamnose Containing Lipopolysaccharide as a Cellular Receptor. PLoS Pathog. *10*, e1003898.

Montero, C., Mateu, G., Rodriguez, R., and Takiff, H. (2001). Intrinsic Resistance of Mycobacteriumsmegmatis to Fluoroquinolones May Be Influenced by New Pentapeptide Protein MfpA. Antimicrob. Agents Chemother. *45*, 3387–3392.

Ni, S., Sheldrick, G., Benning, M., and Kennedy, M. (2009). The 2Å resolution crystal structure of HetL, a pentapeptide repeat protein involved in regulation of heterocyst differentiation in the cyanobacterium Nostoc sp. strain PCC 7120. J. Struct. Biol. *165*, 47–52.

Nummelin, H., Merckel, M.C., Leo, J.C., Lankinen, H., Skurnik, M., and Goldman, A. (2004). The Yersinia adhesin YadA collagen-binding domain structure is a novel left-handed parallel β-roll. EMBO J. *23*, 701–711.

Oppegard, C., Kjos, M., Veening, J.-W., Nissen-Meyer, J., and Kristensen, T. (2016). A putative amino acid transporter determines sensitivity to?the two-peptide bacteriocin plantaricin JK. MicrobiologyOpen *5*, 700–708.

Park, D.M., Overton, K.W., Liou, M.J., and Jiao, Y. (2017). Identification of a U/Zn/Cu responsive global regulatory two-component system in *Caulobacter crescentus*: A metal responsive TCS in *Caulobacter*. Mol. Microbiol. *104*, 46–64.

Pettersen, E.F., Goddard, T.D., Huang, C.C., Couch, G.S., Greenblatt, D.M., Meng, E.C., and Ferrin, T.E. (2004). UCSF Chimera?A visualization system for exploratory research and analysis. J. Comput. Chem. *25*, 1605–1612.

Rea, M.C., Ross, R.P., Cotter, P.D., and Hill, C. (2011). Classification of Bacteriocins from Gram-Positive Bacteria. In Prokaryotic Antimicrobial Peptides, D. Drider, and S. Rebuffat, eds. (New York, NY: Springer New York), pp. 29–53.

Rebuffat, S. (2011). Bacteriocins from Gram-Negative Bacteria: A Classification? In Prokaryotic Antimicrobial Peptides, D. Drider, and S. Rebuffat, eds. (New York, NY: Springer New York), pp. 55–72.

Roelofs, K.G., Coyne, M.J., Gentyala, R.R., Chatzidaki-Livanis, M., and Comstock, L.E. (2016). *Bacteroidales* Secreted Antimicrobial Proteins Target Surface Molecules Necessary for Gut Colonization and Mediate Competition *In Vivo*. mBio *7*, e01055-16.

Ruhe, Z.C., Townsley, L., Wallace, A.B., King, A., Van der Woude, M.W., Low, D.A., Yildiz, F.H., and Hayes, C.S. (2015a). CdiA promotes receptor-independent intercellular adhesion: BamA-independent CdiA-mediated adhesion. Mol. Microbiol. *98*, 175–192.

Ruhe, Z.C., Hayes, C.S., and Low, D.A. (2015b). Measuring Cell–Cell Binding Using Flow-Cytometry. In The BAM Complex, S. Buchanan, and N. Noinaj, eds. (New York, NY: Springer New York), pp. 127–136.

Scholz, R., Molohon, K.J., Nachtigall, J., Vater, J., Markley, A.L., Sussmuth, R.D., Mitchell, D.A., and Borriss, R. (2011). Plantazolicin, a Novel Microcin B17/Streptolysin S-Like Natural Product from Bacillus amyloliquefaciens FZB42. J. Bacteriol. *193*, 215–224.

Schrader, J.M., Zhou, B., Li, G.-W., Lasker, K., Childers, W.S., Williams, B., Long, T., Crosson, S., McAdams, H.H., Weissman, J.S., et al. (2014). The coding and noncoding architecture of the Caulobacter crescentus genome. PLoS Genet. *10*, e1004463.

Shah, S., and Heddle, J.G. (2014). Squaring up to DNA: pentapeptide repeat proteins and DNA mimicry. Appl. Microbiol. Biotechnol. *98*, 9545–9560.

Shi, L., Günther, S., Hübschmann, T., Wick, L.Y., Harms, H., and Müller, S. (2007). Limits of propidium iodide as a cell viability indicator for environmental bacteria. Cytometry A *71A*, 592–598.

Smit, J., Sherwood, C.S., and Turner, R.F. (2000). Characterization of high density monolayers of the biofilm bacterium Caulobacter crescentus: evaluating prospects for developing immobilized cell bioreactors. Can. J. Microbiol. *46*, 339–349.

Strahilevitz, J., Jacoby, G.A., Hooper, D.C., and Robicsek, A. (2009). Plasmid-Mediated Quinolone Resistance: a Multifaceted Threat. Clin. Microbiol. Rev. *22*, 664–689.

Sträuber, H., and Müller, S. (2010). Viability states of bacteria-Specific mechanisms of selected probes. Cytometry A *77A*, 623–634.

Thompson, J.D., Gibson, T.J., and Higgins, D.G. (2002). Multiple Sequence Alignment Using ClustalW and ClustalX. In Current Protocols in Bioinformatics, A.D. Baxevanis, G.A. Petsko, L.D. Stein, and G.D. Stormo, eds. (Hoboken, NJ, USA: John Wiley & Sons, Inc.), p.

Vetting, M.W., Hegde, S.S., Fajardo, J.E., Fiser, A., Roderick, S.L., Takiff, H.E., and Blanchard, J.S. (2006). Pentapeptide Repeat Proteins †. Biochemistry (Mosc.) *45*, 1–10.

Vetting, M.W., Hegde, S.S., Hazleton, K.Z., and Blanchard, J.S. (2007). Structural characterization of the fusion of two pentapeptide repeat proteins, Np275 and Np276, from Nostoc punctiforme: Resurrection of an ancestral protein. Protein Sci. *16*, 755–760.

Waterhouse, A.M., Procter, J.B., Martin, D.M.A., Clamp, M., and Barton, G.J. (2009). Jalview Version 2--a multiple sequence alignment editor and analysis workbench. Bioinformatics *25*, 1189–1191.

de Zamaroczy, M., and Chauleau, M. (2011). Colicin Killing: Foiled Cell Defense and Hijacked Cell Functions. In Prokaryotic Antimicrobial Peptides, D. Drider, and S. Rebuffat, eds. (New York, NY: Springer New York), pp. 255–287.

Chapter 4
Conclusions and future directions

The data presented here are unpublished.

CONCLUSIONS

Bacteriocins are a widely diverse and ubiquitous group of diffusible proteinaceous toxins that mediate interbacterial antagonism. Despite their great impact in microbial communities and their potential as antibiotic alternatives, amongst other promising applications; our current understanding of bacteriocin biology is limited to a narrow group of phylogenetic clades in a small set of growth environments. In the course of my graduate work, I have expanded the current repertoire of characterized bacteriocin diversity by identifying a new and fundamentally different type of small bacteriocin. Although the Cdz system from *Caulobacter crescentus* shares some characteristics with two-peptide bacteriocins from lactic acid bacteria, and others with microcins form enterobacteria, it has the unique property of mediating contact-dependent killing in the dilute and nutrient-poor aquatic conditions where this bacterium thrives. However, this newly discovered family of bacteriocins is not unique to *Caulobacter* or to oligotrophic aquatic environments, as it appears to be broadly distributed across proteobacteria that colonize a diverse range of environments. These results thus highlight the need for the development of more high-throughput methods of screening for contact-dependent antagonism.

Several types of contact-dependent killing systems have been characterized, but they differ profoundly from the Cdz system in their toxin delivery mechanism. These types of systems are based on large macromolecular complexes that allow the toxin to be anchored to the cell surface or to be translocated directly into the inside of the target cell. The exact mechanism that allows the small CDZ toxic proteins to aggregate and remain surface associated has not been elucidated, but is likely to involve β-stacking stabilized by an extended glycine-zipper motif in a hydrophobic span. This hypothesis can be tested through a structural and biochemical characterization of the two peptides that compose the toxin, either in purified form or as part of the fibrils with which they associate to *in vivo*.

Based on the phenotype of prey cells during competition, as well as the results from a suppressor screen for mutations that allow prey cells to escape Cdz-mediated killing, we hypothesize than the inhibitory mechanism of Cdz involves membrane permeabilization to ions . This effect may

be caused by pore formation, but similar to some bacteriocins from lactic acid bacteria that target lipid II, the toxins may have additional effects on the cell wall (Martin and Breukink, 2007). The discovery and initial characterization of the Cdz system in *C. crescentus* thus provide further ammunition for the argument that there may be a link between peptides that undergo β-aggregation and membrane toxicity, as has been proposed for other antimicrobial peptides of eukaryotic origin, most notably the amyloid-β peptide associated with Alzheimer's disease (Golde, 2016). Other examples of eukaryotic antimicrobial peptides thought to cause membrane permeabilization in bacteria and that form amyloid aggregates include Protegrin-1 (pigs) (Jang et al., 2011), Uperin 3.5 (toadlet *Uperoleia mjobergii*) (Calabrese et al., 2016) and CnAMP2 (coconut) (Gour et al., 2016).

Through the suppressor screen, I was able to identify the putative Cdz cell-surface receptor, an envelope-associated protein that is predicted to adopt a square β-helical fold. This structure is reminiscent of other filamentous surface-associated proteins, in particular those adopted by some adhesins and by the toxins in the cdi contact-dependent inhibition system. This newly identified gene, *perA*, is conserved in many *Caulobacte*r relatives and belongs to a family of genes of unknown function that are ubiquitous in bacteria. PerA is important for envelope homeostasis in *C. crescentus,* although its exact physiological role remains to be determined, and appears to be independent of Cdz toxin import. Therefore, a more thorough characterization of PerA could provide great insights into the biology of this new gene family. The screen also allowed the identification of two more genes of unknown function, expressed in one operon, *zerRAB*, which are involved in envelope remodelling and may have a critical role in responding to some types of envelope stress.

Finally, little is known about the regulation of interbacterial antagonism systems under oligotrophic environments. In the following section, I summarize some preliminary results that indicate that regulatory cues for Cdz may be similar to those observed for microcins and two-peptide bacteriocins from lactic acid bacteria. However, under constant nutrient limitation the ecological impact and evolutionary dynamics of the Cdz system may be significantly different than in the copiotrophic and crowded environments where those two groups of bacteria thrive.

Below, I have outlined in more detail some of the remaining open questions, with a particular focus on avenues for future research.

FUTURE DIRECTIONS

Validation of CDZ-like systems in other bacteria

Based on cluster architecture and a hidden Markov model, I was able to identify putative Cdz-like systems in many proteobacteria. The most interesting candidates for future validation are the clusters presents in many clinical isolates of *Klebsiella pneumoniae* and *Pseudomonas aeruginosa*. These clusters have the general characteristics of a polymorphic toxin system, i.e. a conserved secretion machinery coupled to a variable toxin-immunity pair. Interestingly, in *K. pneumoniae* they are adjacent to a fimbrial adhesion cluster. The *Pseudomonas* cdz-like cluster (Fig. 4.1) is present in many isolates, including the lab strain PAO1, which makes it the most amenable to testing. The gene cluster in PAO1 (PA4139 to PA4144) could be replaced by an antibiotic selection marker to allow co-culture experiments with the wild-type strain.

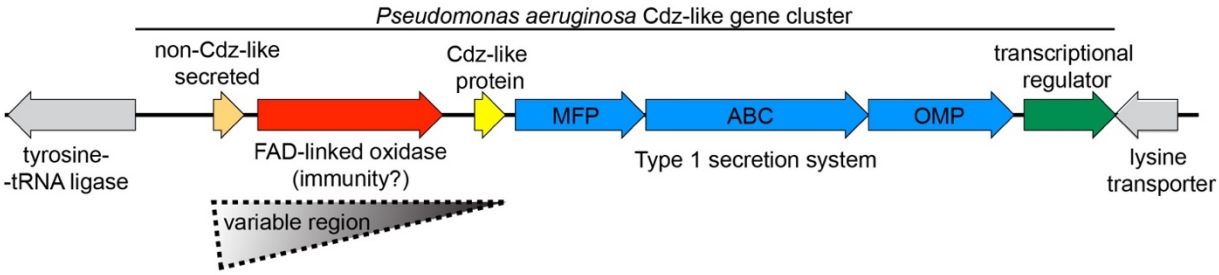

Figure 4.1. Cdz-like gene cluster in *Pseudomonas aeruginosa* PAO1. Components of the T1SS are MFP = membrane fusion protein, ABC = ABC transporter, OMP = outer membrane protein. Genes not thought to be part of the cluster are in grey. The variable region corresponds to the region of the cluster that differs between *P. aeruginosa* strains.

In this species, there are two possible toxin variants for the polymorphic region, with the non-PAO1 variant being present in strain ATCC33359. Each variant is composed of one Cdz-like (PA4141) and one non-Cdz-like peptide (PA4139). Interestingly, the best candidate for the immunity gene is not a small protein but a hypothetical periplasmic/inner membrane FAD-linked oxidase (PA4140), which co-varies with the toxic peptides. One potential mechanism by which

this type of immunity works is that the bacteriocin co-varies with its receptor or target (Roelofs et al., 2016).

Understanding the mechanism of CdzC/D delivery and its link to aggregation

For two-peptide bacteriocins from lactic acid bacteria (LAB), where each peptide by itself lacks killing activity, a cross-complementation phenomenon has been described where the two peptides can be provided sequentially rather than together and still lead to killing activity (Moll et al., 1998). Similarly, the *curli* system in *E. coli* is composed of two small proteins that form amyloid fimbriae that provide structural integrity to biofilms. The fimbriae can form if two partial producer strains, each producing only one of the two fibril components are co-cultured (Chapman, 2002). To examine if EtdC and EtdD needed to be produced within the same cell, I performed cross-complementation assays in which the indicator strain was mixed at an equal ratio to two partial producers, Δ*cdzC* and Δ*cdzD* (Fig. 4.2A). The indicator was inhibited at rates similar to a competition with one full producer, showing that CdzC and CdzD protein molecules secreted from different cells can interact to cause inhibition. Furthermore, all three cell types need to be in direct contact for killing to take place, according to split-well experiments as those described in chapter 2. Killing of the indicator was only observed when using a filter membrane of a 8 µm pore size that allows cells to go through the pores. If a smaller pore size membrane (0.4 µm) was used, such that cells cannot be in direct contact while allowing diffusible molecules to be shared, no killing was observed if one of the three strains was separated by a the membrane from the other two (Fig 4.2B). This result is consistent with the observation that both CdzC and CdzD remain surface associated (Fig 2.10-11), even in the absence of the other peptide. It is thus likely that each peptide toxin can adopt the proper conformation to aggregate and remain surface associated, but toxic activity in the target cell requires the presence of both proteins.

Several avenues could be explored to gain further understanding into the structure adopted by the Cdz toxins in the producer cells. Due to their aggregation propensity, purification of the mature CdzC and CdzD may require recovery from inclusion bodies in an *E. coli* or yeast expression system, and in the presence of a strong denaturing agent (Hammer et al., 2007; Zhong et al., 2014). After purification, fibril formation can be visualized using transmission electron

microscopy, and quantified using Thioflavin T staining and fluorescence measurement (Hammer et al., 2007). Alternatively, the C-DAG *E. coli* system could be used for testing the propensity of CdzC/D to form amyloid fibrils without the need for purification (Sivanathan and Hochschild, 2013). This system would by-pass the current limitation for directly testing for amyloid formation of Cdz in *C. crescentus*: the fact that an unidentified gene different from the *cdz* gene cluster and the HfaA holdfast attachment protein forms amyloid-type structures in the cells, leading to positive results in amyloid stains and other tests, along with presence of fibrils by electron microscopy (Fig. 2.12). This cryptic amyloid in *Caulobacter* is unrelated to the *curli* system, as there are no CsgA/B homologs in the genome. The question remains open of whether the fibrils observed by EM are composed of this uncharacterized amyloid protein and whether they are responsible to cell-cell adhesion in liquid culture. I was unable to find any predicted adhesins or bacterial amyloid fimbriae genes in the *C. crescentus* genome, so their identification remains a challenge for the future.

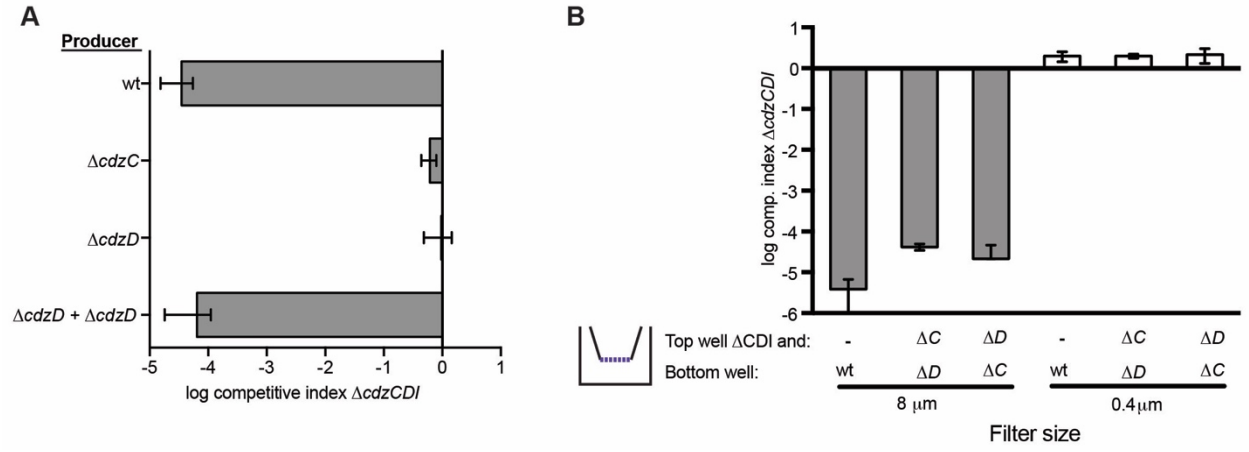

Figure 4.2. CdzC and CdzD can be produced in two separate cells for killing. Competitions were conducted as described in chapter 2. **A.** Competitive index (as defined in Fig.2.3) of *ΔcdzCDI* indicator grown in co-culture with a producer or combination of partial producers mixed at equal ratios. **B.** Competitive index of *ΔcdzCDI* indicator grown in co-culture a wild-type producer or two partial producers, using the split-well set-up shown (left). The membrane separating the two compartments had a pore size of 8 or 0.4 μm, as indicated.

Understanding the physiological role of PerA and ZerA/B

The data presented in chapter 3 indicate that PerA has a key role in cell envelope biogenesis or maintenance. An experimental approach to start elucidating the exact role of PerA would be the

use pull-down experiments to determine potential interaction partners. Additionally, a genetic screen could be conducted for mutations that compensate growth defects in a *ΔperA* strain. This strain is viable under optimal growth conditions, but cannot tolerate many types of stress. The genetic screen could thus be conducted by growing the cells in one of these "stress" conditions. These survivors are expected to have mutations in genes that are implicated in compensating the absence of *perA*. However, depending on the role of PerA, this type of compensatory mutations may not be possible or may be uninformative (e.g. mutations that make the cells grow more slowly to avoid membrane blebbing).

This experimental pipeline can also be implemented to investigate the role of ZerA and ZerB. Additionally, determination of the subcellular localization (e.g. at the division plane, the poles or diffuse localization) of the two proteins may be informative of their role. In the case of ZerA and ZerB, overexpression at very high levels of the two proteins leads to growth inhibition, which could be exploited for a suppressor screen.

Regulation of the Cdz system

As presented in chapter 2, the Cdz system is induced in stationary phase. This could be due to a combination of factors, mainly crowding and nutrient starvation. By conducting competition experiments in diluted medium (PYE diluted 1:4 or 1:10 in distilled water), I was able to show that the system is induced when cell growth starts slowing down (as quantified by optical density), rather than at a specific cell density (Fig 4.3A). This indicates that the system is likely not quorum sensing regulated. I suspected that the major nutrient starvation signal driving induction of the Cdz system was iron starvation. Indeed, the promoter regions of the two divergent operons in the *cdz* gene cluster have consensus *fur* repressor binding boxes (da Silva Neto et al., 2009). Fur (ferric uptake regulator) is a transcriptional repressor that gets released at low iron concentrations. Moreover, according to microarray data, both transcriptional units are upregulated 10-fold upon iron starvation (da Silva Neto et al., 2013). However, when I conducted competition experiments under iron starvation in exponential phase, using the ferric iron chelating agent 2,2'-bipyridyl, there was no inhibition of the indicator strain, even at chelating agent concentrations high enough to arrest growth (Fig 4.3B). Additionally, in a competition in

stationary phase in medium supplemented with excess iron, the indicator strain was significantly less inhibited than without excess iron (Fig 4.3C). These results indicate that iron starvation is a necessary cue to induce the Cdz system, but it is not sufficient to have active Cdz-mediated killing.

Since pH significantly changes from slightly acidic (pH 6.5) to basic (pH 8.5) as the *C. crescentus* culture goes from exponential to stationary phase in PYE (Takacs et al., 2010), I tested the effect of buffering the pH of the medium. In medium buffered at pH 8.5, the killing activity started appearing at a similar time than in unbuffered medium (stationary phase), indicating that a basic culture medium is not sufficient on itself to induce Cdz-mediated killing (Fig 4.3 D). Interestingly, in medium buffered at pH 6.5, no indicator inhibition was observed even in stationary phase, indicating that a basic pH is necessary for Cdz activity (Fig 4.3D). This observation may be explained by the isoelectric point of the mature CdzD, which close to 7, so the shift in pH means it goes from being positively (+0.5) to negatively charged (-1). The mature CdzC goes from cationic (+1.5) to uncharged.

Finally, in medium supplemented with additional 0.2% glucose or 0.3% xylose, a significant reduction in indicator inhibition was observed in stationary phase (Fig 4.1E). Altogether, these results indicate that induction and activation of the system requires a combination of signals, all present in stationary phase: basic medium pH, carbon source depletion and iron starvation. In contrast, high cell density is not a requirement for Cdz activity. Therefore, the Cdz system is active under conditions that *C. crescentus* is likely to encounter often in nature, where cells usually do not reach very high cell densities.

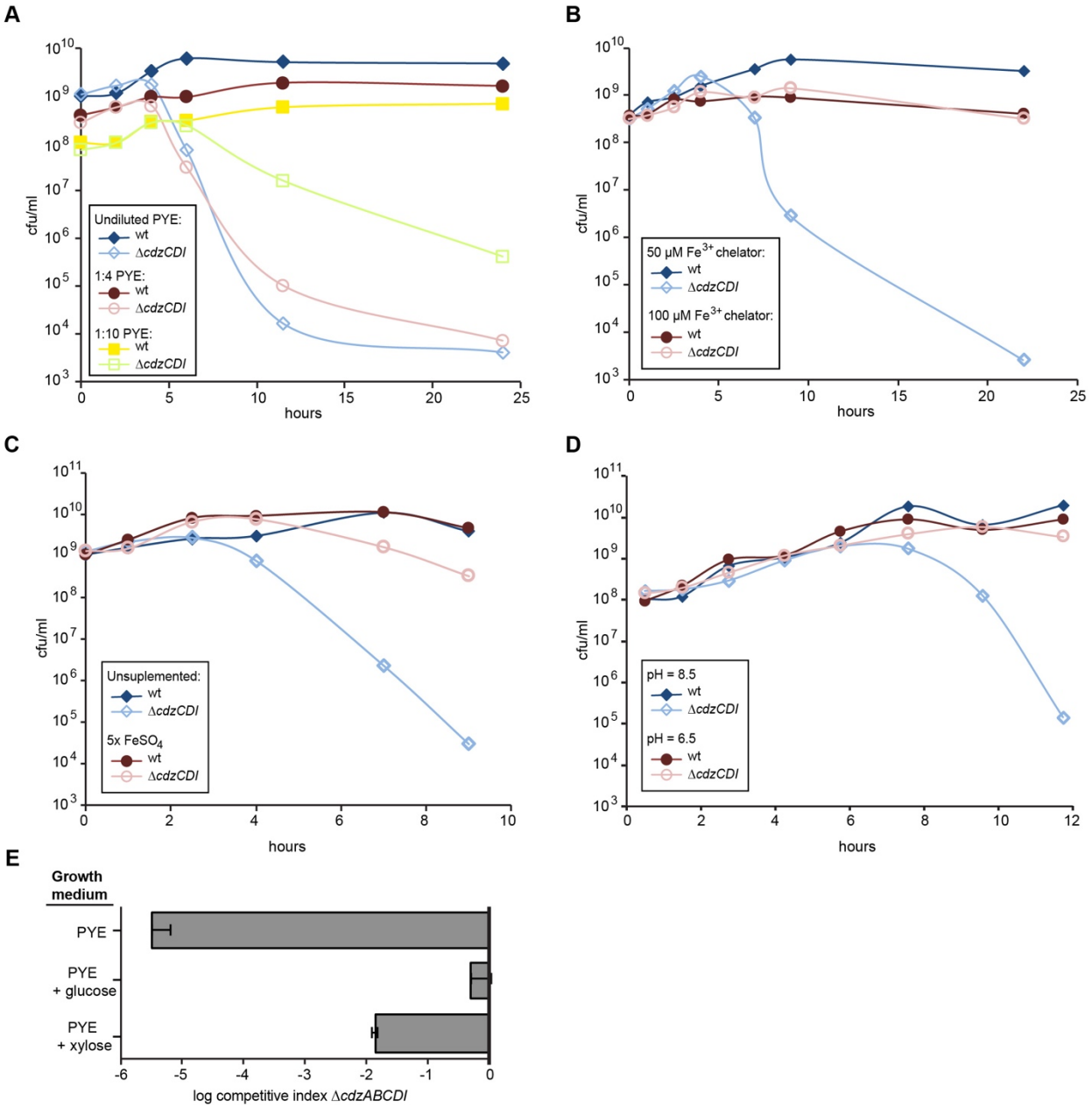

Figure 4.3. Regulation of the Cdz system. Co-culture competition of wild-type *C. crescentus* and *ΔcdzCDI* in rich medium, carried out as described in chapter 2. Strains were mixed 1:1 in exponential phase and co-cultured, with CFUs of each strain measured at each time point (Fig. 2.3). **A.** Competition in PYE, diluted in water at the ratio specified. **B.** Competition under iron starvation: at OD_{600} 0.1, the specified concentration of the ferric iron chelator 2,2'-bipyridyl was added to the culture. **C.** Competition in PYE supplemented with 50 μM $FeSO_4$. **D.** Competition in buffered PYE at the specified pH, prepared as described in (Takacs et al., 2010). **E**. Competition in PYE supplemented with 0.2% (w/v) glucose or 0.3% xylose. Competitive index calculated as described in Fig. 2.3.

According to our exponential phase RNA-seq data from chapter 2, there is a long non-coding RNA that overlaps the *cdzI* gene and the downstream region in the opposite strand (Fig 2.1B). This transcript also has a *fur* binding box. I postulate that this ncRNA may have a role in preventing

spurious transcription or translation under conditions where the system is repressed. Since the *cdzCDI* genes are expressed at such high levels under inducing conditions, the ncRNA could provide a fitness advantage by preventing synthesis of costly proteins when the rest of the system is not active. This model can be tested experimentally: the model would lead to the prediction that ectopic overexpression of the ncRNA in stationary phase would lead to decreased CdzC/D/I protein levels, which can be probed by western blot. It would also lead to absence of killing in stationary phase. Additionally, in a strain where the ncRNA promoter region has been deleted, CdzC/D/I protein levels would be up in exponential phase. This strain could also be used to test if the regulatory effect is due to strand complementarity between the ncRNA and the *cdzCDI* mRNA. Ectopic overexpression of a mutated ncRNA with enough mismatches to inhibit pairing would not affect the higher than normal levels of CdzC/D/I in exponential phase in this strain. If compensatory synonymous mutations are introduced in the *cdzCDI* mRNA to re-establish pairing, CdzC/D/I levels should return to normal. This would constitute the first report of a ncRNA regulating bacteriocin expression.

Discovery of other genes involved in community behaviors in *C. crescentus*

Although expression of the CDZ system does not appear to require high cell density, we cannot rule out that *Caulobacter* may have a quorum sensing signaling system to coordinate community behaviors. The *C. crescentus* genome does not have genes predicted to be involved in the synthesis of acyl-homoserine lactone or other characterized quorum sensing signals from proteobacteria. Very little is known about biofilm regulation in this organism, so a very informative first step would be to conduct RNA-seq of biofilms to identify genes that are upregulated. In addition, a Tn-seq experiment could be conducted to screen for mutants that are unable to form biofilms in glass slides submerged on 96-well plates.

One additional gene that could have a potential role in community behavior is CCNA_03945. CCNA_03945 is a short cationic peptide that, according to our RNA-seq data, is very highly upregulated in stationary phase. Although it is located far from the *cdz* gene cluster on the chromosome, CCNA_03945 has a leader peptide almost identical to that of CdzC. The 28-residue mature peptide does not bear any similarity with characterized proteins and is not adjacent to a

putative immunity gene. I hypothesize that this secreted peptide might be a quorum sensing signal, like the gram-positive peptide pheromones (Kleerebezem and Quadri, 2001). It could alternatively be a bacteriocin targeting unrelated species or could have a role unrelated to interbacterial interactions. The effect of deletion and overexpression of this gene on biofilm formation can be tested. Additionally, If CCNA_03945 is involved on quorum sensing signaling, overexpression in exponential phase should lead to a transcriptional profile comparable to that of a biofilm or of a stationary phase culture.

REFERENCES

Breeuwer, P., and Abee, T. (2008). Section 8 - Molecular tools to assess microbial activities. In Molecular Microbial Ecology Manual, G.A. Kowalchuk, F.J. de Bruijn, I.M. Head, A.D. Akkermans, and J.D. van Elsas, eds. (Dordrecht: Springer Netherlands), pp. 1563–1774.

Calabrese, A.N., Liu, Y., Wang, T., Musgrave, I.F., Pukala, T.L., Tabor, R.F., Martin, L.L., Carver, J.A., and Bowie, J.H. (2016). The Amyloid Fibril-Forming Properties of the Amphibian Antimicrobial Peptide Uperin 3.5. ChemBioChem *17*, 239–246.

Chapman, M.R. (2002). Role of Escherichia coli Curli Operons in Directing Amyloid Fiber Formation. Science *295*, 851–855.

Golde, T.E. (2016). Alzheimer disease: Host immune defence, amyloid-β peptide and Alzheimer disease. Nat. Rev. Neurol. *12*, 433–434.

Gour, S., Kaushik, V., Kumar, V., Bhat, P., Yadav, S.C., and Yadav, J.K. (2016). Antimicrobial peptide (Cn-AMP2) from liquid endosperm of *Cocos nucifera* forms amyloid-like fibrillar structure: AMYLOID FORMATION BY PLANT ANTIMICROBIAL PEPTIDE. J. Pept. Sci. *22*, 201–207.

Hammer, N.D., Schmidt, J.C., and Chapman, M.R. (2007). The curli nucleator protein, CsgB, contains an amyloidogenic domain that directs CsgA polymerization. Proc. Natl. Acad. Sci. *104*, 12494–12499.

Jang, H., Arce, F.T., Mustata, M., Ramachandran, S., Capone, R., Nussinov, R., and Lal, R. (2011). Antimicrobial Protegrin-1 Forms Amyloid-Like Fibrils with Rapid Kinetics Suggesting a Functional Link. Biophys. J. *100*, 1775–1783.

Kirby, J.E., Vogel, J.P., Andrews, H.L., and Isberg, R.R. (1998). Evidence for pore-forming ability by Legionella pneumophila. Mol. Microbiol. *27*, 323–336.

Kleerebezem, M., and Quadri, L.E. (2001). Peptide pheromone-dependent regulation of antimicrobial peptide production in Gram-positive bacteria: a case of multicellular behavior. Peptides *22*, 1579–1596.

Martin, N.I., and Breukink, E. (2007). The expanding role of lipid II as a target for lantibiotics. Future Microbiol. *2*, 513–525.

Moll, G., Hildeng-Hauge, H., Nissen-Meyer, J., Nes, I.F., Konings, W.N., and Driessen, A.J. (1998). Mechanistic properties of the two-component bacteriocin lactococcin G. J. Bacteriol. *180*, 96–99.

da Silva Neto, J.F., Braz, V.S., Italiani, V.C.S., and Marques, M.V. (2009). Fur controls iron homeostasis and oxidative stress defense in the oligotrophic alpha-proteobacterium Caulobacter crescentus. Nucleic Acids Res. *37*, 4812–4825.

da Silva Neto, J.F., Lourenço, R.F., and Marques, M.V. (2013). Global transcriptional response of Caulobacter crescentus to iron availability. BMC Genomics *14*, 549.

Roelofs, K.G., Coyne, M.J., Gentyala, R.R., Chatzidaki-Livanis, M., and Comstock, L.E. (2016). *Bacteroidales* Secreted Antimicrobial Proteins Target Surface Molecules Necessary for Gut Colonization and Mediate Competition *In Vivo*. mBio *7*, e01055-16.

Sivanathan, V., and Hochschild, A. (2013). A bacterial export system for generating extracellular amyloid aggregates. Nat. Protoc. *8*, 1381–1390.

Takacs, C.N., Poggio, S., Charbon, G., Pucheault, M., Vollmer, W., and Jacobs-Wagner, C. (2010). MreB Drives De Novo Rod Morphogenesis in Caulobacter crescentus via Remodeling of the Cell Wall. J. Bacteriol. *192*, 1671–1684.

Zhong, C., Gurry, T., Cheng, A.A., Downey, J., Deng, Z., Stultz, C.M., and Lu, T.K. (2014). Strong underwater adhesives made by self-assembling multi-protein nanofibres. Nat. Nanotechnol. *9*, 858–866.